Atmospheric Research 178–179 (2016) 231–259

Contents lists available at ScienceDirect

Atmospheric Research

journal homepage: www.elsevier.com/locate/atmosres

Invited review article

Physical climatology of Indonesian maritime continent: An outline to comprehend observational studies

Manabu D. Yamanaka

Department of Coupled Ocean–Atmosphere–Land Processes Research (DCOP), Japan Agency for Marine-Earth Science and Technology (JAMSTEC), 2-15 Natsushima-cho, Yokosuka 237-0061, Japan
Department of Planetology, Graduate School of Science, Kobe University, 1-1 Rokkodai-cho, Kobe 657-8501, Japan

ARTICLE INFO

Article history:
Received 7 September 2015
Received in revised form 16 March 2016
Accepted 16 March 2016
Available online 24 March 2016

Keywords:
Maritime continent
Atmosphere–ocean–land interaction
Convective clouds
Multiple scales

ABSTRACT

The Indonesian maritime continent (IMC) is a miniature of our land–sea coexisting planet Earth. Firstly, without interior activity, the Earth becomes an even-surfaced “aqua-planet” with both atmosphere and ocean flowing almost zonally, and solar differential heating generates (global thermal tides and) Hadley's meridional circulations with the inter-tropical convergence zone (ITCZ) along the equator as observed actually over the open (Indian and Pacific) oceans on the both sides of the IMC. The ITCZ involves intraseasonal variations or super cloud clusters moving eastward with hierarchical substructures moving also westward. Secondly, the lands and seas over the actual Earth have been keeping the area ratio of 3:7 (similar to that of islands and inland/surrounding seas in the IMC), but their displacements have produced the IMC near the equator, which turns equatorial Pacific easterly ocean current northward (Kuroshio) and reflects equatorial oceanic waves that affect coupled ocean–atmosphere interannual variations such as ENSO and IOD, or displacements of Walker's zonal circulations. Thirdly, because the IMC consists of many large/small islands with very long coastlines, many narrow straits control the global (Pacific to Indian) ocean circulation, and the land-sea heat capacity contrasts along the coastlines generate the world's largest rainfall with diurnal cycles (sea–land breeze circulations). The diurnal cycles are dominant even in the rainy season (austral summer in Jawa and Bali), because rainfall-induced sprinkler-like land cooling reverses the trans-coastal temperature gradient before sunrise, and subsequent clear sky on land until around noon provides solar heating dependent on season. These processes lead to rapid land/hydrosphere-atmosphere water exchange, local air pollutant washout, and transequatorial boreal winter monsoon (cold surge). In El Niño years, for example, the cooler sea-surface temperature suppresses the morning coastal-sea rainfall, and induces often serious smog diffused from land over the IMC. Lastly, high-resolution observations/models covering both over islands and seas are necessary. A radar-profiler network (HARIMAU) has been constructed during FY2005–09, and capacity building on radar operations and buoy manufacturing has been promoted during FY2009–13 by Japan–Indonesia collaboration projects, which are taken over by an Indonesian national center (MCCOE) established in November 2013. Through these projects, variabilities of local circulations and precipitations with diurnal cycles have been recognized as important targets both in science and application.

© 2016 The Author. Published by Elsevier B.V. This is an open access article under the CC BY license (http://creativecommons.org/licenses/by/4.0/).

Contents

http://dx.doi.org/10.1016/j.atmosres.2016.03.017
0169-8095/© 2016 The Author. Published by Elsevier B.V. This is an open access article under the CC BY license (http://creativecommons.org/licenses/by/4.0/).

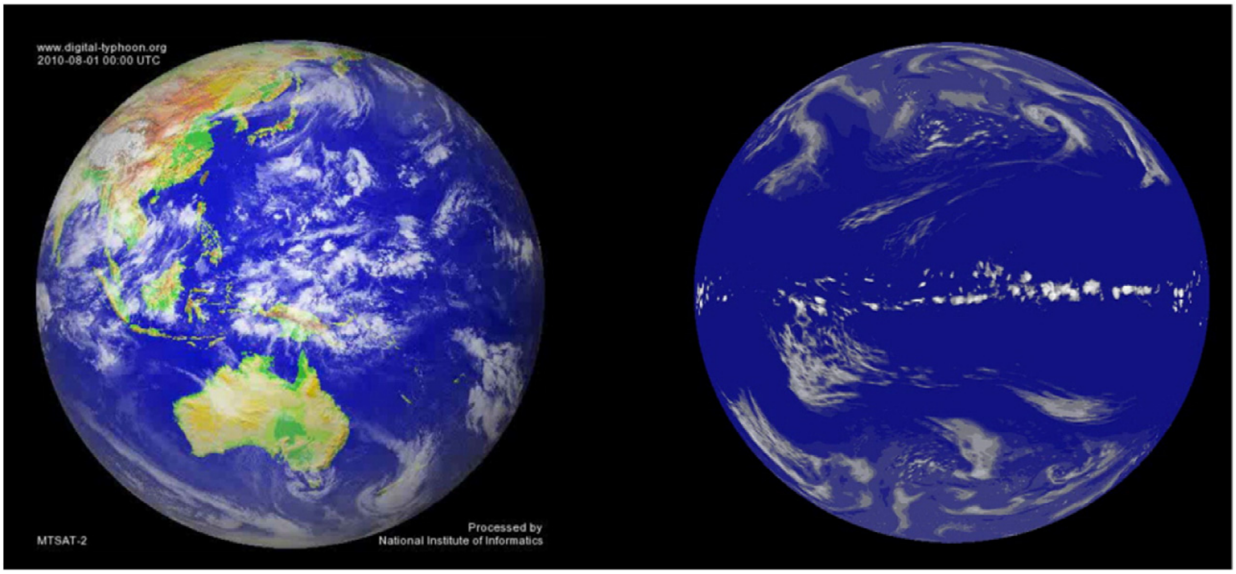

Fig. 1. Cloud distributions over the actual Earth observed by a meteorological satellite (left): http://agora.ex.nii.ac.jp/digital-typhoon/archive/monthly/ and a virtual earth (aqua-planet) with no lands simulated by a high-resolution numerical model (right): http://www.multi.jst.go.jp/theme/img/01_Sato/olr_1.mpeg.

1. Introduction

The Indonesian maritime continent (IMC) consists of five large (Papua, Kalimantan, Sumatera, Sulawesi, and Jawa)[1] and more than 13,000 smaller islands, and has about 5000 km or 1/8 of the equatorial circumference in longitude. In this latitude–longitude region of about 10,000,000 km^2 the land area (including territories of Indonesia, Malaysia, Papua New Guinea, and East Timor) is about 2,720,000 km^2, of which the land–sea ratio (2.7:7.3) is close to that of the whole Earth (3:7). The IMC has been playing the role of a "dam" across global ocean circulation flowing from the Pacific Ocean to the Indian Ocean since 20 million years ago (e.g., Gordon, 2005), interacting with a quasi-periodic change of glacial and inter-glacial periods in global climate. In a glacial period, the western part of the IMC was a true continent called Sundaland. In an inter-glacial period such as the last 10,000 years, the IMC becomes an archipelago in very warm sea water, which is considered to induce very intense convective activities playing the role of a major heat source driving atmospheric circulation. Atmosphere–ocean interactions near the IMC generate interannual global climate variations such as the El Niño–southern oscillation (ENSO) (Bjerknes, 1969) and the Indian Ocean Dipole mode (IOD) (Saji et al., 1999). Intraseasonal variations (ISVs) such as Madden–Julian oscillation (MJO) passing eastward from the Indian to Pacific Oceans (Madden and Julian, 1971) are modified and re-organized over the IMC.

The IMC has meteorological observation stations started in early 19th century (see, e.g., McBride, 1998; Können et al., 1998; and references therein). Many findings concerning tropical meteorology, as well as general meteorology (e.g., atmospheric tides; to be mentioned briefly in the next section), were done there. In particular, van Bemmelen (1913, 1922a, 1922b) described vertical soundings of winds up to the lower stratosphere started in 1909 at Batavia (Jakarta at present), and the results involved equatorial upper-tropospheric easterly and "non-annual" (later found as quasi-biennial, as will be shown later in the top of Fig. 2) wind changes in the stratosphere, annually reversed wind or monsoons (to be described later in Section 3), "anti-trade" winds (westerly bursts associated with ISVs, in Section 2) and sea–land breeze circulations (in Sections 4 and 5). During WWII and independence periods, observations (except for those at Singapore and some Malay stations outside Indonesia) were often interrupted, but after that, Indonesia achieved rapid economic/industrial development. In the present century, the IMC becomes one of the densest observation regions over the world (in Section 6 briefly). There have been published overviews related to climate and weather of the IMC, mainly on interannual variations (Allan, 1991; McBride, 1998), monsoons (e.g., Ramage, 1968; Lau et al., 2000; Chang et al., 2006; Yoden et al., in press; Matsumoto et al., in press), ISVs (e.g., Zhang, 2005, 2013), diurnal cycle (Johnson, 2011), and observation networks (e.g., Fukao, 2006; Yoneyama et al., 2008, 2013; Koh and Teo, 2009; Reid et al., 2013).

This article concerns a unified physical/dynamical viewpoint on observational studies from local to large scales inside the IMC which have been limited until recent decade (Yamanaka et al., 2008; Ando et al., 2010). Such a viewpoint is necessary to comprehend observational evidence increasing rapidly right now and to plan observations in the next step. The IMC is

(i) located in the equatorial ocean
(ii) as a land area
(iii) with alignment islands or archipelago.

In Section 2, observational evidence on (i) is compared with idealistic features of a virtual Earth or an aqua planet without lands (e.g., Hayashi and Sumi, 1986). In Section 3, features of (ii) generated by sea–land co-existence (as considered theoretically by Gill, 1980) are shown. In Section 4, features of (iii) appearing along long coastlines of the IMC, which are dominantly diurnal cycle and differ from a larger-scale discrete forcing case (Matsuno, 1966) over the actual archipelago. In Section 5, larger/longer-scale phenomena will be explained by amplitude modulations of the diurnal cycle. Section 6 concerns a brief summary of observation projects and strategies for future as conclusions of this article.

2. Features in common with an aqua planet: The ITCZ and ISVs

Imagine the Earth is on the same orbit as is in the solar system, but is a completely even-surfaced sphere without interior activity. The

[1] In this article Indonesian names are used for English names: New Guinea, Borneo, Sumatra, Celebes and Java.

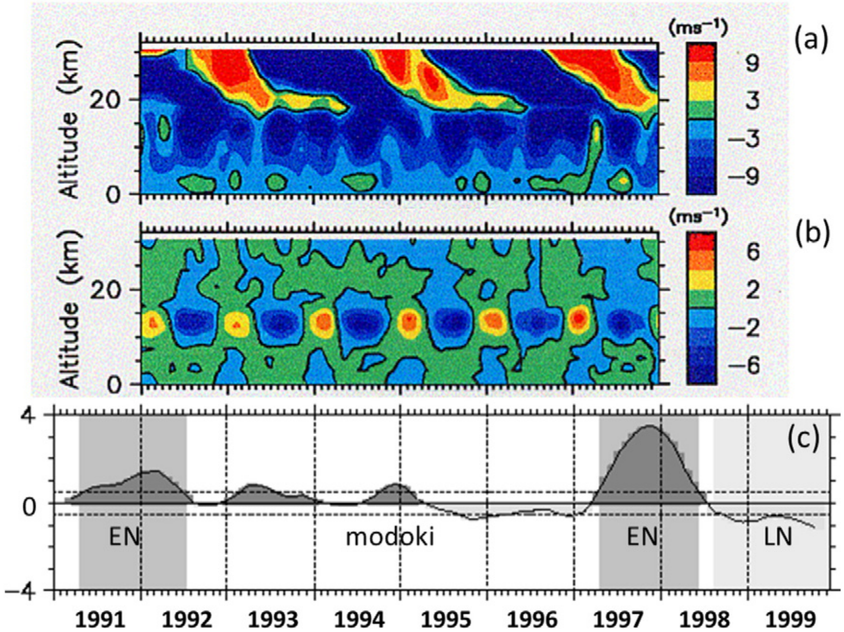

Fig. 2. Interannual-vertical variations of (a) zonal and (b) meridional winds averaged for 11 operational rawinsonde stations in Indonesia (modified from Okamoto et al. (2003) and Hashiguchi et al. (2006)), compared with (c) sea surface temperature over Niño 3 (eastern tropical Pacific: "EN": El Niño; "LN": La Niña; "modoki": weak EN-like situation). In the troposphere, strong westerly appeared in an EN period, and meridional (Hadley) circulation increased in this decade. In the stratosphere, the zonal wind (quasi-biennial oscillation) is almost the same as the zonal mean.

radiative equilibrium between solar heating (decreased by the albedo or parasol effect of Earth's surface and clouds) and infrared cooling (returned partially to the Erath by the greenhouse effect) will maintain liquid water as plenty as the actual Earth, but the water covers the whole Earth with a depth of 2700 m, that is so-called an "aqua-planet" (right-hand side panel of Fig. 1).

Winds observed in the troposphere over the IMC are rather weak in average (Fig. 2), which is a common feature in tropics and may be explained basically even in the aqua planet receiving solar heating with latitudinal difference and annual and diurnal cycles. If the latitudinal differential heating (including that between summer and winter hemispheres) is adjusted completely geostrophically, both atmosphere and ocean flow zonally (as in stripe patterns of dense atmospheres of Jupiter and Saturn, and in the Earth's equatorial stratosphere as shown in Fig. 2). However, in the troposphere, this hydrostatic–geostrophic equilibrium does not hold locally, with over-heating and -cooling in the equatorial and polar regions, respectively, and the equatorial over-heating is partly due to a hydrological cycle (only between atmosphere and ocean; cf. Webster, 1994) associated with a peak 2000 mm/year of rainfall produced by clouds with spatially/temporally small scales. These (heat and water) imbalances must be compensated by meridional circulations (right of Fig. 3, as well as top right of Fig. 5 later),

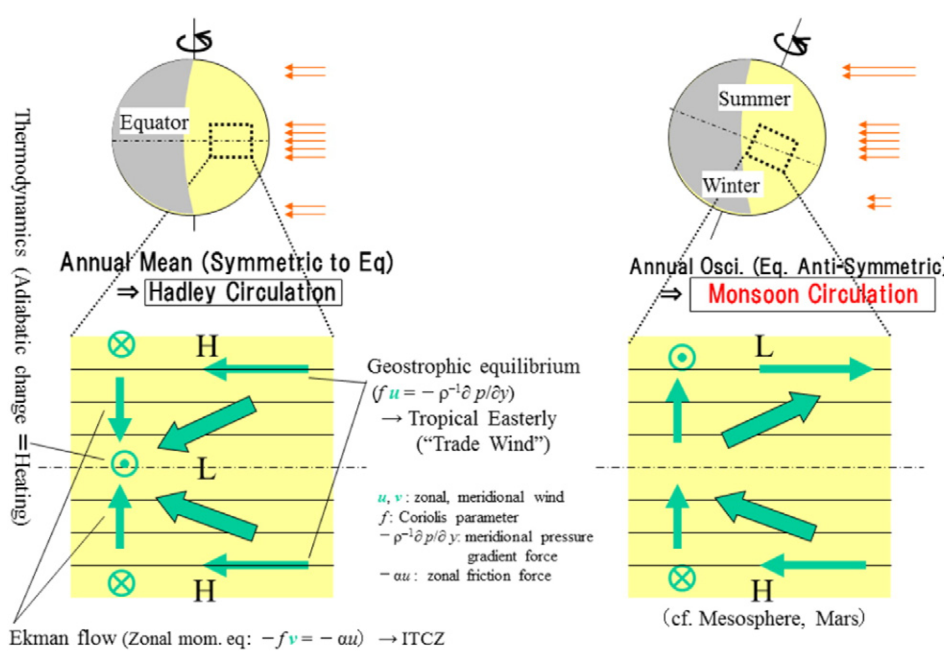

Fig. 3. Schematic figures of geostrophic zonal flow and meridional circulation for equatorially symmetric heating/pressure field associated with Hadley cells (left) and anti-symmetric monsoon-like case (right).

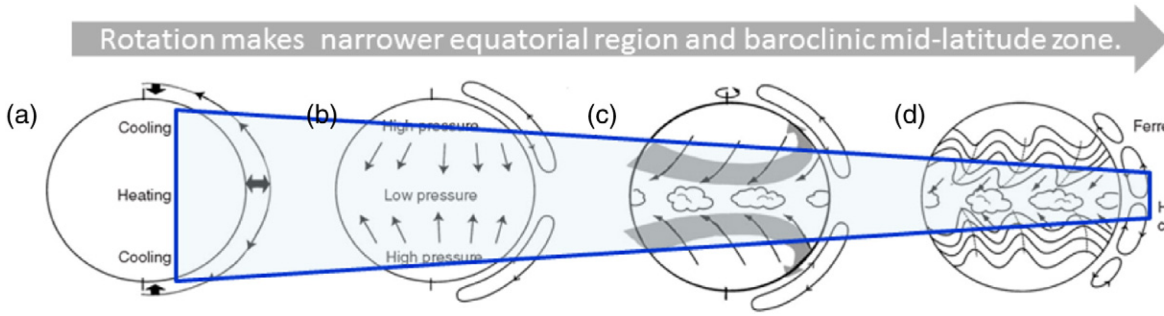

Fig. 4. Schematic depiction of the general circulation as it develops from a state of rest in a climate model for equinox conditions in the absence of land-sea contrasts of the equatorial region (where convective clouds controls circulation) (Wallace, 2002, with modification).

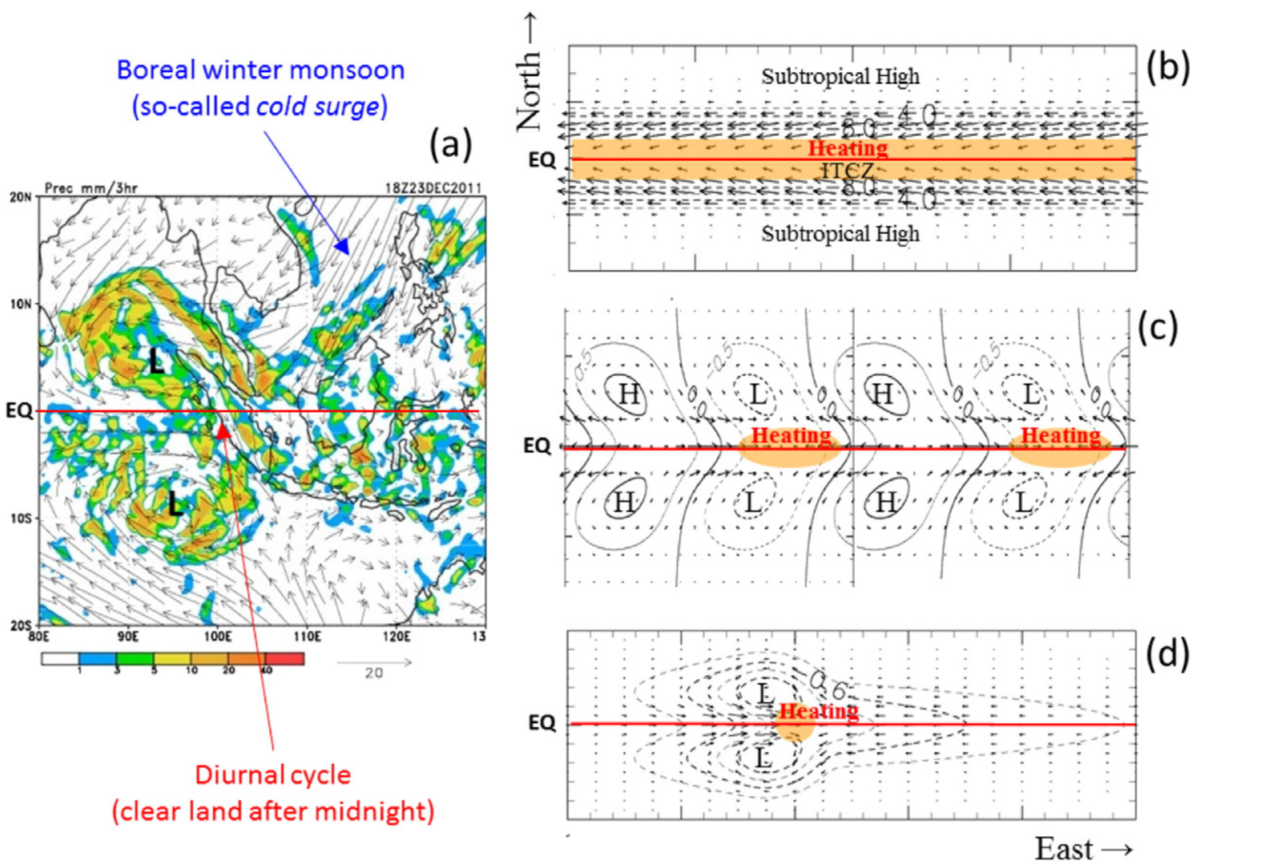

Fig. 5. (a) Observed intraseasonal variation or super cloud cluster over the Indian Ocean (cf. Shibagaki et al., 2006a, 2006b), compared with theoretical (b) the ITCZ-Hadley cells generated by zonally uniform heating (cf. Kosaka and Matsuda, 2005) and the Matsuno–Gill patterns generated by zonally periodic (Matsuno, 1966) and (d) isolated (Gill, 1980) heatings.

known as Hadley twin cells with a meridional scale given by the equatorial deformation radius (see, e.g., Gill, 1982):

$$\lambda_e = \sqrt{\frac{a\sqrt{gh}}{2\Omega}} \approx 1100\ \text{km} \approx 10^\circ \text{ in latitude}, \quad (1)$$

where a, g, and Ω are Earth's radius (6.4×10^6 m), gravity ($9.8\ \text{ms}^{-2}$) and rotation ($7.3 \times 10^{-5}\ \text{s}^{-1}$), and h is the atmospheric equivalent depth (about 80 m for gravity wave phase speed $\sqrt{gh} \approx 28\ \text{m s}^{-1}$). Inside a meridional ($y$) range bordered by (1) ($|y|<\lambda_e$) convective clouds control circulation, whereas outside ($|y|>\lambda_e$) quasi-geostrophic circulation controls clouds (Fig. 4; thus we may use a weather map in middle and high latitudes). It is completely inside (1) that the meridional range of the IMC is located.

Between the twin cells of Hadley circulation, updraft and cloud are concentrated as so-called the inter-tropical convergence zone (ITCZ).[2] The ITCZ is zonally inhomogeneous and intermittent due to ocean–atmosphere interactions, which consists of ISVs and tropical cyclones (e.g., Takayabu and Nitta, 1993). The ISVs or super cloud clusters moving eastward with periods of 1–2 months and zonal scales of a few thousand kilometers are observed over the open (Indian and Pacific) oceans on the both sides of the IMC (Madden and Julian, 1971; Nakazawa, 1988) (seen in Fig. 1 and in the left panel of Fig. 5) and are simulated in the aqua-planet models (e.g., Hayashi and Sumi, 1986). In a steady zonally elongated limit or a zonal/seasonal average,

[2] In this article, the ITCZ is recognized in cloud/rainfall horizontal distributions or as zero meridional wind, so that stationary (or annual-mean) Hadley and monsoon circulations are not separated.

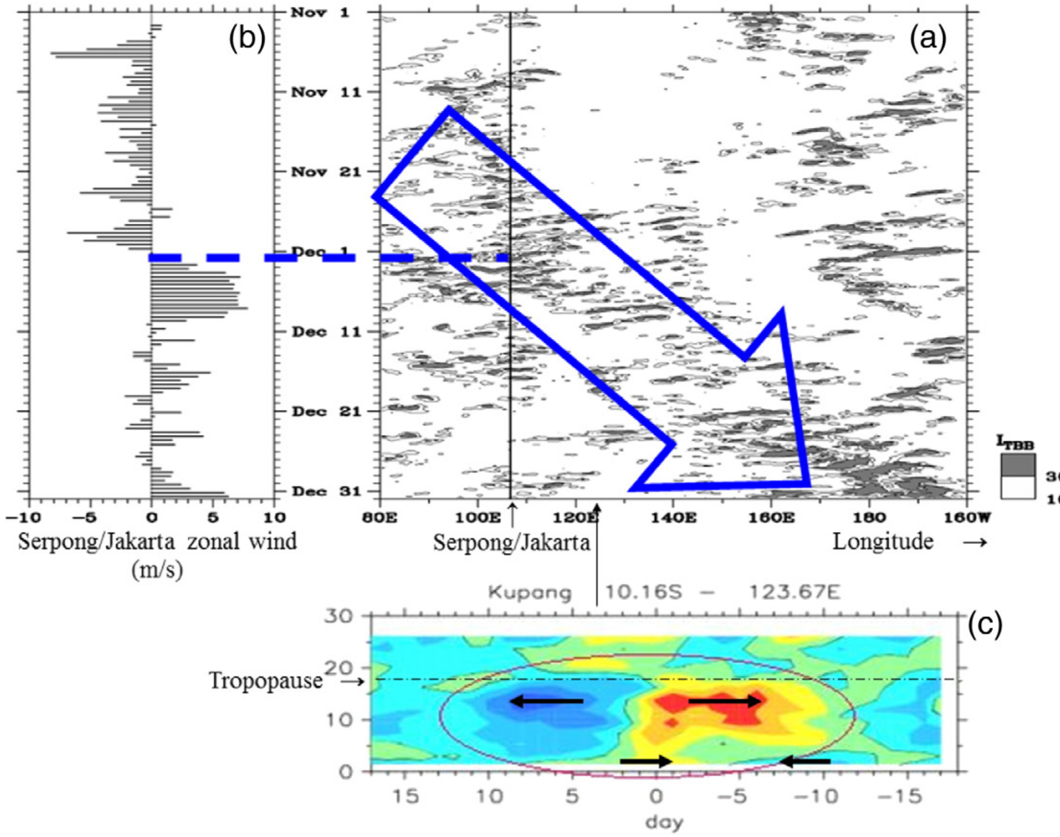

Fig. 6. An ISV passage indicated by (a) meteorological satellite-observed $I_{TBB} = 250$ K — black body temperature, compared with (b) wind profiler-observed lower-tropospheric zonal wind (Hashiguchi et al., 1995a) and (c) a humidity maximum-composite pseudo-zonal vertical cross-section of zonal wind observed by operational rawinsondes at Kupang (10.16°S, 123.67°E), west Timor.

ISVs become the Hadley circulations (Gill, 1980; Lau and Lim, 1982; Matsuda and Kato, 1987; Kosaka and Matsuda, 2005). Due to a superposition of the Kelvin and Rossby wave components (right top of Fig. 5, or left of Fig. 3), winds over the heating area with ISV and over zonally homogeneous equator are weak as observed in Fig. 2.

The rainy season onset of the southern hemispheric part of the IMC (see Section 3) is determined by an ISV (Hashiguchi et al., 1995a) (see Fig. 6), and through the rainy season, rainfall over the IMC increases actually during the active/wet phase of the dominant mode (MJO) of ISVs (Murata et al., 2002, 2006; Shibagaki et al., 2006a, 2006b; Seto et al., 2006; Johnson and Ciesielski, 2013; Marzuki et al., 2013b), in particular on surrounding seas larger than on the large islands (Hidayat and Kizu, 2009)[3]. Shorter hierarchy resembling mixed Rossby-gravity and/or inertio-gravity waves with periods of a few days also has been observed mainly near the eastern/western ends (Pacific and Indian Ocean sides) of the IMC (Takayabu et al., 1996; Widiyatmi et al., 1999, 2001). These are also candidates to amplify diurnal cycles (Section 5) and cause heavy rainfall in the western IMC (Wu et al., 2007, 2013). Recent high-resolution numerical models (e.g., Takasuka et al., 2015) show that MJO/ISVs on an aqua planet are substantially modified if a land such as IMC exists (cf. Section 5).

On the other hand, average annual occurrence of tropical cyclones (called "*badai tropis*" in Indonesia–Malay language) occurred inside the equatorial deformation radius (1) is only two (dispersed between zero and seven each year) on the northern (Philippine and Micronesian) side (during the past century; Kubota et al., 2012; Kubota, 2012) and less than 1.5 on the southern (Australian) sides (for the last two decades of the last century; Hall et al., 2001). They are much rarer (as reported by Chang et al., 2003) and not so much developed over inland seas and islands of the IMC, which could be simulated by high-resolution (cumulus-resolving) numerical models (Fig. 7). Because the ITCZ shifts annually but is not completely following a weak annual cycle of solar radiation (as will be shown in Fig. 8), and it concerns typhoon generation mainly in the northern subtropics (often northern than 20°N in boreal summer), otherwise it involves mainly ISVs (because southward shifts of the ITCZ are not so deep even in the austral summer). However, a few very strong typhoons (such as a case and a "super typhoon" Haiyan (Yolanda, T1330) in 2013, as well as another one in 1912 almost just 100 years ago, and less strong ones such as reported by Holliday and Thompson, 1986, between them almost every about three decades) have been generated and developed very much along (for a few days a little southern than) 10°N (Kubota, private communications)[4].

The annual and diurnal cycles of solar irradiance are calculated astronomically (Fig. 8). The diurnal cycle is dominant in tropics (between the northern and southern tropics, i.e., within ±23.4° in latitude) including the meridional range given by λ_e. Absorption of infrared and ultraviolet components of the solar radiation by tropospheric water vapor and by stratospheric ozone may generate diurnal and semidiurnal atmospheric thermal tides, on which Batavia (Jakarta) was an earliest place of standard observations more than a century ago (Fig. 9; also see, e.g., Chapter 9 of Lindzen, 1990). The most dominant period is semidiurnal (1–2 hPa in surface pressure amplitude), and the second mode is diurnal. These tidal waves with global phase

[3] This ocean-side excess could be explained by characteristics of the local diurnal cycle (Sections 4 and 5) amplified by MJOs/ISVs.

[4] Thus, the generations of those typhoons are not explained by so-called global warming.

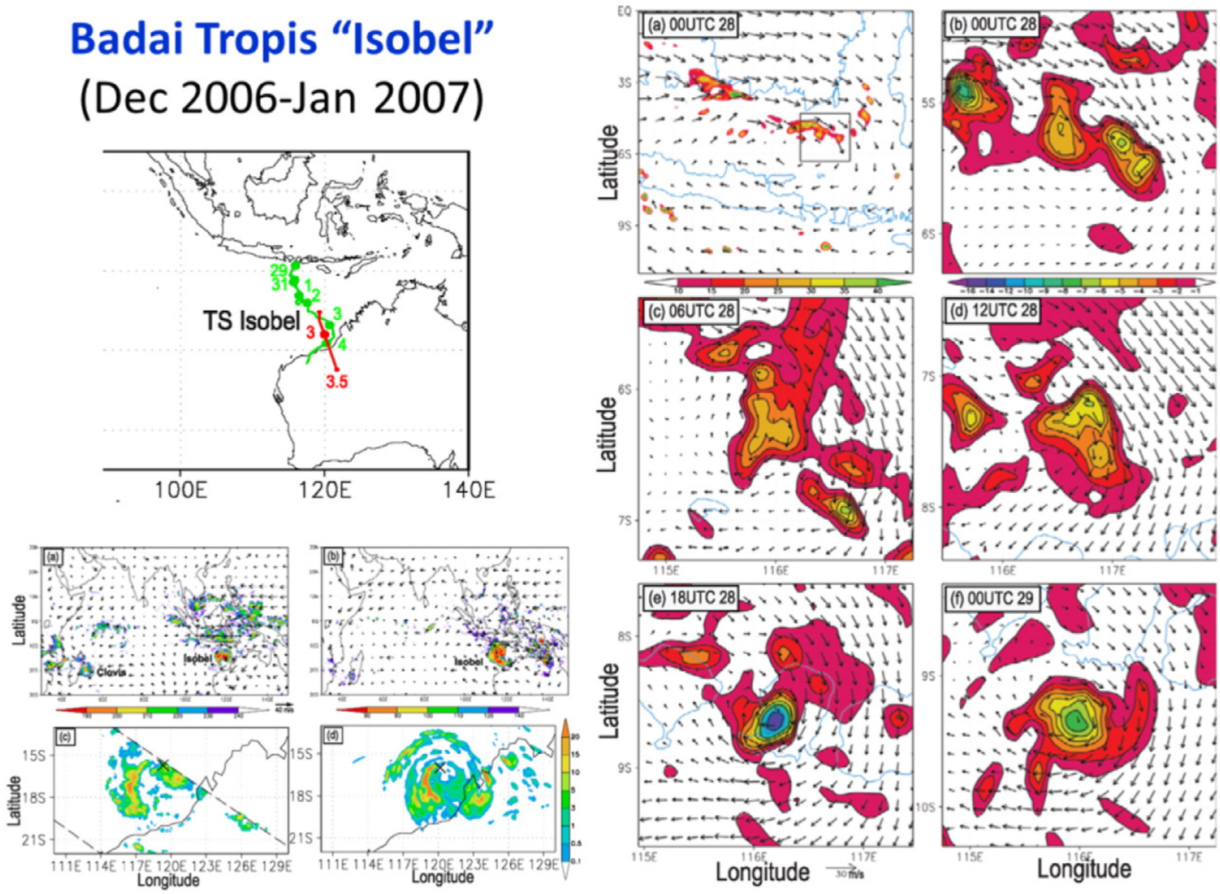

Fig. 7. A very rare example of tropical cyclone generated in the IMC observed by objective analysis and a space-borne radar (TRMM) (left of left bottom) and very high-resolution global numerical simulations (NICAM) (right of left bottom) (Fudeyasu et al., 2008).

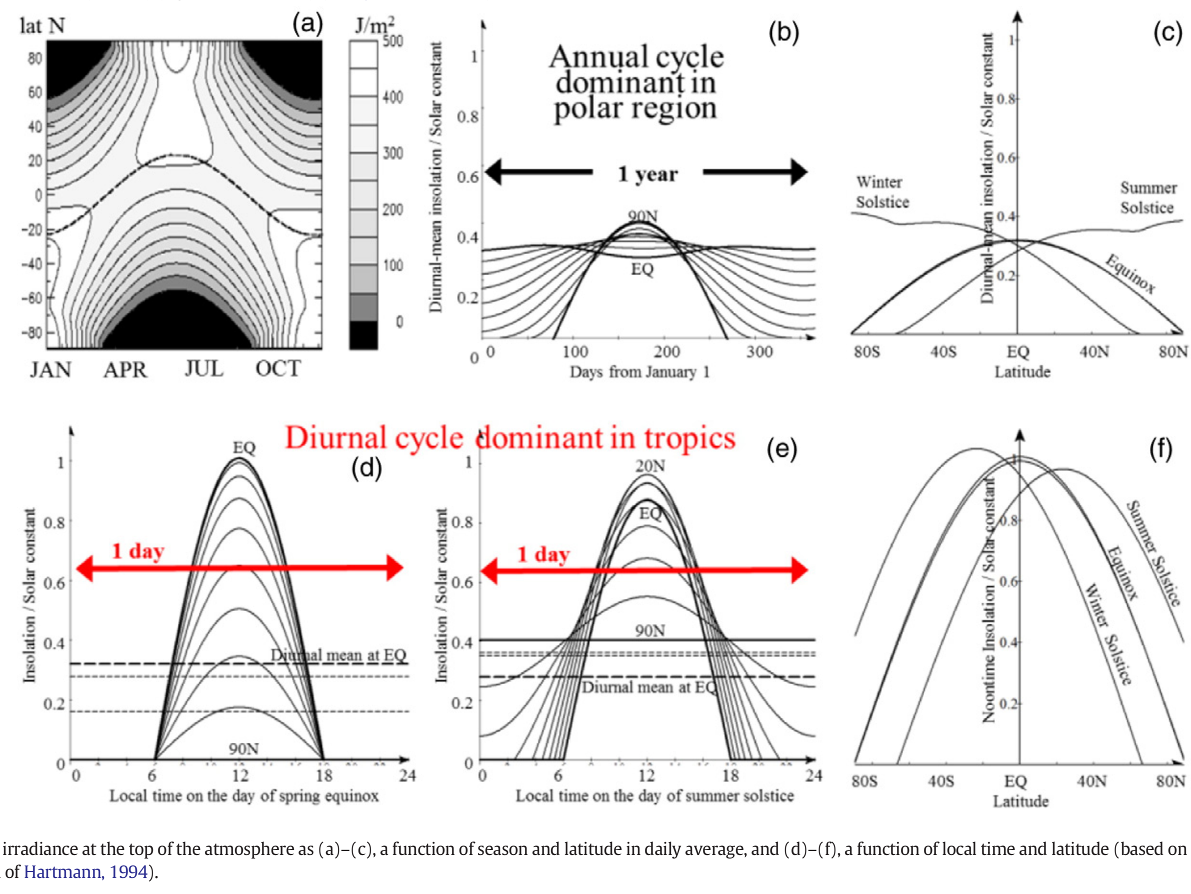

Fig. 8. Solar irradiance at the top of the atmosphere as (a)–(c), a function of season and latitude in daily average, and (d)–(f), a function of local time and latitude (based on Chapter 2 and Appendix A of Hartmann, 1994).

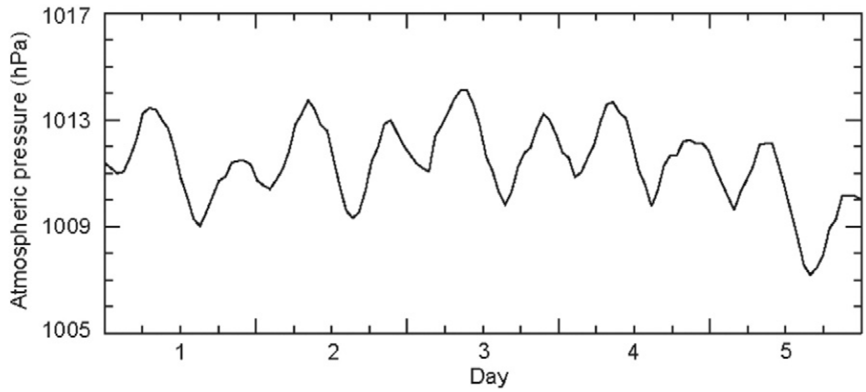

Fig. 9. Reproduced surface pressure record at Batavia (Jakarta) during 1–5 January 1925 (re-plotted by Hagan et al., 2003).

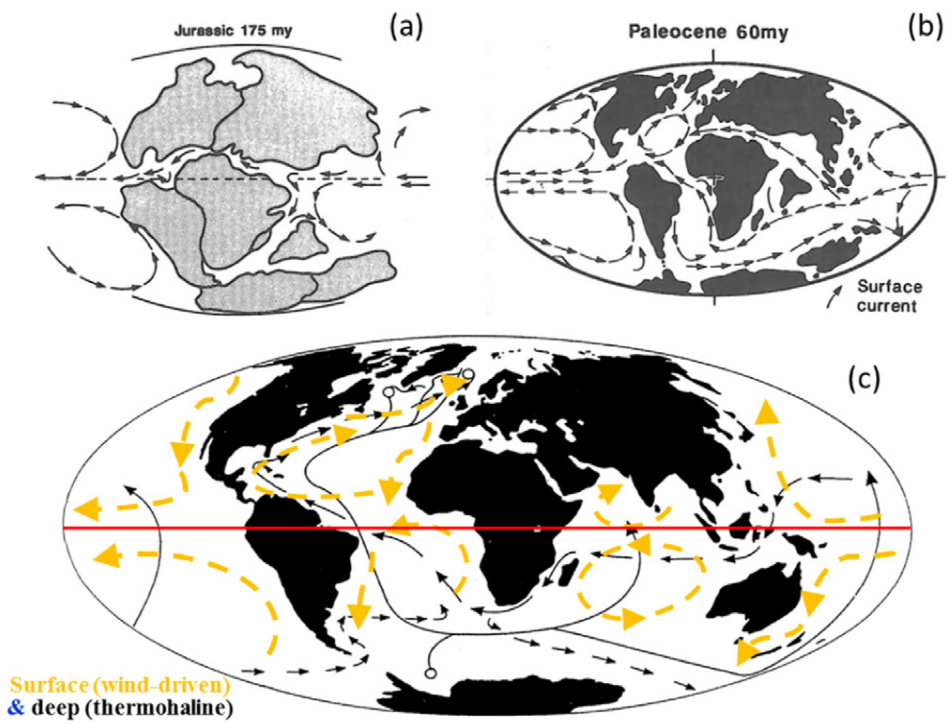

Fig. 10. (a) Mesozoic and (b) Cenozoic Tertiary continent distribution and ocean currents (Van Andel, 1994), compared with the present surface and deep ocean circulations (Bigg, 2003, with modification; originally from Prof. W. S. Broecker's idea proposed in 1987; see Broecker, 1991).

structures are dominant in Mars[5] without oceans and above the middle stratosphere far from the oceans on Earth (e.g., Tsuda et al., 1994a; Sakazaki et al., 2012), but are weaker than another diurnal cycle associated with a sea–land breeze circulation in the troposphere in particular of the Earth's low latitudes (Section 4).

Similarly for the annual cycle, the winter–summer hemispheric difference induces a monsoon-like meridional circulation (right panel of Fig. 3), in particular in the Indian Ocean (see Webster et al., 2002, who suggested a self-regulation between monsoon and its Ekman ocean transport), although the other cause, the continent–ocean contrast, is more important. In addition, a superimposition of the monsoon-like circulation may be seen also as the dominance (both in size/cross-equatorial shift and in intensity) of winter-hemispheric cell of Hadley circulations to the summer-hemispheric cell (see the lower panel of Fig. 2; also the left panels of Fig. 12 later).

[5] On Venus, however, the diurnal tide (day–night circulation) is suppressed by a zonally homogeneous superrotation (Matsuda, 1980).

3. Climatic features due to land–sea coexistence: Monsoon, ENSO, and IOD

The Earth is not an aqua planet but has lands and seas. The global land–sea area ratio 3:7 has been kept since at least 400 million years ago, but their displacements produced the IMC on the equator, which turns equatorial Pacific easterly ocean current northward (Kuroshio) (Fig. 10; see, e.g., Broecker, 1991; Van Andel, 1994; Bigg, 2003). In the atmosphere, the continent–ocean (liquid–solid) contrast of heat capacity toward the solar radiation produces seasonal (monsoonal) variations (Fig. 11). Because there are Eurasian and Australian continents to the north and south of the IMC, the both boreal and austral summer monsoons associated with the annual–meridional shift of the ITCZ are very clear, which is also seen as the stronger/larger winter-hemispheric Hadley cell, as mentioned in the previous section. Because of this basic behavior of the ITCZ and monsoon, the rainy season over the IMC differs/moves meridionally, and thus the IMC may be divided into roughly three climatic regions on the both sides and vicinity of the equator with austral/boreal summer single peak and with semiannual

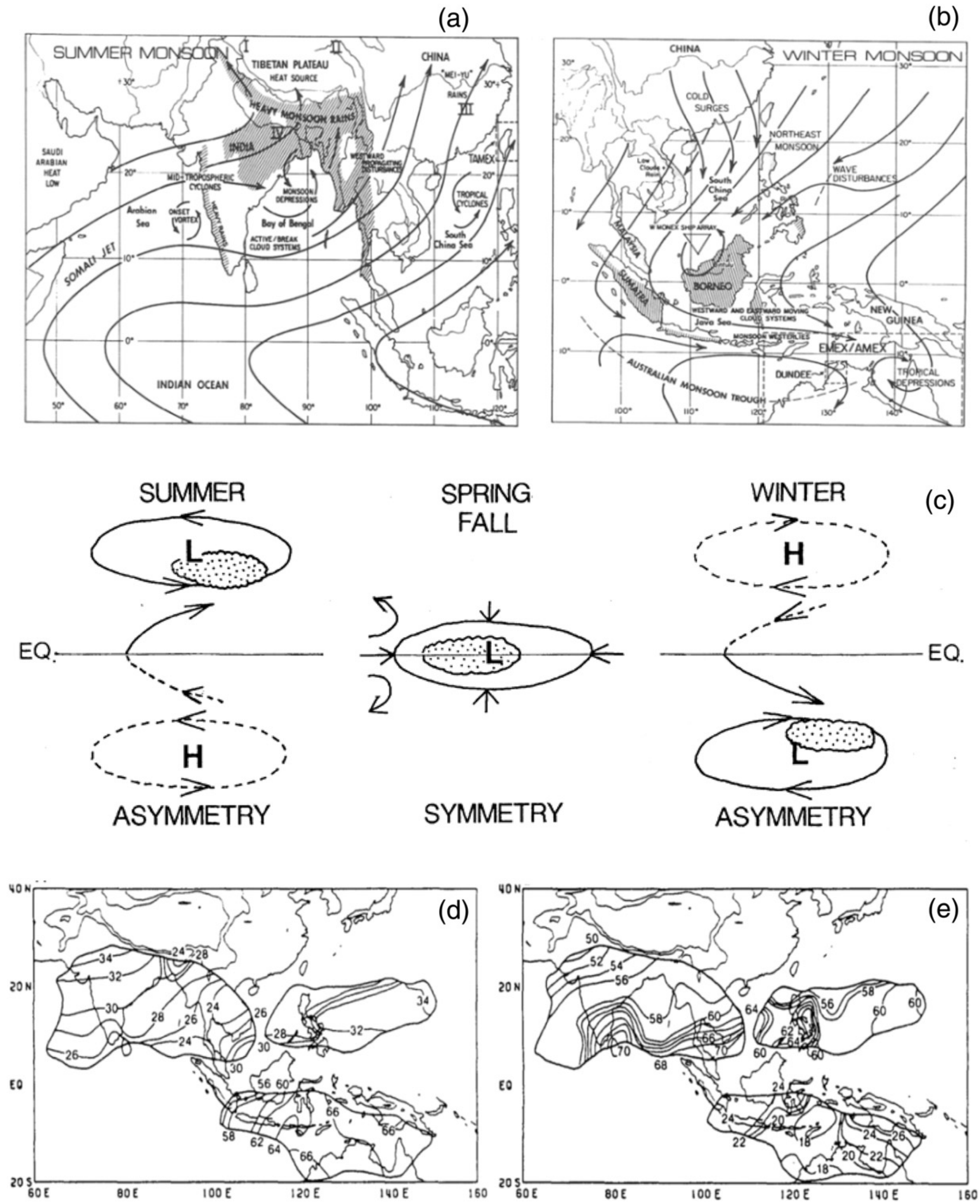

Fig. 11. Boreal (a) summer and (b) winter Asia monsoon circulations (Johnson, 1992), (c) the seasonal cycle of the ITCZ location indicated by dotted area (Matsumoto and Murakami, 2000), and rainy-season (d) onset and (e) withdrawal isochrones indicated by pentad number (Murakami and Matsumoto, 1994).

double or unclear peaks, respectively (Schmidt and Ferguson, 1951; Eguchi, 1983; Murakami and Matsumoto, 1994; Hamada et al., 2002; Hendon, 2003; Aldrian and Susanto, 2003; Chang et al., 2004b, 2005)[6]. More precisely, there are two onset migration routes of the austral summer rainy season (Murakami and Matsumoto, 1994): one starts from the Indian Ocean side of Jawa in the middle September and propagates northward (in Jawa) and eastward (to Nusa Tenggara in middle December); the other one is from Papua to Nusa Tenggara (Lesser Sunda Islands from Timor to Bali). The withdrawal of the austral-type rainy season starts from western Nusa Tenggara in March and goes eastward (to eastern Nusa Tenggara) and westward (to Jawa), until late May.

However, annual-cycle-based description seems to have limitations, because there are two geographical (equatorially asymmetric

[6] Schmidt and Ferguson (1951) distinguished climate of Jawa roughly from other major islands. Eguchi (1983), Matsumoto (1992), and Murakami and Matsumoto (1994) recognized the three types (see text) in monthly rainfalls, wind directions and cloud activities, respectively. Hamada et al. (2002), Hendon (2003), and Aldrian and Susanto (2003) showed them clearly from daily 46, monthly 43, and 100 rainfall station data, respectively. Chang et al. (2005) used satellite rainfall and wind (TRMM and QuikSCAT) data.

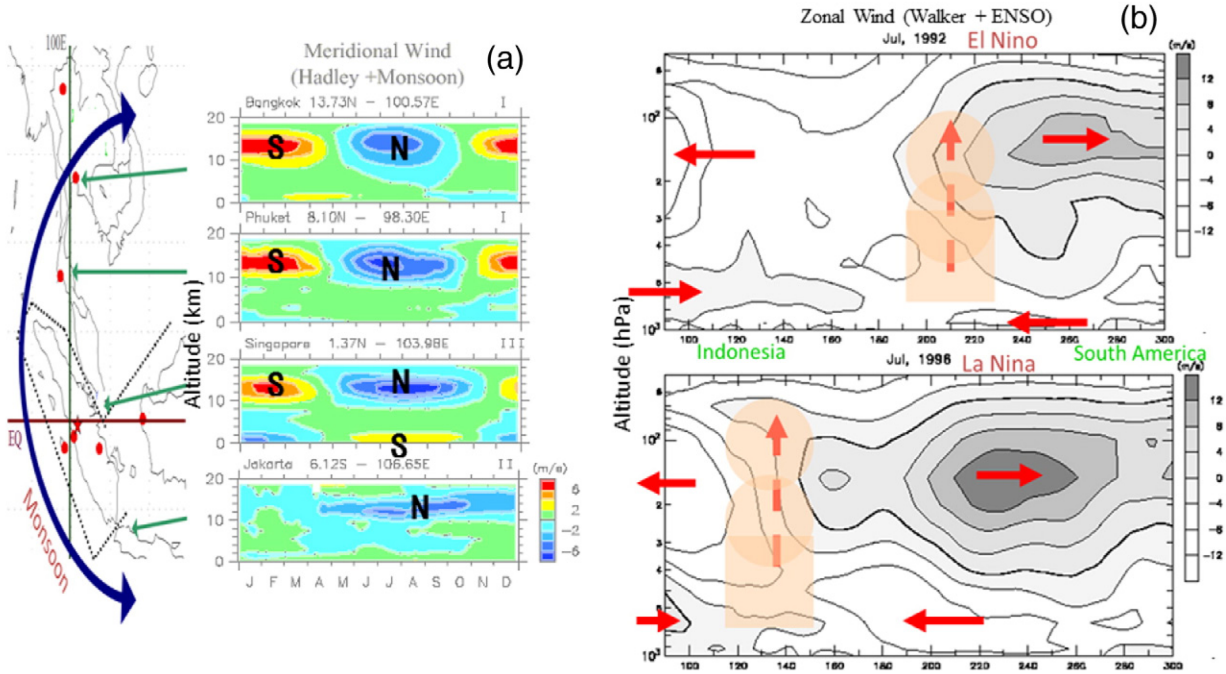

Fig. 12. (a) Seasonal-vertical variations of meridional wind at stations along 100°E meridian showing a seasonal-meridional shift of the Hadley circulation, and (b) zonal-vertical distributions of zonal wind in El Niño–La Niña years showing an ENSO-correlated zonal shift of the Walker circulation (modified from Okamoto et al. (2003) and Hashiguchi et al. (2006)).

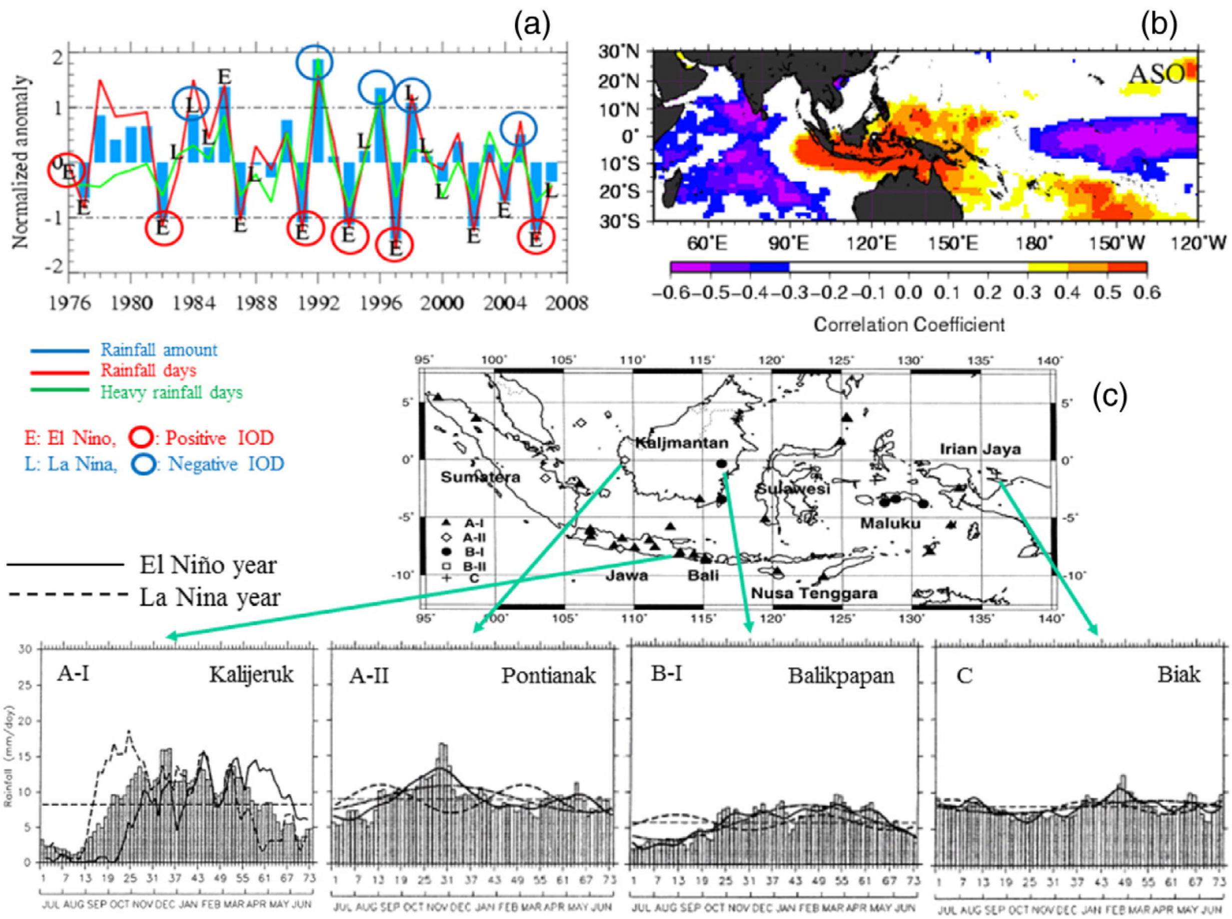

Fig. 13. (a) Interannual variations of dry-season (Aug–Sep–Oct) rainfall in Jakarta (shown by 9-station-averaged normalized anomaly of rainfall (bars), rainy days (red line), and 5th percentile heavy rain days (green line) compared with "E"l Niño, "L"a Niña, and ±IOD (red/blue circle) years and (b) their simultaneous correlation with SST (colored above the 95% confidence level (Hamada et al., 2012); and (c) pentad-mean rainfall variations averaged for all (bars), El Niño (solid) and La Niña (dashed) years at typical stations, compared with each mean pentad rainfall (horizontal dashed line) (Hamada et al., 2002).

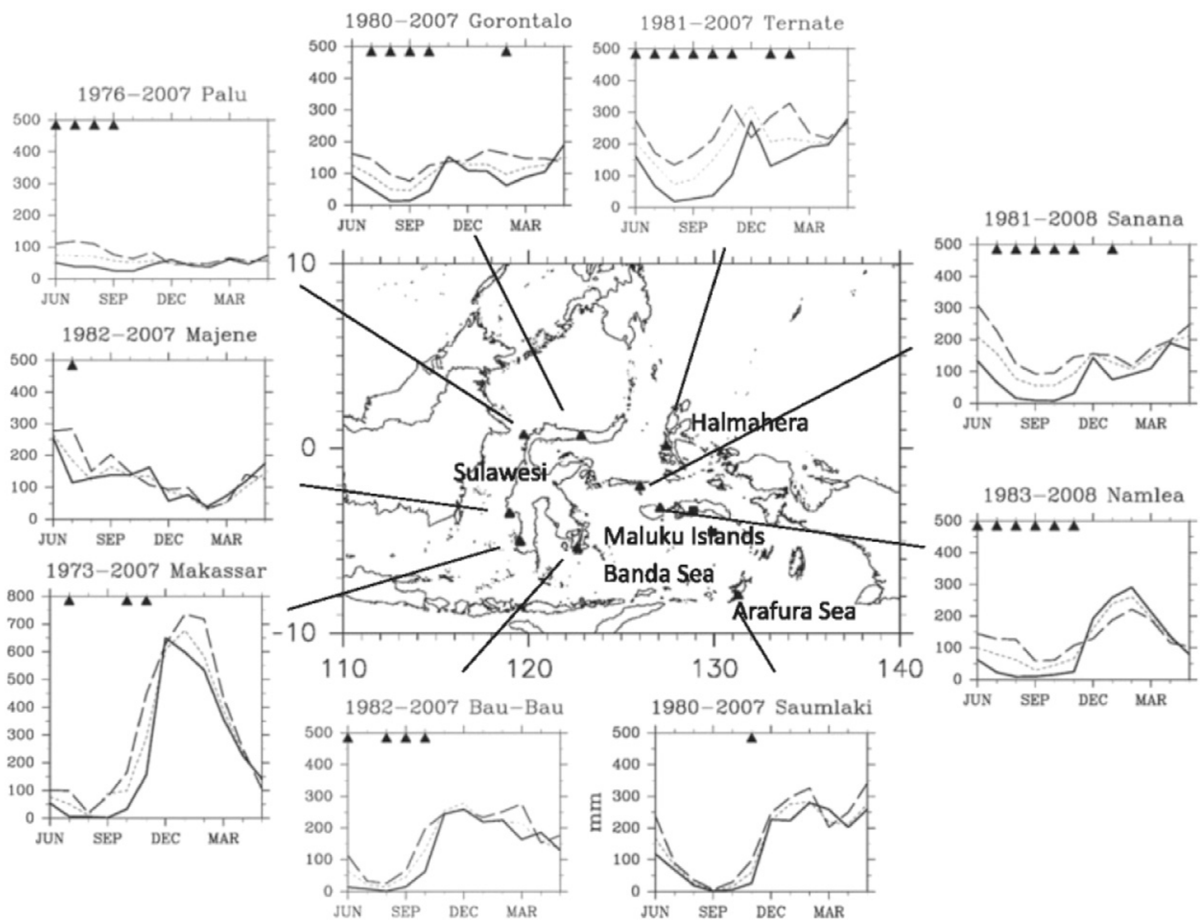

Fig. 14. Monthly rainfalls (in mm) averaged on El Niño (solid), La Niña (dashed), and all years (dotted line) for the eastern IMC. Triangles indicate months with statistically significant El Niño–La Niña rainfall differences at the 95% confidence level (Kubota et al., 2011).

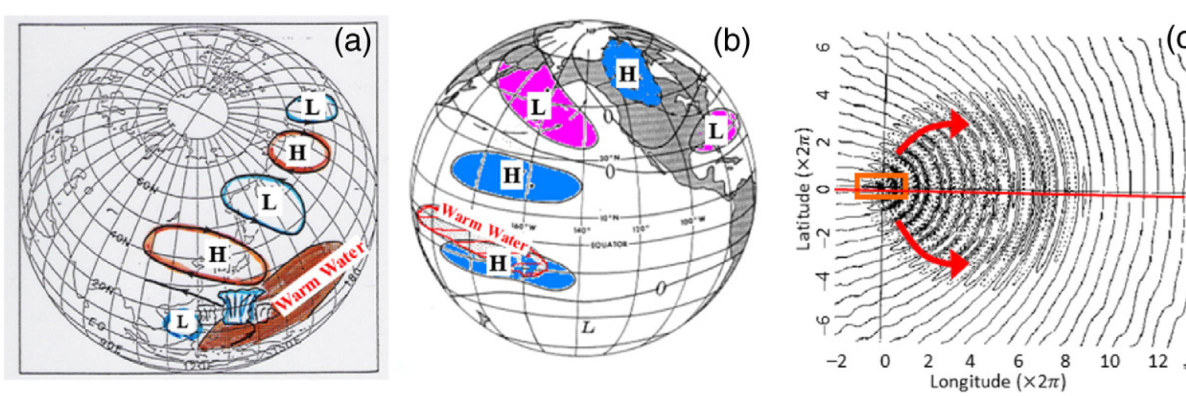

Fig. 15. Observed (a) La Nina (Nitta, 1987)–(b) El Nino (Horel and Wallace, 1981) and (c) theoretical (Hayashi, 1987) patterns of teleconnections between tropical anomalies and global abnormal weathers.

continent–ocean placement and steep mountain topography) and two spectral reasons (dominant interannual and intraseasonal variations). In other words, the annual cycle over the IMC is not so uniquely dominant as in the extratropics (as so far suggested in the radiative forcing of Fig. 3), and these are why the climatological description could not be done until 1980s in spite of about 2000 rain gauge stations constructed until the end of the 19th century. Many high (often active) volcanoes and deep jangles have been covered by neither old rain gauge nor recent radar networks,[7] which are also related to the last item: ISVs and their modifications over the IMC (see subsequent sections). Due to asymmetrically gigantic and small continents, Eurasia and Australia, the northward invasions of the ITCZ and boreal summer monsoon are deeper

[7] A satellite-borne radar described in the next subsection may cover the whole IMC including mountain and sea areas, but it cannot be used for continuous observations because of its polar orbit (with a recurrent period of 1 day or longer).

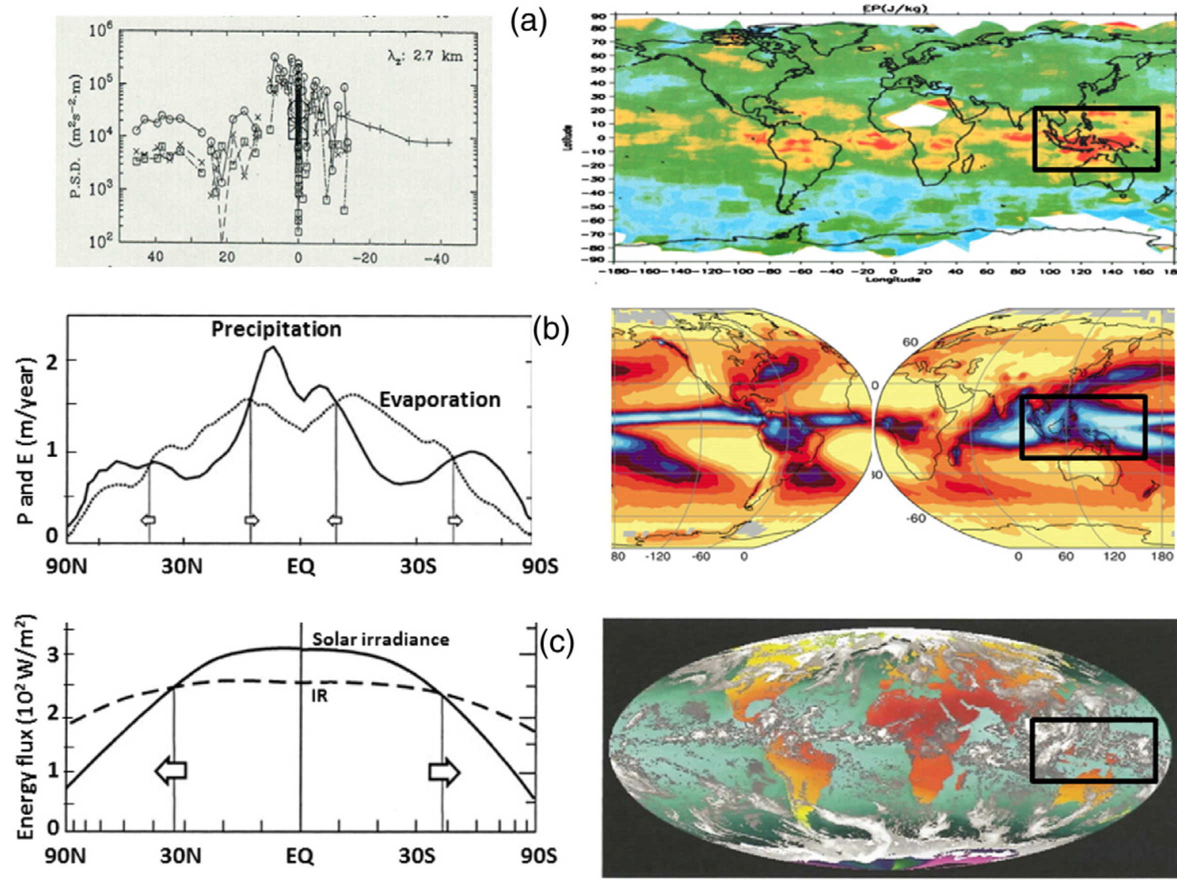

Fig. 16. Meridional (left) and global (right) distributions of (a)(d) gravity wave momentum flux (Ogino et al., 1995; Tsuda et al., 2000), (b)(e) water and (c)(f) radiation budgets (Hartmann, 1994; IPCC, 2007; Wallace and Hobbs, 2006). (b) shows both precipitation and evaporation, but (e) shows precipitation only (based on Xie and Arkin, 1997). (c) shows solar irradiance and infrared radiation, whereas (f) shows temperatures of cloud, land and sea surfaces.

(at least zonal mean) than the southward one with boreal winter monsoon, but the latter becomes an important cause of torrential rainfall in the IMC (so-called cold surges or northern Australia and Indonesian monsoon; Murakami and Matsumoto, 1994; Wu et al., 2007; Hattori et al., 2011; Matsumoto et al., in press), in particular in Jawa in the rainy season (by amplifying local diurnal cycles as will be mentioned in the next section), together with the other cause, interannual variability such as ENSO (see Fig. 12) and IOD induced by another land effect of the IMC which reflects oceanic waves propagating along the equator (e.g., Battisti and Hirst, 1989) and modifies/damps atmospheric ISVs (e.g., Nitta et al., 1992). The cold surges induce heavy rainfalls along the western coast of the South China Sea (Vietnam and Malay) near the northern boundary of (1) or of the IMC, in particular, when synoptic-scale cyclonic disturbances are formed near Kalimantan and southern Philippines (e.g., Cheang, 1977; Tangang and Juneng, 2004; Yokoi and Matsumoto, 2008; Wu et al., 2011; Chen et al., 2013), which Chen et al. (2015) considers important also for transequatorial impacts in Jawa.

Observed, the IMC rainfall–ENSO/IOD correlation has seasonality and locality. Hamada et al. (2002) showed that the rainy season onset comes later (earlier) in El Niño (La Niña) years than the average at most stations (particularly in the southeastern part of Jawa) (lower panels of Fig. 13). Correlations between rainfall amounts at those stations, and the southern oscillation index in SON, are significantly high. Hamada et al. (2012) have shown that northwestern Jawa including Jakarta, drought in the dry season (May − October) occurs in conjunction with simultaneous development of positive IOD and El Niño, whereas wet conditions tend to appear in negative IOD with or without La Niña (upper panels of Fig. 13). Large-scale divergence (convergence) and lower (higher) atmospheric water vapor content tend to suppress (induce) rainfall in northwestern Jawa during the dry seasons of positive (negative) IOD years with cooler (warmer) SST.

However, as Haylock and McBride (2001) and McBride et al. (2003) described, such a clear correlation in the west IMC is not seen in the rainy season. Hamada et al. (2002) showed that the rainfall amount throughout a rainy season is not dependent upon the length of the rainy season (between onset and withdrawal) in many areas (except southern Sulawesi). Chang et al. (2004a) suggested low correlations of the western IMC rainfalls with ENSO due to anomalous Walker circulation patterns on the Indian Ocean side and steep mountains barriers there. Hamada et al. (2012) showed that rainfall in west Jawa in the rainy season (November − April) is influenced more directly by the cold surges rather than ENSO/IOD. Similar conclusion had been obtained also for Malay on the western side of the IMC (Tangang et al., 2008). Such larger-scale conditions including ENSO/IOD, cold surges, and ISVs may generate heavy rainfall in some areas (but not in others) through amplifying local diurnal cycles, as described in Sections 4 and 5. On the other hand, for the eastern part or Pacific Ocean side of the IMC (roughly to the east of central Kalimantan mountains), Aldrian and Susanto (2003) and Kubota et al. (2011) showed strong correlations with ENSO (Fig. 14), and the latter authors suggested that the drought condition in an El Niño year might be intensified by SST decrease and subsidence over inland (Banda and Arafura) seas due to both boreal/austral summer monsoons. Recent detailed analysis (Lestari et al., 2016) shows that ENSO influences in Sulawesi and Maluku are more dominant in boreal summer and transitional seasons than in austral summer.

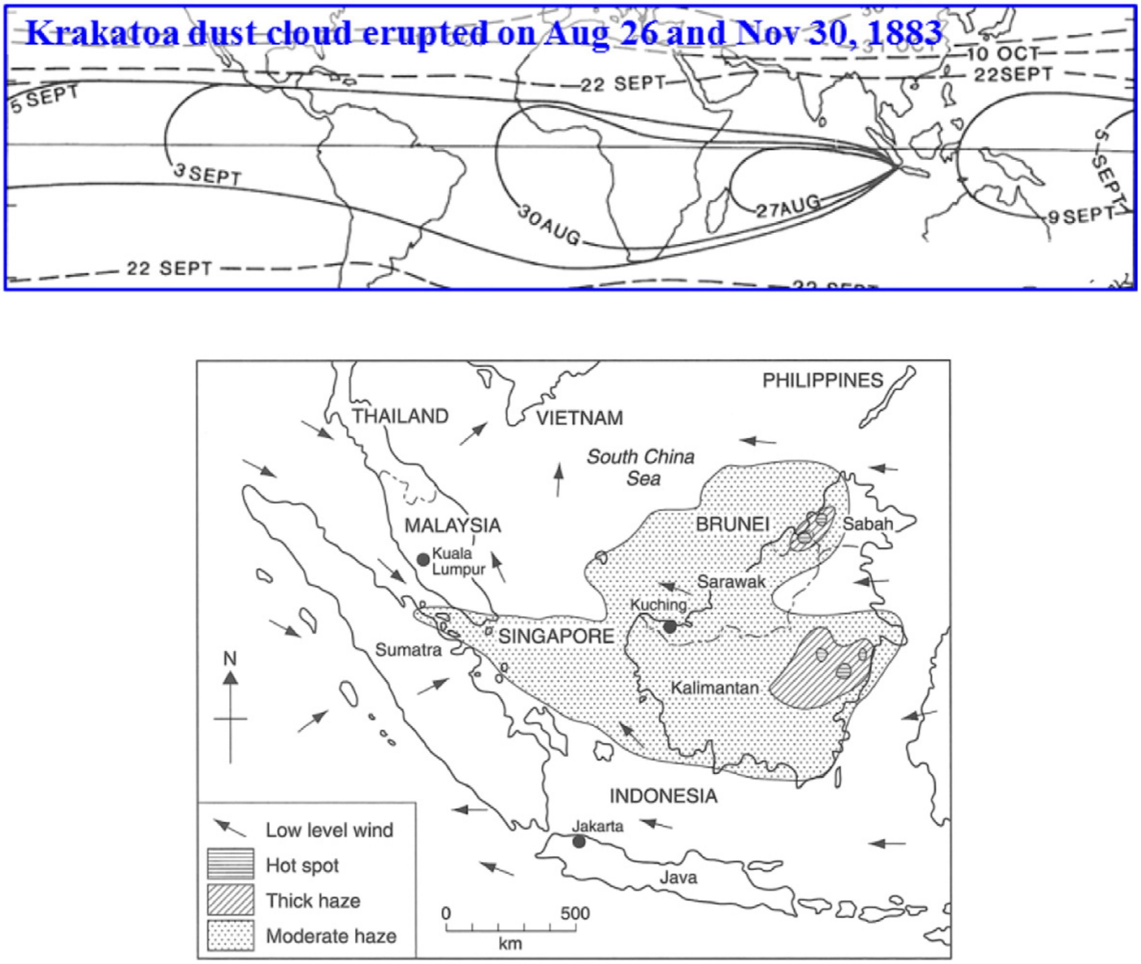

Fig. 17. Material transports from the IMC: (upper panel) mainly stratospheric volcanic material spread after the Krakatoa eruption on 26 August 1888, from Fig. 2. 12 of Barry and Chorley (2003); (lower panel) mainly lower-tropospheric forest-fire smog in the developing stage of 1997/98 El Niño, from Window 2.5 of Goudie (2001).

Some (non-divergent barotropic Rossby) wave modes generated from temperature anomalies due to ENSO/IOD near the IMC may propagate beyond the equatorial region (1) and cause abnormal weathers in middle and high latitudes (Fig. 15). Other (equatorial Kelvin, mixed Rossby-gravity, and inertia-gravity) waves (see, e.g., Tsuda et al., 1994a, 1994b, 1995, 2000; Ogino et al., 1995; Shimizu and Tsuda, 1997, 2001) generated by the most active convective clouds over the IMC (e.g., Xie and Arkin, 1997; also see global climatological overviews by Hartmann, 1994; Wallace and Hobbs, 2006; IPCC, 2007) may propagate vertically (Fig. 16) and contribute to the middle and upper atmospheric circulations such as stratospheric quasi-biennial oscillation (as shown in upper panel of Fig. 2). The IMC concerned also an earliest estimation of the equivalent depth h, which appeared in (1) and is an important parameter also for wave propagations, was carried out in 1930s by using Krakatau[8] (Krakatoa) eruption in 1883 (Fig. 17). Such Indonesian volcano eruptions often caused remarkable parasol effect and global cooling. A larger case was the 1815 eruption of Mt. Tambora of Sumbawa, Nusa Tenggara (see a very recent review by Brönnimann et al., 2015), although observations were limited two centuries ago. The largest was at Sumatera 74,000 years ago, making the world's largest caldera lake Toba (Ambrose, 1998; Robock et al., 2009). Although detailed discussions on these effects on global climate are out of the scope of this article, recent observational evidence (such as importance of local diurnal cycles to be mentioned later) must be considered to estimate climatic impacts of such volcanic eruptions.

4. Archipelago effects: Diurnal cycles

The IMC is inside the equatorial deformation radius (1) in latitude, and its land–sea ratio is close to that of the whole Earth. However, because the IMC is not a continent but an archipelago, many narrow straits are produced between very long coastlines surrounding large/small islands, through which a part of the Pacific water is escaped to the Indian Ocean (see, e.g., Wyrtki, 1987; Gordon, 2005). The northeastern-central (Philippine, Sulawesi, and Banda) seas are deeper than the western (Natuna and Jawa) and southeastern (Arafura and Coral) seas, and sea water flow these deeper seas (Makassar and Lombok Straits). This so-called Indonesian throughflow (ITF) is interacted with situations of the two oceans and prevailing atmospheric conditions (winds and rainfalls), i.e., Pacific decadal oscillation, ENSO/IOD, monsoons, MJOs/ISVs, and the global climate (e.g., Lukas et al., 1996; Sprintall et al., 2014; Hu et al., 2015). By recent Japan–Indonesia collaborations projects (see Section 6) detailed variability of inland seas and coastal oceans has been clarified (e.g., Kashino et al., 2009, 2011, 2013; Horii et al., 2009, 2011, 2012, 2013; Iskandar et al., 2009, 2010; Hasegawa et al., 2009, 2010a, 2010b, 2013; Syamsudin et al., 2010; Syamsudin and Kaneko, 2013; Ueki et al., 2010; Ueki, 2011).

[8] The worldwide popular name Krakatoa is considered due to misspelling of the locally correct name Krakatau by journalism (see pp.27–28, 177–179, 182–184, 23–239 of Winchester, 2003).

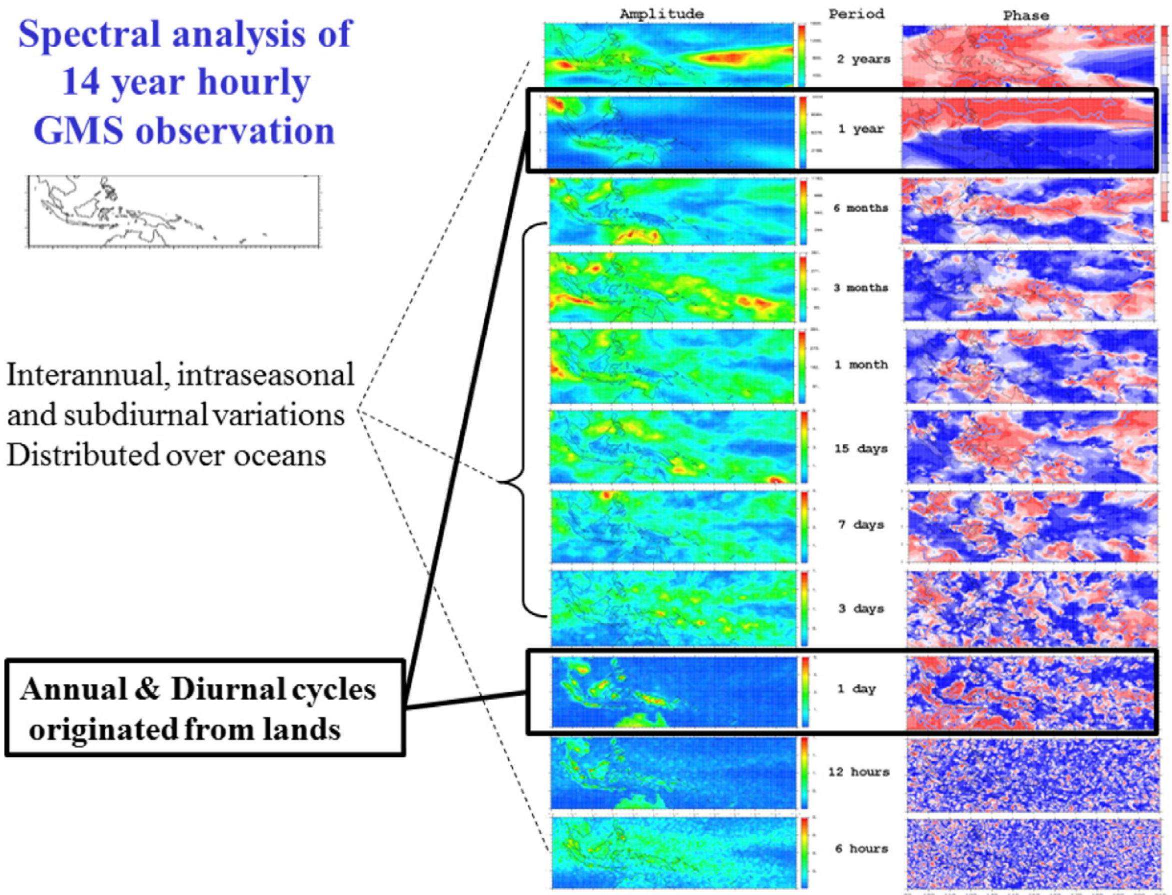

Fig. 18. Geographical distributions of power spectral densities (left) and phases (right) of 6 h to 2-year components analyzed from 14-year hourly GMS-IR cloud top temperature data.

Each island in the IMC has a coastline with land–sea heat capacity contrast, along which the diurnal-cycle dominant solar heating (Fig. 8) induces convective activity with diurnal cycles in the almost cyclone-free equatorial atmosphere (see, e.g., Johnson, 2011). Steep slopes of many volcanoes over 2000 m near coastlines amplify the sea–land diurnal cycles, and on the southern side of Papua, diurnal cycles are more dominant along the baseline of mountains (5000 m at highest) than the coastline facing very shallow Torres Strait between Arafura and Coral Seas. The horizontal scale of an island (or a peninsula) larger than a few kilometers is appropriate to generate internal gravity wave modes, which are called sea–land breeze circulations reversed with diurnal cycle. Because the atmosphere over the IMC is quite humid, i.e., conditionally unstable, convective clouds may be generated in particular in the afternoon until evening. Therefore, diurnal-cycle rainfalls are dominant along the coastlines of the IMC as shown in Figs. 18 and 19 (Houze et al., 1981; Hendon and Woodberry, 1993; Nitta and Sekine, 1994; Hashiguchi et al., 1995a, 1995b; Sugimoto et al., 2000; Yang and Slingo, 2001; Ohsawa et al., 2001; Kubota and Nitta, 2001; Renggono et al., 2001; Hadi et al., 2002; Murata et al., 2002; Wu et al., 2003; Mori et al., 2004; Sakurai et al., 2005; Araki et al., 2006; Tabata et al., 2011b; and many othres). Microphysical features such as raindrop size distributions have also been observed (Renggono et al., 2001, 2006; Kozu et al., 2006).

The diurnal cycles over the IMC near the equator are dominant even in the rainy season (austral summer in Jawa and Bali) because rainfall-induced sprinkler-like land cooling reverses the trans-coastal temperature gradient before sunrise (Fig. 20, right), and subsequent clear sky on land until around noon provides solar heating dependent on season (Wu et al., 2008a). In the western coast of Sumatera as one of the most striking places of the diurnal cycle (Mori et al., 2004), a convective rainfall peak appears near the coastline in the daytime and migrates toward inland until the evening (see Figs. 21 and 22). Another equally convective-stratiform rainfall peak starts from the coastline and migrates offshore until the morning. Each rainfall peak migration has a distance up to 400 km and a speed around 10 m/s. These features may be simulated by (both regional and global) numerical models with resolution sufficiently higher than 100 km (Saito et al., 2001; Wu et al., 2003; Sasaki et al., 2004; Arakawa and Kitoh, 2005; Hara et al., 2009; T. Sato et al., 2009) (see Figs. 20 and 22), and they are quite different from extratropical sea–land breeze circulations dominant only in clear days with infrared cooling in nighttime. The diurnal cycles are almost unique causes of surface winds stronger than 10 m/s (see Fig. 23) in the IMC almost free from cyclones (except for a rare case as in Fig. 7). Although a local wind called “Sumatras” has been known (e.g., Scott, 1956; Nieuwolt, 1968; Chen et al., 2014), probably partially due to steep mountains (up to 3800 m), strong winds appear near active convective clouds usually in local evening with diurnal cycle. Seasonal and meridional variations of the diurnal cycle in Sumatera associated with the ITCZ displacement have been analyzed (Sakurai et al., 2005).

As shown in Fig. 24 very clearly, the most dominant mode is changed beyond the coastline from oceanic ISVs to diurnal cycle on land. Theoretically, the horizontal scale λ_d of the diurnal-cycle sea–land breeze circulation in the low latitudes may be given essentially by the dispersion relation of internal gravity waves (e.g., Rotunno, 1983; Niino, 1987):

$$\lambda_d = 1 \text{ day} \times \sqrt{gh'} \approx 100 - 300 \text{ km}, \qquad (2)$$

where the phase speed $\sqrt{gh'} \approx 5 - 10$ km/h $\approx$ 1-3 m/s, which is one order slower than that for the large-scale equatorial waves (1).

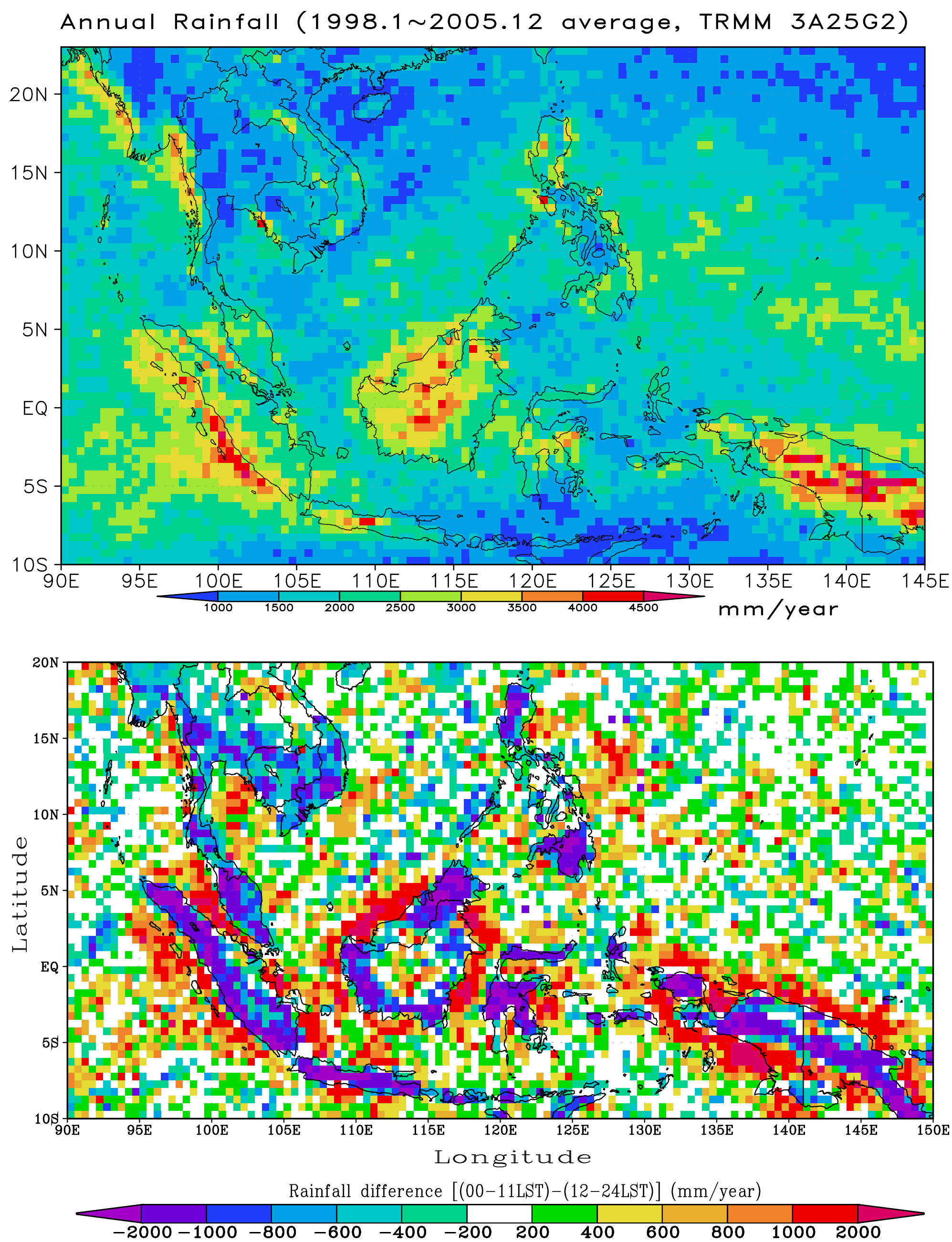

Fig. 19. Geographical distributions of annual rainfall amounts (upper) and AM-PM differences (lower) of 3-year TRMM-PR rainfall data over Indonesia maritime continent (Mori et al., 2004).

Observed values of λ_d in the IMC are 100 km or more (Wu et al., 2003, 2008a, 2009b; Mori et al., 2004; see Figs. 19–22), and the rainfall is concentrated in a distance within about 300 km (both on the land and sea sides) from the coastline (Ogino et al., 2016; see the middle panel of Fig. 26 later). Thus, the land with clear diurnal cycle must be larger than 100 km, which has been suggested by earlier studies (e.g., Kubota and Nitta, 2001). In case of adjacent small and large islands (the former located inside the coastal area of the latter), the smaller one (such as Siberut in the west of Sumatera, and Biak in the northwest of Papua as shown in the right of Fig. 25), a little complex feature appears due to the diurnal cycles of the both islands (Wu et al., 2008b; Tabata et al., 2011b; Kamimera et al., 2012). In narrow straits such as Melaka (Malacca; between Sumatera and Malay) and Makassar (between Kalimantan and Sulawesi), the diurnal cycles of the both islands are interfered and sometimes seem to propagate from one island to the other (e.g., Ichikawa and Yasunari, 2007; Wu et al., 2009a; Fujita et al., 2011). They correspond to the confluence of wind known in particular in the Melaka Strait (e.g., Ramage, 1971; Fujita et al., 2010).

The diurnal cycles over the IMC are excited by solar radiation every day and developed almost spontaneously by processes mentioned above. Therefore, as well as their amplifications at maxima (two times a year) of solar heating and moisture transport by monsoon and or ISVs, any suppression processes may induce their temporal/spatial variability. Larger scale may concern such amplification and suppression, as considered since earlier studies around the IMC (e.g., Houze et al., 1981; Johnson and Priegnitz, 1981; Johnson and Kriete, 1982) (also see next section). Western coast predominance in comparison to

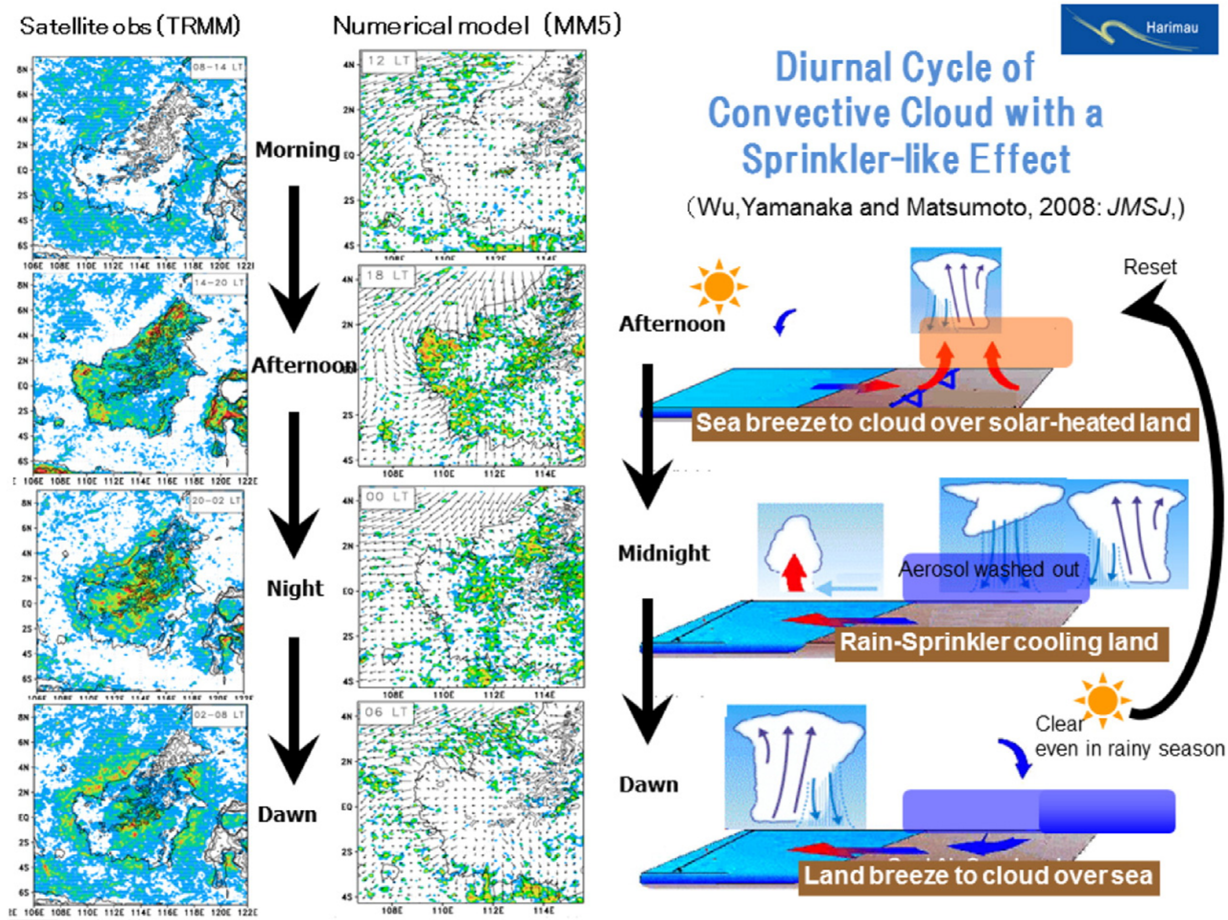

Fig. 20. TRMM-observed rainfall (left) and MM5-simulated wind and rainfall (middle) over Kalimantan Island. A schematic model (right) for the diurnal cycle (Wu et al., 2008a, 2009a) is also shown.

eastern coast (in Sumatera and Kalimantan, as well as Malay, Indochina Peninsula, and Indian Subcontinent) has been reported (cf. Figs. 20 and 21) and discussed in view of prevailing winds and/or gravity-wave propagations to enhance a circulation cell on the western side and suppress the other one on the eastern side (e.g., Murata et al., 2002; Mori et al., 2004; Xie et al., 2006; Wu et al., 2009a, 2009b).

Horizontally quasi-continuous observations of rainfall over tropics including the IMC could not be achieved, until the TRMM space-borne precipitation radar was launched in November 1997 (see, e.g., Hirose and Nakamura, 2004). We (Mori et al., 2004, 2011; Wu et al., 2008a, 2009b) have analyzed the TRMM data over the IMC and noticed that the diurnal-cycle rainfall is heavier on the sea side (called coastal heavy rainband, or CHeR) than on the land side. Prior to them, several observational (e.g., Chang et al., 2004a) and numerical (e.g., Ogura and Yoshizaki, 1988) studies noticed substantially similar phenomena of convective activities and considered mainly orography (mountain range) effects on monsoons. After starting TRMM, other studies for various areas in tropics (e.g., Xie et al., 2006) also noticed what we call CHeR and studied mainly the orographic effect. Finally, we (Ogino et al., 2016) show very recently that tropical rainfall may be approximately expressed in general by a function of the coastal distance with dominance on the sea side. Mechanisms generating the sea-side dominance have been shown numerically (Wu et al., 2008a, 2009b) by nocturnal outflow (land breeze) and seaward migration of land clouds.

In summary, the diurnal cycles over the IMC have north–south hemispheric/seasonal differences and other localities probably dependent mainly on coastline/mountain range and larger-scale wind directions, in addition on SST and land surface features (forest, ground, or city etc.). Further observations are necessary to clarify details on locality, seasonality, and interannual variability of the diurnal cycles over the IMC and their elegant explanations.

The dominance of diurnal cycles suggests that the hydrologic cycle is very quick over the IMC (as shown in the top panel of Fig. 26). It has been observed and understood well (since Wu et al., 2003; Mori et al., 2004) that rainfall comparable to the annual amount (both on the sea and land sides of the coastlines) and water vapor transport by sea winds are clearly following the diurnal cycle. A recent study (Sulistyowati et al., 2014) has shown a diurnal cycle of river water level, that is, water transport from land to sea, which must be balanced with sea–wind water vapor transport, if the water budget is closed in a river basin, a coastal sea just outside the river mouth and the atmosphere over them. This hypothesis is not so bad because all of river flow, sea–land breeze circulation, and raincloud migration are approximately perpendicular to the coastline, and also because the water is conserved by so-called cold trap mechanism at the top of tall convective clouds near the very low-temperature tropopause (often around −80 °C or cooler; see e.g., Holton et al., 1995) which also follow the diurnal cycle. Although quantitative evidence has not yet been sufficient, if the evaporation from sea surface and evapotranspiration from land surface also follow the diurnal cycle, this hypothesis should hold. By this very quick water cycle over the IMC, the water is almost conserved, whereas the (sensible and latent) heat transport from the earth's surface to the whole troposphere is effective enough to satisfy the global energy budget.

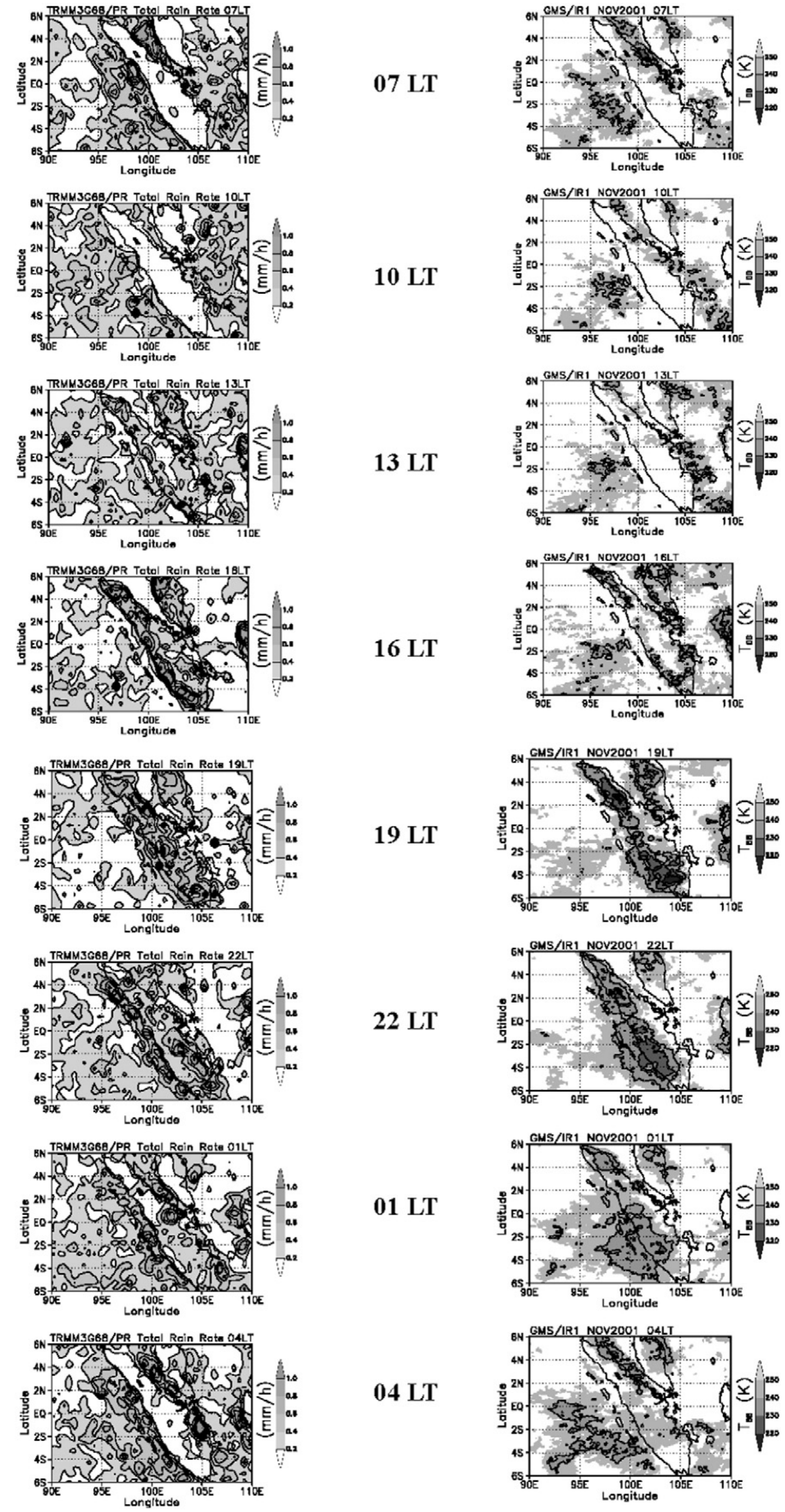

Fig. 21. Diurnal cycles of TRMM rainfall averaged for 1998–2000 and GMS cloud top temperature averaged for November 2001. Modified from Mori et al. (2004). For GMS data, also see Sakurai et al. (2005). Both rain and cloud and also both polar-orbit and geostationary observations show clear diurnal cycles.

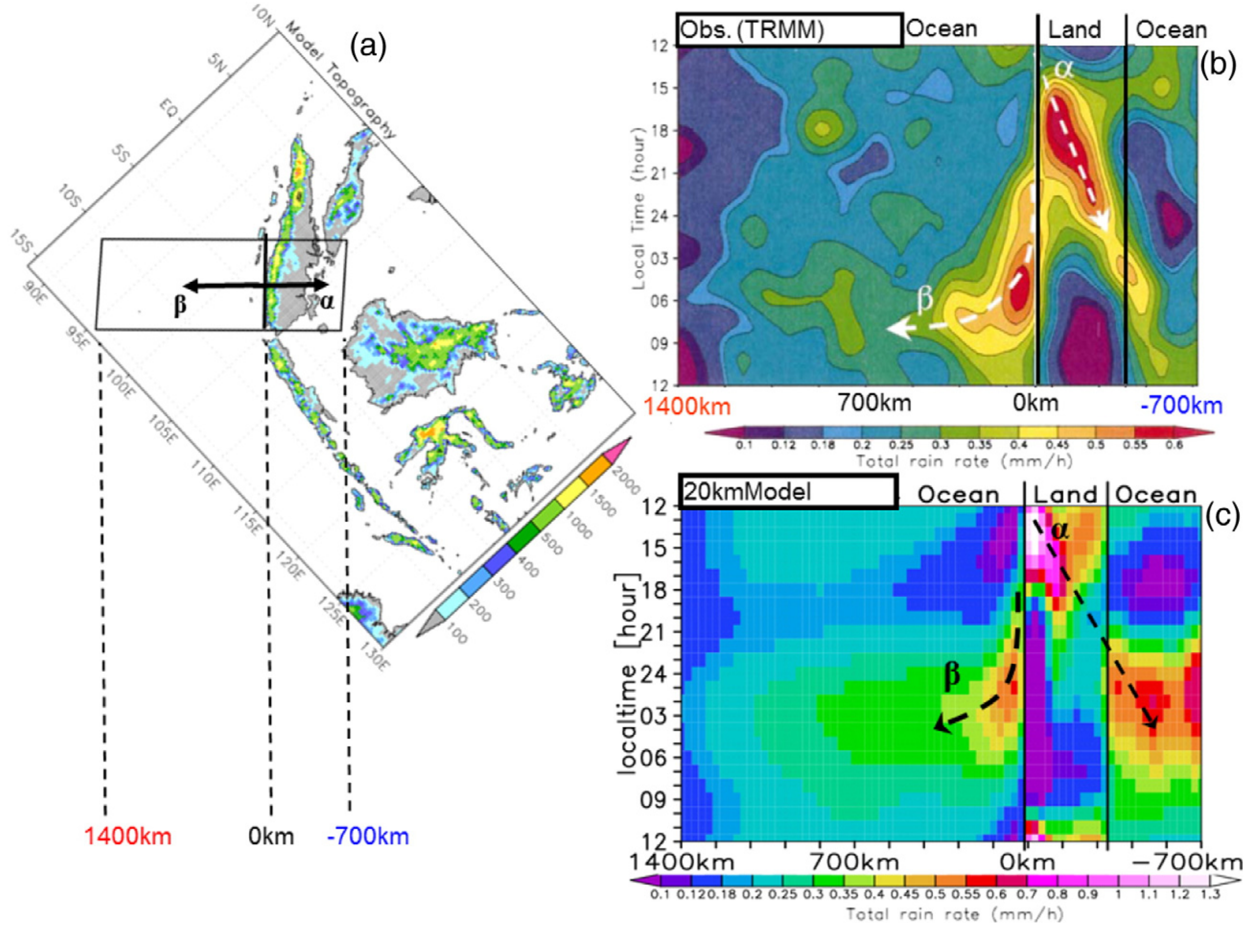

Fig. 22. Hovmöller diagrams along the direction shown in (a), concerning diurnal-cycle migrations of rainfalls (b) observed by TRMM as shown already in Fig. 21 (Mori et al., 2004) and (c) analyzed from numerical simulations by a global high-resolution numerical model (Arakawa and Kitoh, 2005).

5. Large-scale effects of local diurnal cycle over the IMC

The smaller-scale diurnal cycle rainfalls may be modified by larger-scale ISVs (Hashiguchi et al., 1995a, 1995b; Widiyatmi et al., 1999, 2001; Murata et al., 2002, 2006; Shibagaki et al., 2006a, 2006b; Rauniyar and Walsh, 2011; Kanamori et al., 2013; Peatman et al., 2014), seasonal cycle/monsoons (Hashiguchi et al., 1995a, 1995b; Renggono et al., 2001; Hamada et al., 2002; Okamoto et al., 2003; Sakurai et al., 2005; Xie et al., 2006; Araki et al., 2006; Koseki et al., 2013) and ENSO and/or IOD (Hamada et al., 2002; Sakurai et al., 2005; Hashiguchi et al., 2006; Qian et al., 2013; Rauniyar and Walsh, 2013). On the other hand, locally roughly closed water cycle and a little opened energy release over the IMC mentioned in the last paragraph of the previous section are consistent with most of ISVs (super cloud clusters) decaying/modifying after landing the IMC (found since Nitta et al., 1992).[9] Cloud systems involved/maintained in an ISV migrating eastward over the Indian Ocean are decayed by almost complete consumption of water for rainfall in the local evening followed by clear atmosphere in the local morning. In this process, the local rainfall keeps the diurnal cycle but its amount may be affected by moisture, stratification stability, and wind field associated with the ISV. Therefore, the diurnal cycle may be amplified by ISVs and, in longer time scale, by the annual cycle of the ITCZ (Figs. 27-29). Mori et al. (2004); Wu et al. (2009b) and Ogino et al. (2016) have demonstrated the sea-side dominance of diurnal-cycle rainfall as CHeR (see Section 4), which is consistent with other evidence by Hidayat and Kizu (2009) that the ISV-correlated rainfall is also heavier than on the sea side.

Concerning interannual variations of rainfall correlated strongly (at least partly) with ENSO/IOD (Section 2), we may consider also the variations of SST. Because the sea–land breeze circulations are directly enforced by the land–sea temperature difference (e.g., Estoque, 1962; Rotunno, 1983; Niino, 1987), cooler SST in El Niño and/or positive dipole mode may induce weaker land breeze and suppress sea-side rainfall in the early morning than in La Niña and/or negative dipole mode. Complex topography of coastlines, land surfaces, and ocean bottoms may induce highly inhomogeneous regionality of correlations between atmosphere and ocean interacting each other. Serious flood events were caused by the diurnal cycles amplified by La Niña/negative IOD, transequatorial boreal winter monsoons (cold surges from Siberia), and ISVs (Wu et al., 2007, 2013; Figs. 28 and 29), although the general relationship among the diurnal cycle, ISV, monsoon, and ENSO/IOD is still a target for future studies.

It is the diurnal-cycle rainfalls along the world's longest coastlines associated with many large islands of the IMC that generate the equatorial rainfall peak controlling the global climate (see Fig. 30). The rainfall concentration is about 2000 mm/year for a “coastline density” 10^{-2} km^{-1} (corresponding to 10^2 km coastline around 10^4 km^2 area), which is consistent with the coastal peak 1300 mm/year in Fig. 26(b)

[9] A rare ISV travelling through the equatorial circumference has been reported by Takayabu et al. (1999).

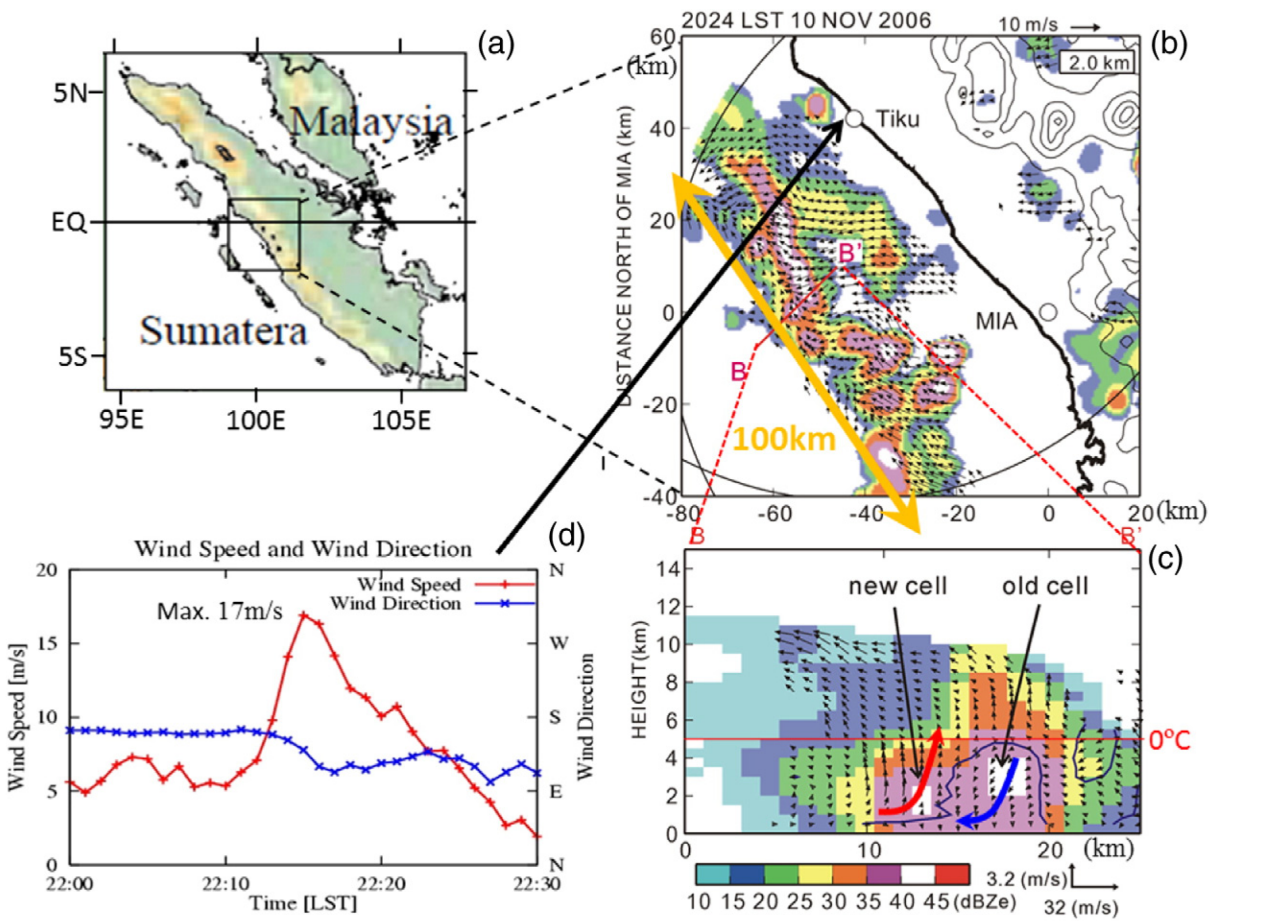

Fig. 23. Observations of development of a convective cloud system at the western coast of Sumatera shown in (a). (b) Horizontal and (c) vertical displays of rainfalls (contours) and winds (arrows) observed with dual X-band Doppler radars installed at Tiku and MIA indicated in (b) (Sakurai et al., 2009, 2011), and (d) strong gust observed with surface anemometer (Kawashima et al., 2006, 2011).

and also with the equatorial rainfall peak 2000 mm/year in Fig. 16(b), considering that the total tropical coastline length (almost in the IMC) is almost equivalent to the equatorial circumference (40,000 km). Although it has been explained often directly by the warmest seawater surrounding the IMC, rainfall over the open ocean is less than over the islands in the IMC (cf. Qian, 2008). Indeed, the solid land is heated easier than the liquid sea, but convective precipitating clouds generated over the true continents (Africa and South America) are less active than over the IMC as seen in Fig. 16(e) obtained from IPCC (2007) for example. Instead, the diurnal cycles generated around the longest coastlines of the IMC are essential to generate the largest rainfall there. For each heavy rainfall condition produced by large-scale phenomena such as ENSO/IOD, monsoon surges or ISVs (Section 3), only some areas have actual heavy rainfall (Wu et al., 2007, 2013), but an integration over the long coastlines may achieve the world's largest annual rainfall amount over the IMC.[10] The concentration of rainfall has been shown as a function of the coastal distance in Fig. 27 (b). Another empirical formula between mean regional annual rainfall and coastline length divided by land area is obtained (as shown in the right panel of Fig. 30), which seems satisfied by several equatorial regions over the world.

These relationships indicating importance of the local diurnal cycles imply that a climate model needs to resolve the equatorial coastlines with a scale sufficiently smaller than 100 km. Actually, recent global models have satisfied such high resolutions (e.g., Neale and Slingo, 2003; Arakawa and Kitoh, 2005; Hara et al., 2009; Satoh et al., 2008; T. Sato et al., 2009; Love et al., 2011). Their downscaling and regional model applications are also progressed for usual diurnal cycles (Wu et al., 2003, 2008a, 2009a, 2009b) and extreme rainfalls making floods (Trilaksono et al., 2011, 2012).

Because the sea–land circulation is a horizontal convection, that is a superimposition of upward and downward propagating internal gravity waves, they may be modified if the background wind is changed. Actually, the amplitude distributions of gravity waves in the lower stratosphere resemble those of convective activity and their cause (solar radiation) as so far shown in Fig. 16. Local instability and turbulence generation has been also observed at the cloud top (e.g., Mega et al., 2010, 2012). The spectral features of cloud top temperature (corresponding to height of cloud convection) (Fig. 31) are also similar to so-called universal shapes of gravity waves (e.g., Gage and Nastrom, 1985; Nastrom and Gage, 1985; Hashiguchi et al., 1997). Generations of gravity waves from cloud systems actually observed over the IMC and their emissions to the whole middle atmosphere have been simulated by numerical models (e.g., Horinouchi and Yoden, 1996; Horinouchi et al., 2002, 2003). Momentum flux of such gravity waves have been requested to simulate the stratospheric dynamics such as equatorial quasi-biennial oscillations (Sato et al., 1999; Kawatani et al., 2010a, 2010b), which implies also a link between climates in the

[10] Recent high-resolution numerical simulations (e.g., Takasuka et al., 2015) look to support this.

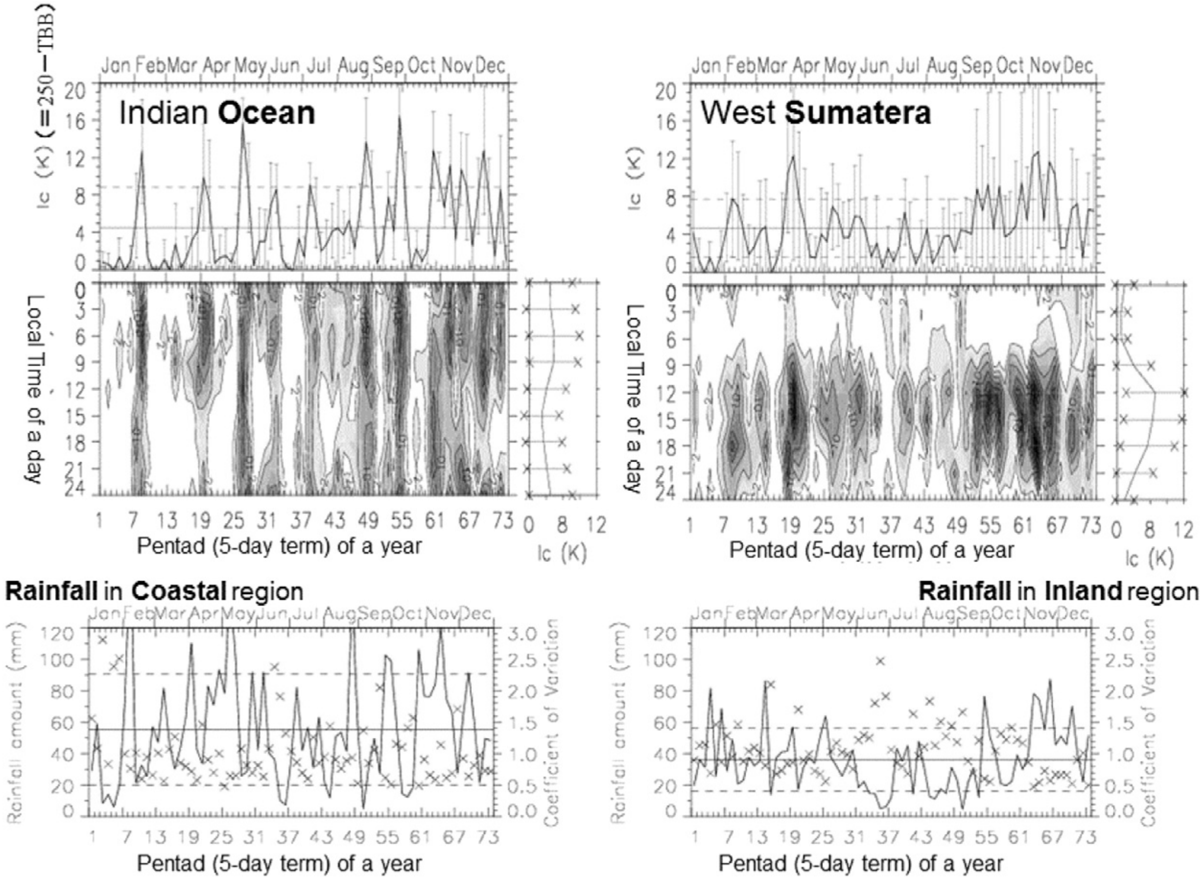

Fig. 24. Seasonal variations of pentad-mean (top) and seasonal-local time plots (middle) of pentad-mean cloud top temperature, compared with pentad-mean rainfall amounts (bottom), on the Indian Ocean (left) and inland (right) sides of the western coast of Sumatera Island. (Hamada et al., 2008).

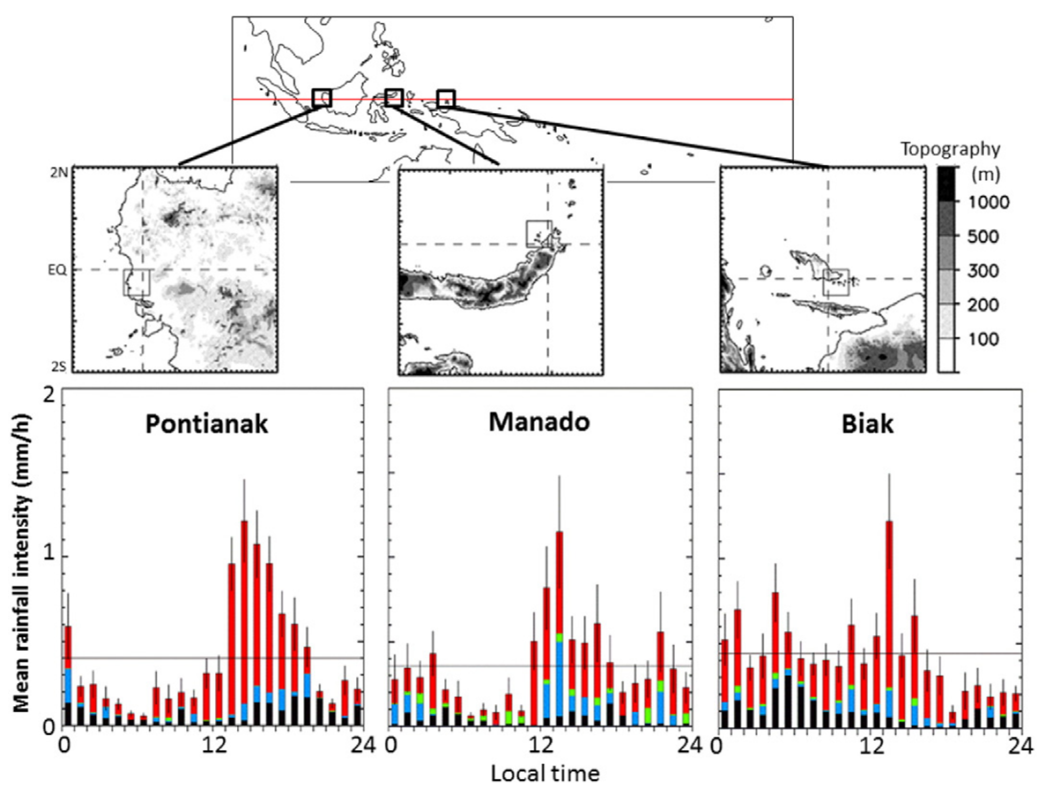

Fig. 25. Diurnal cycles of rainfall intensity observed by wind profilers at Pontianak (Kalimantan), Manado (Sulawesi), and Biak (near Papua) (Tabata et al., 2011b). Rainfall is classified as stratiform (black), mixed stratiform/convective (blue), shallow convective (green), and deep convective (red) types.

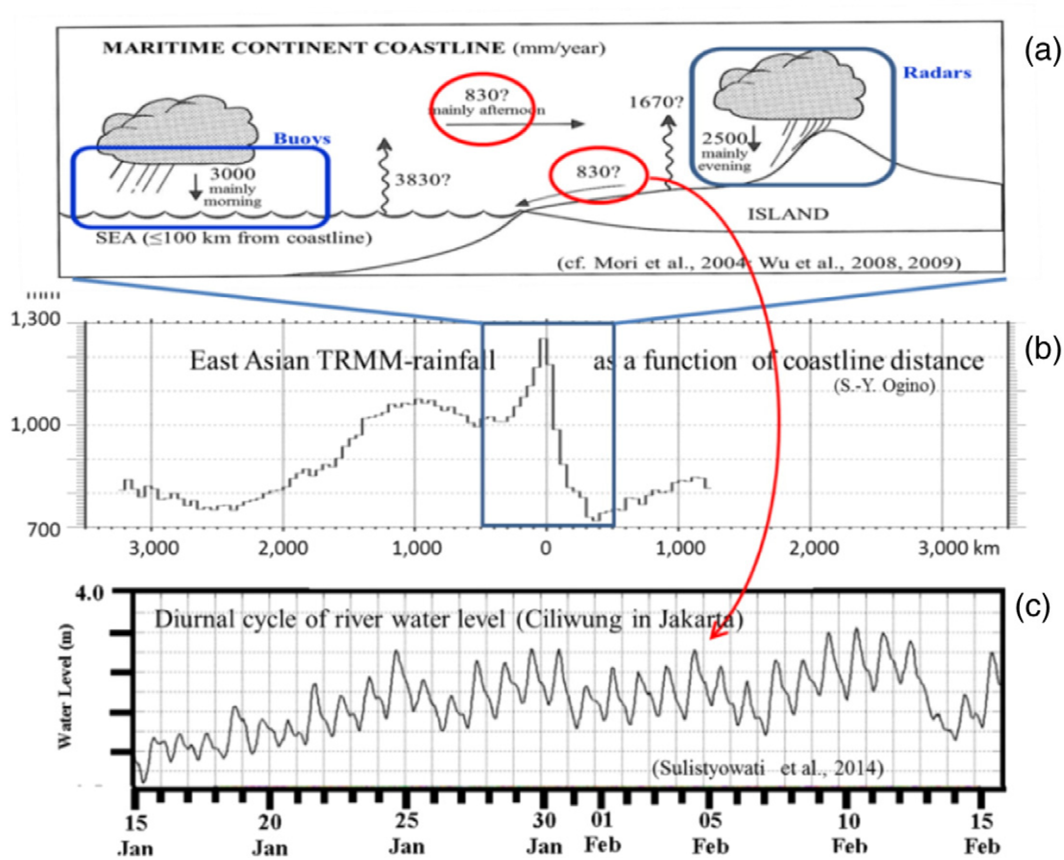

Fig. 26. (a) Schematic hydrologic cycle near the coastline of the IMC, (b) rainfall as a function of distance from the coastline over tropical Asia observed by TRMM (Ogino et al., 2016), and (c) diurnal cycle observed at a river in west Jawa (Sulistyowati et al., 2014).

troposphere and stratosphere (e.g., Kawatani and Hamilton, 2013). Furthermore, the global–vertical structures of diurnal tides are also studied, in particular on their excitation/amplification in the tropics (e.g., Sakazaki et al., 2012).

Another process linking atmosphere vertically may be electricity including thunderstorms. Concerning lightning, Hidayat and Ishii (1998) analyzed seasonal and diurnal variations around Jawa, Hamid et al. (2001) showed ENSO impacts over the IMC, Kodama et al. (2006) showed lightening activation due to stronger convective instability in dry (El Niño) phase, and Virts et al. (2013a, 2013b) studied MJO and diurnal cycles based on a global network. They are in general consistent with the convective cloud activities described in this article, but more studies are needed for the significance of vertical (atmosphere–ionosphere) coupling and for a practical application to warn local torrential rainfall.

Recent global climate change appears also in the IMC. Manton et al. (2001) found that the number of rainy days has generally decreased significantly throughout Southeast Asia during 1961–1998. Hamada et al. (2002) showed that the dominant time scale of interannual variations of rainy season onset in Jawa and Bali during 1961–90 is 2–3 years, which looks somewhat shorter than that during 1910–41. Weakening of monsoonal strength, lengthening of dry season, and decreasing of rainfall are observed in the East Jawa during 1955–2005 (Aldrian and Djamil, 2008). Endo et al. (2009) also confirmed the decreasing trend of number of rainy days as a dominant feature during 1950s–2000s over Southeast Asia, although data of the IMC were limited to Malaysian territory. Very recently, Villafuerte and Matsumoto (2015) have examined the long-term changes of extreme rainfall in Southeast Asia including the IMC and their relationship with global temperature and ENSO. Long-term changes of the Hadley and Walker circulations and their effects on the IMC rainfall have been suggested (e.g., Okamoto et al., 2003; Hashiguchi et al., 2006; Nguyen et al., 2013).

More locally, Hamada et al. (2012) suggested that rainfall in the rainy season (November — April) in west Jawa near Jakarta has a decreasing tendency through recent decades with global warming. However, urbanization effects are more serious particularly in the very rapidly developed megacity Jakarta (Fig. 32). Können et al. (1998) pointed out rain day increase during 1950s–90s around Jakarta and considered urbanization as its likely cause. Siswanto et al. (2015) have analyzed the diurnal cycles of temperature in Jakarta historically and showed that the maximum temperature increased 2.5 °C during recent hundred years. The diurnal-cycle convections and rainfalls in this megacity may transport and wash out the anthropogenic gases and aerosols (air pollutant) every day (e.g., Sugimoto et al., 2000). More studies are necessary concerning soil moisture, underground hydrological processes and land-atmosphere humidity exchange to consider effectiveness of convective cloud generation over such city area in the afternoon.

6. Brief retrospect and future strategy

Historical records on monthly (Braak, 1929; Berlage, 1949, 1957; Schmidt and Ferguson, 1951; LMG, 1973a, 1973b; Yasunari, 1981; Eguchi, 1983; Yasunari and Suppiah, 1988; McBride, 1992, 1998; Können et al., 1998; Haylock and McBride, 2001) or daily (Hamada et al., 2002, 2012; Siswanto et al., 2015) rainfalls observed by stations of the operational agency (Meteorological Climatological and

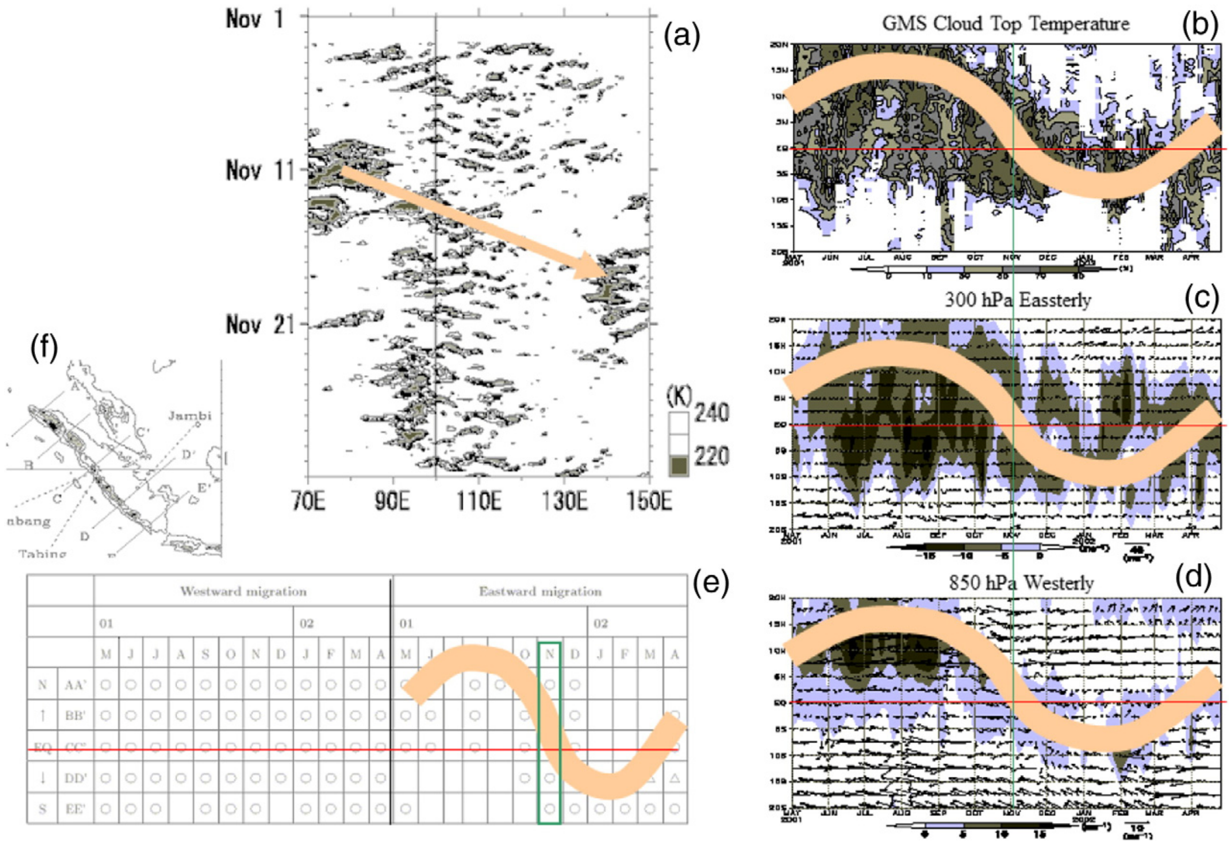

Fig. 27. (a) Hovmöller diagrams of GMS-IR cloud-top black-body temperature along the equator in November 2001; latitude-time cross-sections of (b) occurrence frequency of cloud top temperature between 170 and 270 K, (c) 300- and (d) 850-hPa horizontal wind (arrows: upward is northward, shaded: easterly in (c) and westerly in (d)) along 100°E for May 2001–April 2002; and (e) seasonal variations of westward/eastward migration occurrences along the lines AA′ to EE′ indicated in (f). These results show amplitude variations of the diurnal cycles by ISVs and annual cycle shift of the ITCZ (Sakurai et al., 2005). In (a), the diurnal cycle at the west coast of Sumatera (at 100°E, indicated by a straight line) is seen, even during an ISV passage (a colored arrow). All peaks (indicated by colored curves) of (b) cloud activity (associated with ITCZ over the Indian Ocean), (c) upper-tropospheric easterly, (d) lower-tropospheric westerly (associated with ISVs), and (e) eastward-migrating diurnal-cycle occurrence have similar seasonal variations.

Geophysical Agency, abbreviated as BMKG in Indonesian language),[11] as well as those by other governmental agencies (e.g., Inoue and Nakamura, 1990; Nakamura, 1994; Können et al., 1998), are valuable and important for climatic change analysis. However, to resolve diurnal-cycle local circulations and cloud convections emphasized in the previous section and to provide accurate observations of rainfalls and reliable predictions of floods or droughts for societal request with very rapid development of Indonesia (Wu et al., 2007, 2013; Sulistyowati et al., 2014), high-resolution/broad-band observations/models covering both over islands and seas are necessary. Actually, the objective analysis for the IMC is improved after BMKG rawinsonde launches (at 23 stations as of the end of 2014) have been drastically increased (daily or 12-hourly) in 2006 (Okamoto et al., 2003; Seto et al., 2009).

On the other hand, scientific observation projects for the IMC under Solar-Terrestrial Energy Program (STEP: 1990–97), Tropical Ocean Global Atmosphere-Coupled Ocean Atmosphere Response Experiment (TOGA-COARE: 1992–93), and Coupling Processes in the Equatorial Atmosphere (CPEA: 2001–2007) have been led by Kyoto University of Japan and the Indonesian Institute for Space and Aeronautics (LAPAN), mainly for dynamical processes of vertical (troposphere, stratosphere, mesosphere, and ionosphere) coupling (see, e.g., Tsuda et al., 1995; Hashiguchi et al., 1995b; Widiyatmi et al., 1999, 2001; Fukao, 2006). In particular, VHF (Equatorial Atmosphere Radar, or EAR at Kototabang near Padang) and UHF (boundary layer radar and wind profiler) observations of three-dimensional (3D) wind velocity components with high time and vertical resolution are very important, particularly in the tropics, because geostrophic approximation (the indirect estimation of wind from a pressure field) is not useful and cloud systems with diurnal and shorter scales are dominant. In particular, the vertical velocity variations in clear air or associated with precipitating clouds (Mori et al., 2006; Kozu et al., 2009) are observed by EAR, compared with meteorological radars and raindrop size observation at the bottom (Renggono et al., 2001, 2006; Kozu et al., 2006; Marzuki et al., 2009, 2010, 2012, 2013a, 2013c) and with a millimeter radar and optical observations at the top (Yamamoto et al., 2008, 2009; K. Sato et al., 2009; Mega et al., 2012).

Special radiosonde/rawinsonde/GPSsonde observations (3-hourly at a maximum) have been carried out in some campaign or intense observation periods led by Kyoto University and LAPAN (e.g., Tsuda et al., 1994a, 1994b; Shimizu and Tsuda, 1997, 2001; Bhatnagar et al., 2013), and by Kobe University and Japan Agency for Marine-Earth Science and Technology (JAMSTEC) of Japan and the Agency for the Assessment and Application of Technology (BPPT) of Indonesia (e.g., Murata et al.,

[11] The operational observation history was started at a personal station in Bogor in 1841. After increasing activities and stations, and they were organized as the Magnetic and Meteorological Observatory of Dutch colonial government in 1866. After independence it became a national bureau (JMG) in 1949 (joined WMO in 1950), an institute (LMG) in 1955, again a bureau (JMG) in 1960, a directorate (DMG) in 1965, and a center (PMD) in 1972. In 1980 Meteorological and Geophysical Agency (BMG) was established, and had reinstalled stations including those established by other agencies until it became belonged directly to the Presidential Office in 2002. BMG was expanded in the field of climatology as BMKG in 2008.

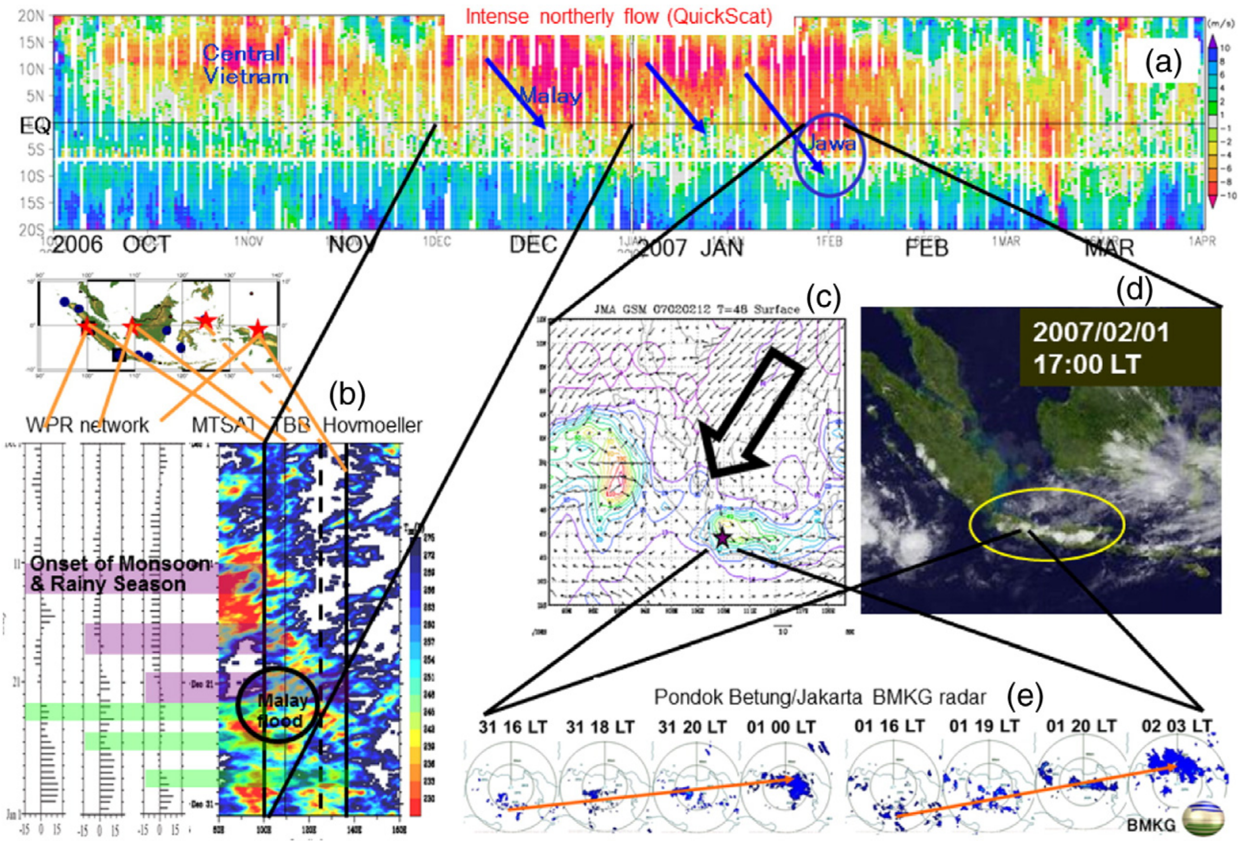

Fig. 28. A heavy rainfall event caused by amplification of diurnal-cycle evening rain (migrating from land to sea in this case) due to La Niña, cold surge, and ISV during 31 January to 2 February 2007 near Jakarta, west Jawa (Wu et al., 2007; Yamanaka et al., 2008). (a) Time-latitude plot of NASA's QuikSCAT sea-surface meridional wind (red: northerly) along 108° in October 2006–March 2007; (b) HARIMAU-profilers' zonal wind variations in 2–3 km altitude and a Hovmöller diagram of GMS-IR cloud-top black-body temperature along the equator in December 2006; (c) JMA-GSM 48-h forecast of surface wind and precipitation at 19 LT 2 Feb 2007; (d) GMS-IR clouds at 17 LT 1 Feb 2007; and (e) BMKG X-band radar PPI images around Jakarta in continuous two nights 31 Jan–1 Feb and 1–2 Feb 2007.

2002; Mori et al., 2004). At some stations (not only in the IMC but also other regions of monsoon Asia), rainwater samples have been obtained and their isotope ratios have been analyzed in order to study their origin (e.g., Ichiyanagi, 2007; Kurita et al., 2009; Fudeyasu et al., 2011; Suwarman et al., 2013). Other observational projects concerning atmospheric constituents, aerosols, and their variability by forest fires (correlated with rainfall, hence also with ENSO/IOD) etc. have been being carried out by various international frameworks (e.g., Nurhayati and Nakajima, 2012; Reid et al., 2013).

Satellite (hourly[12] geostationary, such as GMS/MTSAT series; or spatially high-resolution polar-orbit such as GPS, TRMM/GPM, etc.) observations of both operational and scientific objectives have been also being carried out. Examples of GMS (e.g., Fig. 1 left; also diurnal cycle studies by Sakurai et al., 2005), TRMM (e.g., Mori et al., 2004), and GPS (e.g., Tsuda et al., 2000) observations have been already mentioned in previous sections.

The Hydrometeorological ARray for Isv-Monsoon AUtomonitoring (HARIMAU, meaning tiger in Indonesia–Malay language), a 5-year Japan EOS Promotion Program (JEPP) project contributing to the Global Earth Observation System of Systems (GEOSS), was conducted during August 2005–March 2010, under collaborations by JAMSTEC, Kyoto University, and Hokkaido University of Japan, and the Agency for the Assessment and Application of Technology (BPPT), LAPAN, and BMKG of Indonesia. A radar-profiler network with meteorological Doppler radars (C-band near Jakarta and X-band near Padang; e.g., Kawashima et al., 2006, 2011; Sakurai et al., 2009, 2011; Mori et al., 2011) and wind profilers (Pontianak, Manado, and Biak; Tabata et al., 2011a, 2011b) has been constructed as shown in Fig. 33 (Yamanaka et al., 2008). In parallel, meteorological radars of BMKG have been being replaced from a few stations of classical SHF-band measuring only spatial distributions of raindrops to more than 30 stations of C-band Doppler measuring also radial wind velocity in rainy atmosphere.

Furthermore, over the Indonesian exclusive economic zone (EEZ) surrounding the IMC, independent JAMSTEC-BPPT collaboration projects of installation and maintenance of buoys, as well as research vessel observations, have been continued as a part of the global network of Tropical Ocean Climate Study (TOCS) (Ando et al., 2010). In particular, the Indian Ocean side network was named by Indian holy word, RAMA (Research Moored Array for African–Asian–Australian Monsoon Analysis and Prediction) (McPhaden et al., 2009a, 2009b) and have been operated by another JEPP project between JAMSTEC and BPPT during 2005–10, just in parallel with the HARIMAU project on land. Also, another project called MISMO (Mirai Indian Ocean Cruise for the Study of the MJO-Convection Onset) has also been carried out using radars and radiosondes at a vessel of JAMSTEC and at stations of islands and surrounding countries in 2006 (see Yoneyama et al., 2008).

Following those foregoing successful collaborations, capacity building on radar operations and buoy manufacturing has been promoted during FY2009–13 by another Japan–Indonesia collaboration project funded by the Science and Technology Research Partnership for Sustainable Development (SATREPS) of two Japanese funding agencies (JICA and JST) as an item of the official development assistance (ODA)

[12] Japanese meteorological satellite launched very recently (Himawari-8, October 2014) has much improved horizontal resolution and time interval.

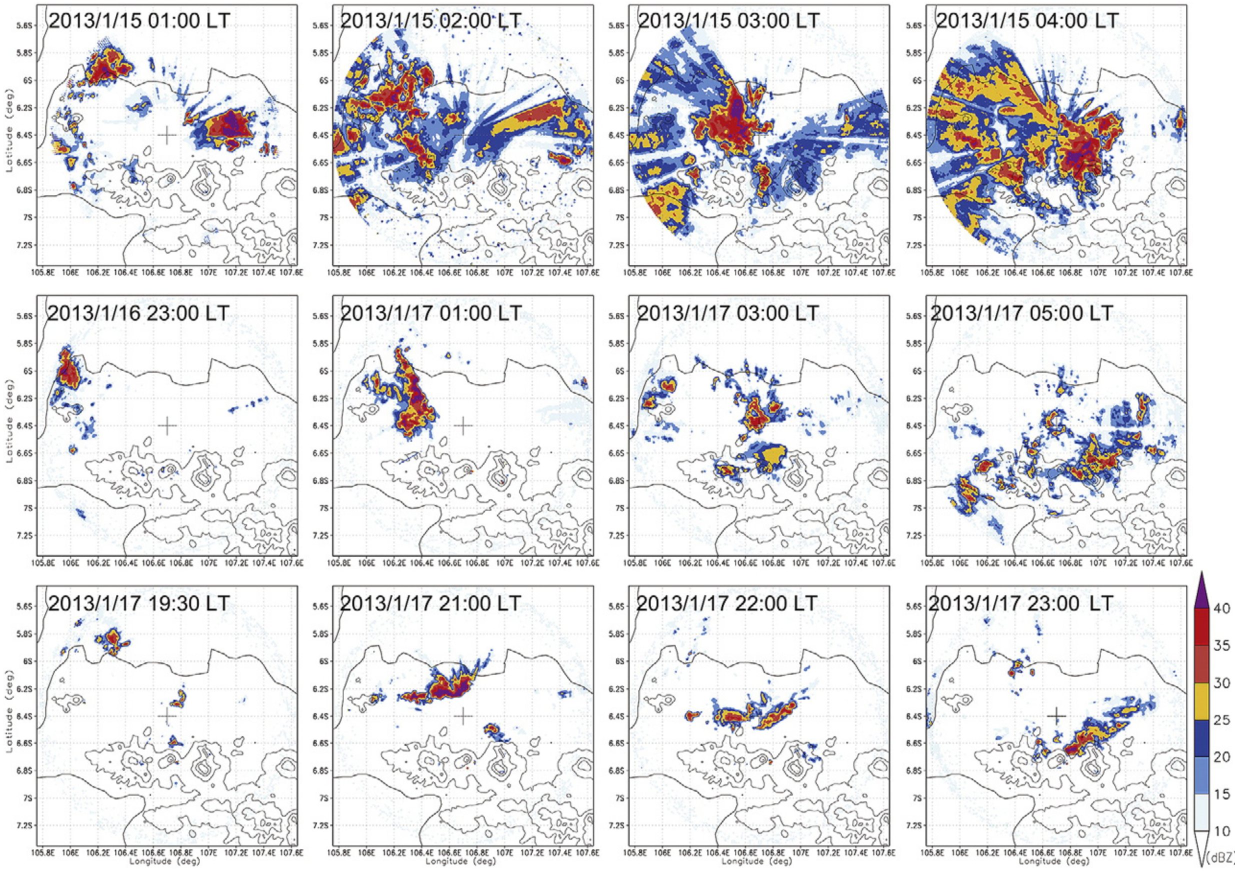

Fig. 29. A heavy rainfall event associated with morning rain (migrating from sea to land) amplified mainly by ISV, partly by cold surge, observed with 2-km altitude CAPPI (constant-altitude plan position indicator) images of the HARIMAU C-band radar at Serpong/Jakarta during 15–17 January 2013 near Jakarta, west Jawa (Wu et al., 2013).

of Japanese government. All the instruments have been taken over by an international center of tropical climatology, meteorology, and oceanography, called "Maritime Continent Center of Excellence" (MCCOE), established under BPPT in November 2013. The building of MCCOE

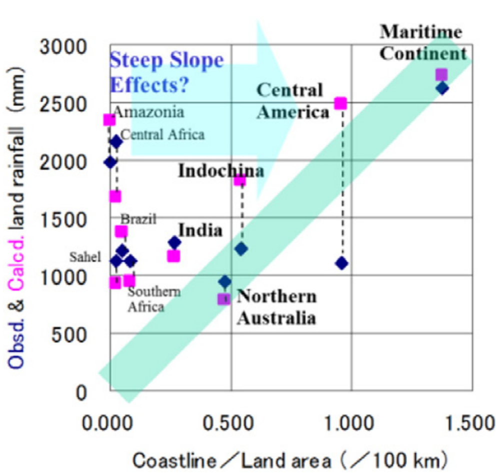

Fig. 30. Relationship between coastline length (divided by land area, in 100 km resolution) and rainfall (right) for low-latitude regions in climate modeling (left top). Results suggest cloud/rainfall distribution around the IMC coastlines almost equivalent to the equatorial circumference.

was constructed near CDR and the buoy factory of BPPT in Serpong (located in the southwestern suburb of Jakarta) completely by the Indonesian budget. The MCCOE has three functions: (i) an observation center maintaining/operating radar (HARIMAU) and buoy (TOCS) networks, (ii) a data center collaborating with BPPT's data integration facility (NEONET), and (iii) a research center promoting advanced studies concerning the climatological sciences of the IMC (as described in the foregoing sections) together with international visitors. A campaign observation (HARIMAU2011) of this project has been collaborated with other projects called CINDY2011 (Cooperative Indian Ocean Experiment on Intraseasonal Variability in the Year 2011; see Yoneyama et al., 2013) and DYNAMO (Dynamics of the MJO; see e.g., Zhang, 2013; Johnson and Ciesielski, 2013).

Those ground-based observations suggest rainfall amount approximately as functions of distance and length of the coastline, which have been confirmed by recent analysis of space-borne observations (e.g., Ogino et al., 2016). Applications of these features for disaster prevention and agriculture are now going on. However, separation between synthesis and variabilities is still under progress, mainly because the increase of facilities is more rapid than the building of capacities. In the next step, more detailed variabilities of the diurnal cycles and their causes should be studied.

For the future, much more multi-lateral observations are now being planned toward so-called the Years of Maritime Continent (YMC) in 2017–19. Historically, this new project is the first true international collaborations based on equal contributions from Asian countries including Indonesia. This is also based on the first true densely organized network both on lands and in the ocean of this region. It is

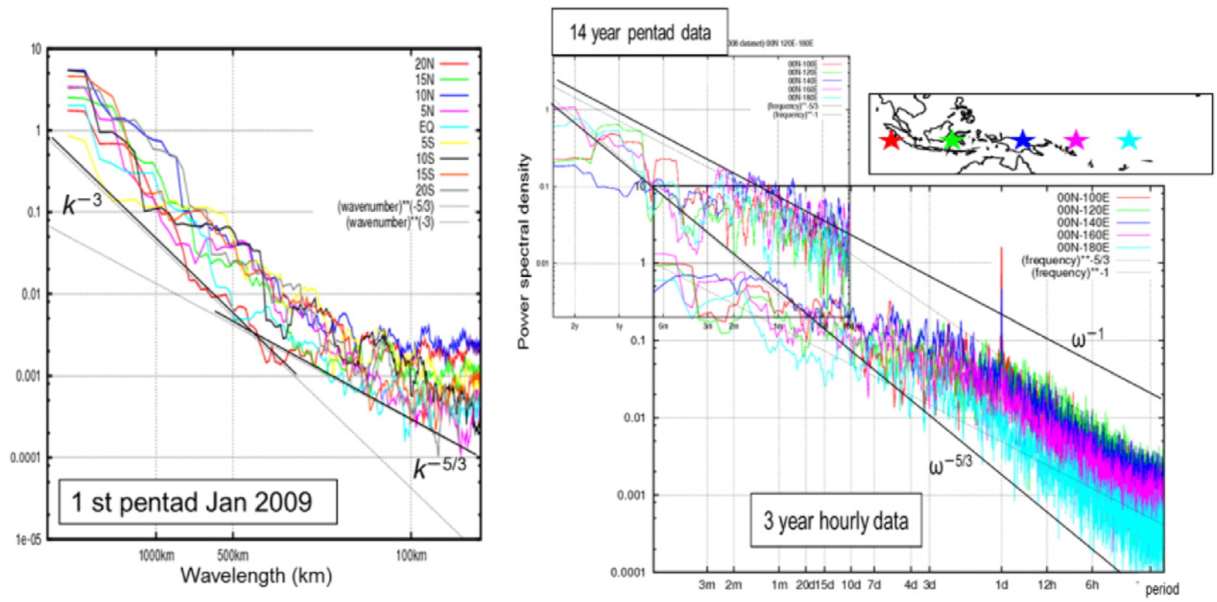

Fig. 31. Examples of zonal wavenumber (left) and frequency (right) spectra analyzed from 14-year hourly GMS-IR cloud top temperature data. The former is calculated for 90°E–150°W longitude range at every 10° latitude around the equator. The latter is for five locations at every 20° longitude in 100–180°E along the equator, based on the same calculations as plotted in Fig. 18.

strongly expected that through this international air–sea–land coupled project, many of the outstanding issues seen in the previous sections of this article are solved and that the results will contribute also to significant breakthrough of the global climate and domestic disaster–environment issues. In conclusion, the IMC is truly a miniature of Earth as so far mentioned at the beginning of the Abstract, not only

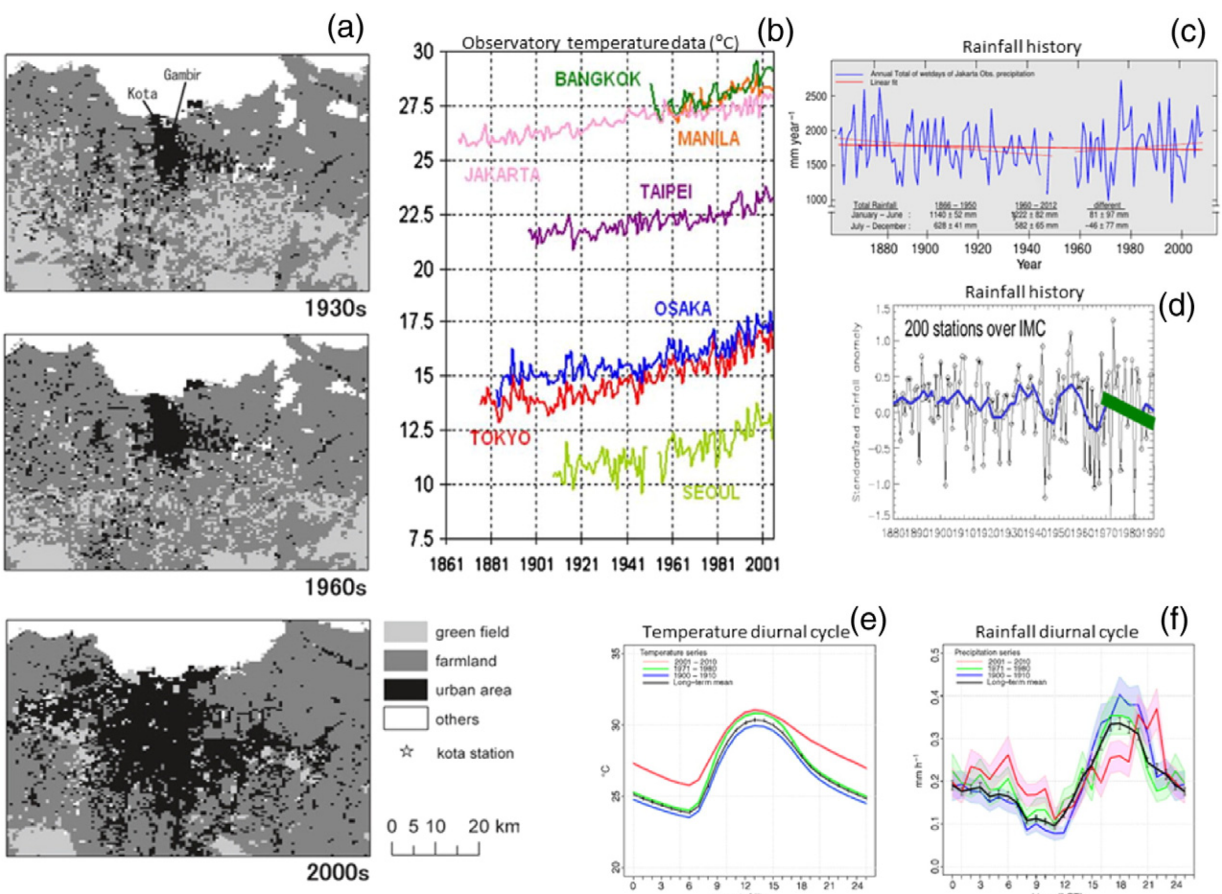

Fig. 32. (a) Urbanization (Yamashita, 2011), historical changes of (b) mean (Kataoka et al., 2009; in comparison with other Asian megacities), (c) annual rainfall (Siswanto et al., 2015) in comparison with (d) all Indonesian 200-station average standardized anomaly (Hamada et al., 2002), and diurnal-cycle (e) temperature and (f) rainfall (Siswanto et al., 2015) at Batavia-Jakarta.

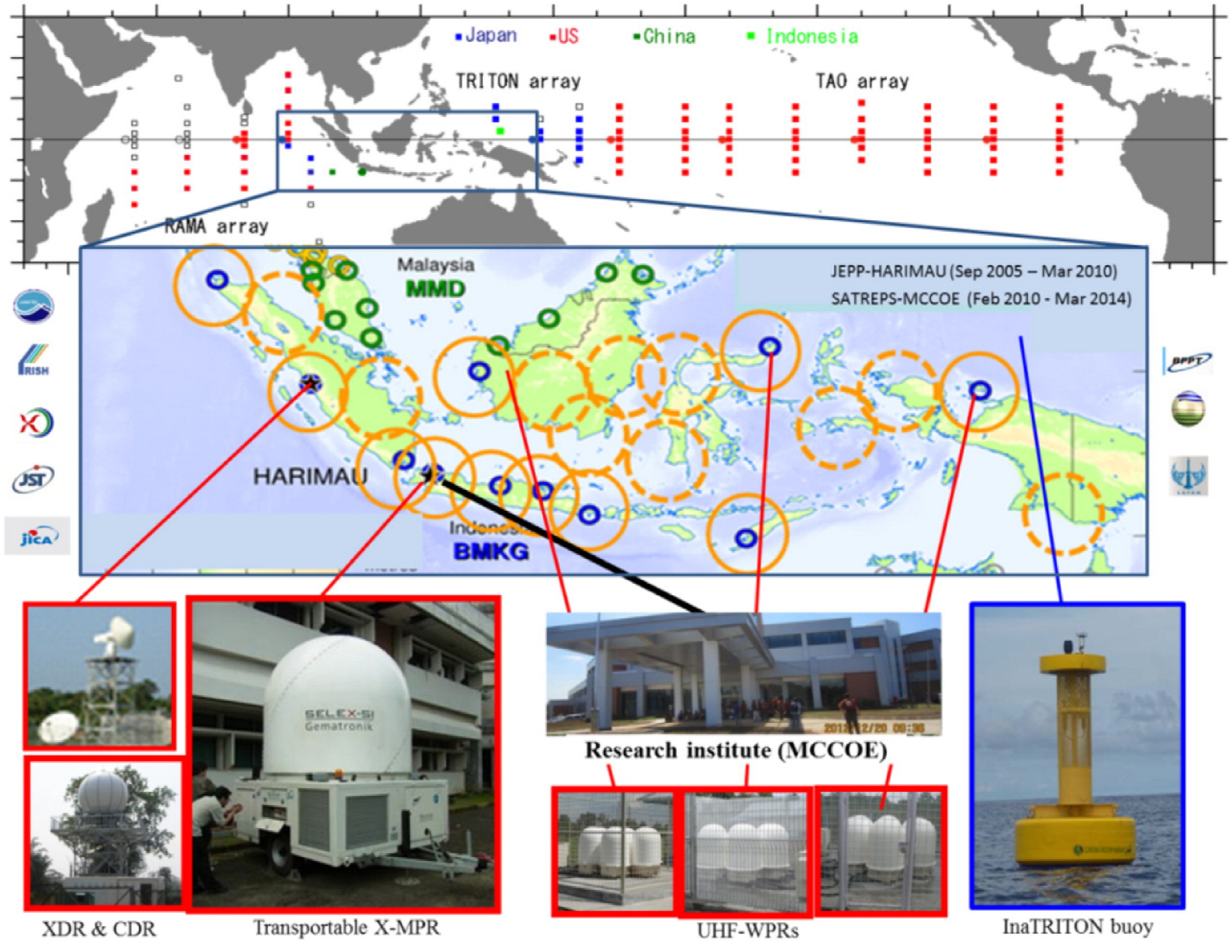

Fig. 33. Observation networks used in JEPP-HARIMAU (2005–2010) and SATREPS-MCCOE (2010–2014) projects (see Yamanaka et al., 2008; Ando et al., 2010), in collaborations with US–Japan–China RAMA-TRITON-TAO climate buoy arrays over the Indian–Pacific Oceans (upper map) and Indonesian BMKG operational radars (lower map).

concerning the climatological mechanisms but also regarding the human activities to interact them.

Acknowledgments

To close this article, I would like to acknowledge many members of JEPP-HARIMAU, SATREPS-MCCOE, and YMC projects: in particular, Drs. Shuichi Mori and Hamada Jun-Ichi for many materials throughout this article, Prof. Jun Matsumoto for monsoon studies including recent ones (co-authored with Prof. Mike Chen), and Dr. Hisayuki Kubota for evidence of the northern adjacent regions (Philippines and Micronesia) such as typhoons including his own recent results prior to publications. Dr. Fadli Syamsudin cooperated all the observations and data collections as the leader of Indonesian team and coauthored many original papers cited here. Dr. Miki Hattori, Ms. Mariko Hayashi and Mr. Toshiki Okuda provided Figs. 5(a), 5(b) and 6(c), respectively. Messrs. Mitsunori Nakamoto and Tomoya Suga provided Figs. 18 and 31. This article is based on an invited talk at a maritime continent session of AGU Fall Meeting 2014, and I would like to thank sincerely the session organizer Professor Chidong Zhang who provided also many valuable comments on the first draft of this article. I am also deeply indebted to Dr. Kunio Yoneyama, the Director of DCOP/JAMSTEC and the principal investigator of YMC team in Japan. My last but not least thanks are due to the reviewers of this article for their truly constructive comments.

References

Aldrian, E., Djamil, Y.S., 2008. Spatio-temporal climatic change of rainfall in East Java Indonesia. Int. J. Climatol. 28, 435–448.

Aldrian, E., Susanto, D., 2003. Identification of three dominant rainfall regions within Indonesia and their relationship to sea surface temperature. Int. J. Climatol. 23, 1435–1452.

Allan, R.J., 1991. Australasia. Teleconnections linking worldwide climate anomalies. In: Glantz, M.H., et al. (Eds.), Scientific Basis and Societal Impact. Cambridge University Press, pp. 73–120.

Ambrose, S.H., 1998. Late Pleistocene human population bottlenecks, volcanic winter, and differentiation of modern humans. J. Hum. Evol. 34, 623–651.

Ando, K., Syamsudin, F., Ishihara, Y., Pandoe, W., Yamanaka, M.D., Masumoto, Y., Mizuno, K., 2010. Development of new international research laboratory for maritime-continent seas climate research and contributions to global surface moored buoy array. In: Hal, J., Harrison, D.E., Stammer, D. (Eds.), *Proceedings of the "OeanObs'09: sustained Ocean Observations and Information for Society" Conference (Annex), Venice, Italy, 21-25 September 2009*. ESA Publication WPP-306.

Arakawa, O., Kitoh, A., 2005. Rainfall diurnal variation over the Indonesian maritime continent simulated by 20 km-mesh GCM. SOLA 1, 109–112.

Araki, R., Yamanaka, M.D., Murata, F., Hashiguchi, H., Oku, Y., Sribimawati, T., Kudsy, M., Renggono, F., 2006. Seasonal and interannual variations of diurnal cycles of local circulation and cloud activity observed at Serpong, West Jawa, Indonesia. J. Meteorol. Soc. Jpn. 84A, 171–194.

Barry, R., Chorley, R., 2003. *Atmosphere, Weather and Climate*. eighth ed. Routledge (472 pp).

Battisti, D.S., Hirst, A.C., 1989. Interannual variability in a tropical atmosphere–ocean model: influence of the basic state, ocean geometry and nonlinearity. J. Atmos. Sci. 46, 1687–1712.

Berlage, H.P., 1949. Rainfall in Indonesia. Verhandelingen 37 (212 pp).

Berlage, H.P., 1957. Fluctuations in the general atmospheric circulation of more than one year, their nature and prognostic value. Verhandelingen 69 (152 pp).

Bhatnagar, R., Panwar, V., Shibagaki, Y., Hashiguchi, H., Fukao, S., Kozu, T., Takahashi, M., Dhaka, S.K., 2013. Hourly radiosonde observation of humidity and temperature and high resolution vertical wind using the Equatorial Atmosphere Radar during convection over Koto Tabang, Indonesia in CPEA-II campaign. Indian J. Radio Space Phys. 42, 277–291.

Bigg, G.R., 2003. The Oceans and Climate. second ed. Cambridge University Press (288 pp).

Bjerknes, J., 1969. Atmospheric teleconnections from the equatorial Pacific. Mon. Weather Rev. 97, 163–172.

Braak, C., 1929. The climate of the Netherlands indies. 8. Verhandelingen 1602pp.

Broecker, W.S., 1991. The great ocean conveyor. Oceanography 4 (2), 79–89.

Brönnimann, S., Grosjean, M., Joos, F., Tinner, W., Rohr, C., Raible, C.C., Arfeuille, F., 2015. Bicentenary of the great Tambora eruption: implications for stratosphere-troposphere processes. SPARC Newsl. 45, 26–30 ((image of Krakatoa eruption, p.1) http://www.sparc-climate.org/fileadmin/customer/6_Publications/Newsletter_PDF/45_SPARCnewsletter_Jul2015_web2.pdf).

Chang, C.P., Liu, C.-H., Kuo, H.-C., 2003. Typhoon Vamei: an equatorial tropical cyclone formation. Geophys. Res. Lett. 30, 1150. http://dx.doi.org/10.1029/2002GL016365.

Chang, C.P., Wang, Z., Ju, J., Li, T., 2004a. On the relationship between western maritime continent monsoon rainfall and ENSO during northern winter. J. Clim. 17, 665–672.

Chang, C.P., Harr, P.A., McBride, J.C., Hsu, H.H., 2004b. Maritime continent monsoon: annual cycle and boreal winter variability. In: Chang, C.P. (Ed.), *East Asia Monsson*, pp. 107–152.

Chang, C.P., Wang, Z., McBride, J.L., Liu, C.-H., 2005. Annual cycle of Southeast Asia–Maritime Continent rainfall and the asymmetric monsoon transition. J. Clim. 18, 287–301.

Chang, C.-P., Wang, Z., Hendon, H., 2006. The Asian winter monsoon. In: Wang, B. (Ed.), *The Asian Monsoon*. Springer, pp. 89–127.

Cheang, B.K., 1977. Synoptic features and structures of some equatorial vortices over the South China Sea in the Malaysian region during the winter monsoon, December 1973. Pure Appl. Geophys. 115, 1303–1333.

Chen, H., Malanotte-Rizzoli, P., Koh, T.-Y., Song, G., 2014. The relative importance of the wind-driven and tidal circulations in Malacca Strait. Cont. Shelf Res. 88, 92–102.

Chen, T.C., Tsay, J.-D., Yen, M.-C., Matsumoto, J., 2013. The winter rainfall of Malaysia. J. Clim. 26, 936–958.

Chen, T.C., Tsay, J.-D., Matsumoto, J., Alpert, J., 2015. Development and formation mechanism of the Southeast Asian winter heavy rainfall events around the South China Sea. Part I: Formation and propagation of cold surge vortex. J. Clim. 28, 1417–1443.

Eguchi, T., 1983. Rainfall distribution and air streams over Indonesia. Geogr. Rev. Jpn 56, 151–170 (in Japanese with English abstract).

Endo, N., Matsumoto, J., Lwin, T., 2009. Trends in precipitation extremes over Southeast Asia. SOLA 5, 168–171.

Estoque, M.A., 1962. The sea breeze as a function of the prevailing synoptic situation. J. Atmos. Sci. 19, 244–250.

Fudeyasu, H., Wang, Y., Satoh, M., Nasuno, T., Miura, H., Yanase, W., 2008. Global cloud-system-resolving model NICAM successfully simulated the lifecycles of two real tropical cyclones. Geophys. Res. Lett. 35, L22808. http://dx.doi.org/10.1029/2008GL036003.

Fudeyasu, H., Ichiyanagi, K., Yoshimura, K., Mori, S., Sakurai, N., Hamada, J.-I., Yamanaka, M.D., Matsumoto, J., Syamsudin, F., 2011. Effects of large-scale moisture transport and mesoscale processes on precipitation isotope ratios observed at Sumatera, Indonesia. J. Meteorol. Soc. Jpn. 89A, 49–59.

Fujita, M., Kimura, F., Yoshizaki, M., 2010. Morning precipitation peak over the Strait of Malacca under a calm condition. Mon. Weather Rev. 138, 1474–1486.

Fujita, M., Yoneyama, K., Mori, S., Nasuno, T., Satoh, M., 2011. Diurnal convection peaks over the eastern Indian Ocean off Sumatra during different MJO phases. J. Meteorol. Soc. Jpn. 89A, 317–330.

Fukao, S., 2006. Coupling Processes in the Equatorial Atmosphere (CPEA): a project overview. J. Meteorol. Soc. Jpn. 84A, 1–18.

Gage, K.S., Nastrom, G.D., 1985. On the spectrum of atmospheric velocity fluctuations seen by MST/ST radar and their interpretation. Radio Sci. 20, 1339–1347.

Gill, A.E., 1980. Some simple solutions for heat-induced tropical circulation. Q. J. R. Meteorol. Soc. 106, 447–462.

Gill, A.E., 1982. Atmosphere–Ocean Dynamics. Academic Press (662 pp).

Goudie, A., 2001. The Nature of the Environment. fourth ed. Blackwell Publ. (544 pp).

Gordon, A.L., 2005. Oceanography of the Indonesian seas and their throughflow. Oceanography 18 (4), 14–27.

Hadi, T.W., Horinouchi, T., Tsuda, T., Hashiguchi, H., Fukao, S., 2002. Sea-breeze circulation over Jakarta, Indonesia: a climatology based on boundary layer radar observations. Mon. Weather Rev. 130, 2153–2166.

Hagan, M., Forbes, J., Richmond, A., 2003. Atmospheric tides. *Encyclopedia of Atmospheric Sciences*. Academic Press, pp. 159–165.

Hall, J.D., Matthews, A.J., Karoly, D.J., 2001. The modulation of tropical cyclone activity in the Australian region by the Madden–Julian oscillation. Mon. Weather Rev. 129, 2970–2982.

Hamada, J.-I., Yamanaka, M.D., Matsumoto, J., Fukao, S., Winarso, P.A., Sribimawati, T., 2002. Spatial and temporal variations of the rainy season over Indonesia and their link to ENSO. J. Meteorol. Soc. Jpn. 80, 285–310.

Hamada, J.-I., Yamanaka, M.D., Mori, S., Tauhid, Y.I., Sribimawati, T., 2008. Differences of rainfall characteristics between coastal and interior areas of central western Sumatera, Indonesia. J. Meteorol. Soc. Jpn. 86, 593–611.

Hamada, J.-I., Mori, S., Yamanaka, M.D., Haryoko, U., Lestari, S., Sulistyowati, R., Syamsudin, F., 2012. Interannual rainfall variability over northwestern Jawa and its relation to the Indian Ocean dipole and El Niño-southern oscillation events. SOLA 8, 69–72.

Hamid, E.Y., Kawasaki, Z.-I., Mardiana, R., 2001. Impact of the 1997–98 El Niño event on lightning activity over Indonesia. Geophys. Res. Lett. 28, 147–150.

Hara, M., Yoshikane, T., Takahashi, H.G., Kimura, F., Noda, A., Tokioka, T., 2009. Assessment of the diurnal cycle of precipitation over the Maritime Continent simulated by a 20 km mesh GCM using TRMM PR data. J. Meteorol. Soc. Jpn. 87A, 413–424.

Hartmann, D.L., 1994. Global Physical Climatology. Academic Press (411 pp).

Hasegawa, T., Ando, K., Mizuno, K., Lukas, R., 2009. Coastal upwelling along the north coast of Papua New Guinea and SST cooling over the Pacific warm pool: a case study for the 2002/03 El Niño event. J. Oceanogr. 65, 803–817.

Hasegawa, T., Ando, K., Sasaki, H., 2010a. Cold water flow and upper-ocean currents in the Bismarck Sea from December 2001 to January 2002. J. Phys. Oceanogr. 41, 827–834.

Hasegawa, T., Ando, K., Mizuno, K., Lukas, R., Taguchi, B., Sasaki, H., 2010b. Coastal upwelling along the north coast of Papua New Guinea and El Niño event during 1981–2005. Ocean Dyn. 60, 1255–1269.

Hasegawa, T., Ando, K., Ueki, I., Mizuno, K., Hosoda, S., 2013. Upper-ocean salinity variability in the tropical Pacific: case study for quasi-decadal shift during the 2000s using TRITON buoys and Argo floats. J. Clim. 26, 8126–8138.

Hashiguchi, H., Fukao, S., Yamanaka, M.D., Tsuda, T., Harijono, S.W.B., Wiryosumarto, H., 1995a. Boundary layer radar observations of the passage of the convection center over Serpong, Indonesia (6°S, 107°E) during the TOGA-COARE intensive observation period. J. Meteorol. Soc. Jpn. 30, 543–548.

Hashiguchi, H., Fukao, S., Tsuda, T., Yamanaka, M.D., Tobing, D.L., Sribimawati, T., Harijono, S.W.B., Wiryosumarto, H., 1995b. Observations of the planetary boundary layer over equatorial Indonesia with an L-band clear-air Doppler radar: initial results. Radio Sci. 30, 1043–1054.

Hashiguchi, H., Fukao, S., Yamanaka, M.D., Tsuda, T., 1997. Frequency spectra of wind velocity fluctuations between 1 hour and 1 month in the atmospheric boundary layer over equatorial Indonesia. J. Geomagn. Geoelectr. 49, S187–S195.

Hashiguchi, N.O., Yamanaka, M.D., Ogino, S.-Y., Shiotani, M., Sribimawati, T., 2006. Seasonal and interannual variations of temperature in tropical tropopause layer (TTL) over Indonesia based on operational rawinsonde data during 1992–1999. J. Geophys. Res. 111, D15110. http://dx.doi.org/10.1029/2005JD006501.

Hattori, M., Mori, S., Matsumoto, J., 2011. The cross-equatorial northerly surge over the maritime continent and its relationship to precipitation patterns. J. Meteorol. Soc. Jpn. 89A, 27–47.

Hayashi, Y.-Y., 1987. Linear theory of two dimensional steady Rossby waves. *Meteor. Res. Note*. J. Meteorol. Soc. Jpn. 156, 29–48 (in Japanese).

Hayashi, Y.-Y., Sumi, A., 1986. The 30–40 day oscillations simulated in an “aqua-planet” model. J. Meteorol. Soc. Jpn. 64, 451–467.

Haylock, M., McBride, J., 2001. Spatial coherence and predictability of Indonesian wet season rainfall. J. Clim. 14, 3882–3887.

Hendon, H.H., 2003. Indonesian rainfall variability: impacts of ENSO and local air–sea interaction. J. Clim. 16, 1775–1790.

Hendon, H.H., Woodberry, K., 1993. The diurnal cycle of tropical convection. J. Geophys. Res. 98, 16623–16637.

Hidayat, R., Kizu, S., 2009. Influence of the Madden–Julian Oscillation on Indonesian rainfall variability in austral summer. Int. J. Climatol. 30, 1816–1825.

Hidayat, S., Ishii, M., 1998. Spatial and temporal distribution of lightning activity around Java. J. Geophys. Res. 103, 14001–14009.

Hirose, M., Nakamura, K., 2004. Spatiotemporal variation of the vertical gradient of rainfall rate observed by the TRMM Precipitation Radar. J. Clim. 17, 3378–3397.

Holliday, C.R., Thompson, A.H., 1986. An unusual near-equatorial typhoon. Mon. Weather Rev. 114, 2674–2677.

Holton, J.R., Haynes, P.H., Mcintyre, M.E., Douglass, A.R., Rood, R.B., Pfister, L., 1995. Stratosphere-troposphere exchange. Rev. Geophys. 33, 403–439.

Horel, J.D., Wallace, J.M., 1981. Planetary-scale atmospheric phenomena associated with the southern oscillation. Mon. Weather Rev. 109, 813–829.

Horii, T., Masumoto, Y., Ueki, I., Hase, H., Mizuno, K., 2009. Mixed layer temperature balance in the eastern Indian Ocean during the 2006 Indian Ocean dipole. J. Geophys. Res. 114, C07011. http://dx.doi.org/10.1029/2008JC005180.

Horii, T., Masumoto, Y., Ueki, I., Kumar, S.P., Mizuno, K., 2011. Intraseasonal vertical velocity variation caused by the equatorial wave in the central equatorial Indian Ocean. J. Geophys. Res. 116, C09005. http://dx.doi.org/10.1029/2011JC007081.

Horii, T., Ueki, I., Hanawa, K., 2012. Breakdown of ENSO predictors in the 2000s: decadal changes of recharge/discharge-SST phase relation and atmospheric intraseasonal forcing. Geophys. Res. Lett. 39. http://dx.doi.org/10.1029/2012GL051740.

Horii, T., Ueki, I., Ando, K., Mizuno, K., 2013. Eastern Indian Ocean warming associated with the negative Indian Ocean dipole: a case study of the 2010 event. J. Geophys. Res. Oceans 118, 536–549.

Horinouchi, T., Yoden, S., 1996. Excitation of transient waves by localized episodic heating in the tropics and their propagation into the middle atmosphere. J. Meteorol. Soc. Jpn. 74, 189–210.

Horinouchi, T., Nakamura, T., Kosaka, J.-i., 2002. Convectively generated mesoscale gravity waves simulated throughout the middle atmosphere. Geophys. Res. Lett. 29 (21), 2007. http://dx.doi.org/10.1029/2002GL016069.

Horinouchi, T., Pawson, S., Shibata, K., Langematz, U., Manzini, E., Giorgetta, M.A., Sassi, F., Wilson, R.J., Hamilton, K., de Grandpré, J., Scaife, A.A., 2003. Tropical cumulus convection and upward-propagating waves in middle-atmospheric GCMs. J. Atmos. Sci. 60, 2765–2782.

Houze Jr., R.A., Geotis, S.G., Marks Jr., F.D., West, A.K., 1981. Winter monsoon convection in the vicinity of north Borneo. Part I: structure and time variation of the clouds and precipitation. Mon. Weather Rev. 109, 1595–1614.

Hu, D., Wu, L., Cai, W., Gupta, A.S., Ganachaud, A., Qiu, B., Gordon, A.L., Lin, X., Chen, Z., Hu, S., Wang, G., Wang, Q., Sprintall, J., Qu, T., Kashino, Y., Wang, F., Kessler, W.S., 2015. Pacific western boundary currents and their roles in climate. Nature 522, 299–308.

Ichikawa, H., Yasunari, T., 2007. Propagating diurnal disturbances embedded in the Madden–Julian Oscillation. Geophys. Res. Lett. 34, L18811. http://dx.doi.org/10.1029/2007GL030480.

Ichiyanagi, K., 2007. Review: Studies and applications of stable isotopes in precipitation. J. Jpn. Assoc. Hydrol. Sci. 37 (4), 165–185.

Inoue, T., Nakamura, K., 1990. Physical and biological background for insect studies in Sumatra. *Natural History of Social Wasps and Bees in Equatorial Sumatra*. Hokkaido University Press, pp. 1–11.

IPCC (Intergovernmental Panel on Climate Change), 2007. *Climate Change 2007 – The Physical Science Basis: Working Group I Contribution to the Fourth Assessment Report of the IPCC*. Cambridge University Press (1009 pp).
Iskandar, I., Masumoto, Y., Mizuno, K., 2009. Subsurface equatorial zonal current in the eastern Indian Ocean. J. Geophys. Res. 114, C06005. http://dx.doi.org/10.1029/2008JC005188.
Iskandar, I., Sasaki, H., Sasai, Y., Masumoto, Y., Mizuno, K., 2010. A numerical investigation of eddy-induced chlorophyll bloom in the southeastern tropical Indian Ocean during Indian Ocean Dipole-2006. Ocean Dyn. 60, 731–742.
Johnson, R.H., 1992. Heat and moisture sources and sinks of Asian monsoon precipitating systems. J. Meteorol. Soc. Jpn. 70, 353–372.
Johnson, R.H., 2011. Diurnal cycle of monsoon convection. In: Chang, C.-P., et al. (Eds.), *The Global Monsoon System: Research and Forecast*, second ed. World Scientific Pub. Co., pp. 257–276.
Johnson, R.H., Ciesielski, P.E., 2013. Structure and properties of Madden–Julian Oscillations deduced from DYNAMO sounding arrays. J. Atmos. Sci. 70, 3157–3179.
Johnson, R.H., Kriete, D.C., 1982. Thermodynamic and circulation characteristics of winter monsoon tropical mesoscale convection. Mon. Weather Rev. 110, 1898–1911.
Johnson, R.H., Priegnitz, D.L., 1981. Winter monsoon convection in the vicinity of north Borneo. Part II: Effects on large-scale fields. Mon. Weather Rev. 109, 1615–1628.
Kamimera, H., Mori, S., Yamanaka, M.D., Syamsudin, F., 2012. Modulation of diurnal rainfall cycle by the Madden–Julian oscillation based on one-year continuous observations with a meteorological radar in West Sumatera. SOLA 8, 111–114.
Kanamori, H., Yasunari, T., Kuraji, K., 2013. Modulation of the diurnal cycle of rainfall associated with the MJO observed by a dense hourly rain gauge network at Sarawak, Borneo. J. Clim. 26, 4858–4875.
Kashino, Y., España, N., Syamsudin, F., Richards, K., Jensen, T., Dutrieux, P., Ishida, A., 2009. Observations of the north equatorial current, Mindanao current, and Kuroshio current system during the 2006/07 El Niño and 2007/08 La Niña. J. Oceanogr. 65, 325–333.
Kashino, Y., Ishida, A., Hosoda, S., 2011. Observed ocean variability in the Mindanao Dome region. J. Phys. Oceanogr. 41, 287–302.
Kashino, Y., Atmadipoera, A., Kuroda, Y., Lukijanto, 2013. Observed features of the Halmahera and Mindanao eddies. J. Geophys. Res. Oceans 118, 6543–6560.
Kataoka, K., Matsumoto, F., Ichinose, T., Taniguchi, M., 2009. Urban warming trends in several large Asian cities over the last 100 years. Sci. Total Environ. 407, 3112–3119.
Kawashima, M., Fujiyoshi, Y., Ohi, M., Honda, T., Kozu, T., Shimomai, T., Hashiguchi, H., 2006. Overview of Doppler radar observations of precipitating cloud systems in Sumatera Island during the first CPEA campaign. J. Meteorol. Soc. Jpn. 84A, 33–56.
Kawashima, M., Fujiyoshi, Y., Ohi, M., Honda, T., Mori, S., Sakurai, N., Abe, Y., Harjupa, W., Syamsudin, F., Yamanaka, M.D., 2011. Case study of an intense wind event associated with a mesoscale convective system in west Sumatera during the HARIMAU2006 campaign. J. Meteorol. Soc. Jpn. 89A, 239–257.
Kawatani, Y., Hamilton, K., 2013. Weakened stratospheric quasibiennial oscillation driven by increased tropical mean upwelling. Nature 497, 478–481.
Kawatani, Y., Sato, K., Dunkerton, T.J., Watanabe, S., Miyahara, S., Takahashi, M., 2010a. The roles of equatorial trapped waves and internal inertia-gravity waves in driving the quasi-biennial oscillation, part I: zonal mean wave forcing. J. Atmos. Sci. 67, 963–980.
Kawatani, Y., Sato, K., Dunkerton, T.J., Watanabe, S., Miyahara, S., Takahashi, M., 2010b. The roles of equatorial trapped waves and internal inertia-gravity waves in driving the quasi-biennial oscillation, part II: three-dimensional distribution of wave forcing. J. Atmos. Sci. 67, 981–997.
Kodama, Y.-M., Tokuda, M., Murata, F., 2006. Convective activity over the Indonesian maritime continent during CPEA-I as evaluated by lightning activity and Q1 and Q2 profiles. J. Meteorol. Soc. Jpn. 84A, 133–149.
Koh, T.-Y., Teo, C.-K., 2009. Toward a mesoscale observation network in Southeast Asia. Bull. Am. Meteorol. Soc. 39, 481–488.
Können, G.P., Jones, P.D., Kaltofen, M.H., Allan, R.J., 1998. Pre-1866 extensions of the southern oscillation index using early Indonesian and Tahitian meteorological readings. J. Clim. 11, 2325–2339.
Kosaka, Y., Matsuda, Y., 2005. Roles of Rossby and gravity waves on circulation associated with tropical and subtropical heating. J. Meteorol. Soc. Jpn. 83, 481–498.
Koseki, S., Koh, T.-Y., Teo, C.-K., 2013. Effects of the cold tongue in the South China Sea on the monsoon, diurnal cycle and rainfall in the Maritime Continent. Q. J. R. Meteorol. Soc. 139, 1566–1582.
Kozu, T., Reddy, K.K., Mori, S., Thurai, M., Ong, J.T., Rao, D.N., Shimomai, T., 2006. Seasonal and diurnal variations of raindrop size distribution in Asian monsoon region. J. Meteorol. Soc. Jpn. 84A, 195–209.
Kozu, T., Kodama, Y., Shibagaki, Y., Shimonai, T., Kawashima, M., Alexander, S., 2009. Diurnal and intraseasonal variation of UTLS vertical wind disturbance in equatorial region and its relation to tropospheric convective activities. Earth Planets Space 61, 534–544.
Kubota, H., 2012. Variability of typhoon tracks and genesis over the western North Pacific. In: Oouchi, K., Fudeyasu, H. (Eds.), Cyclones: *Formation, Triggers and Control*. Nova Science Publ., pp. 95–114.
Kubota, H., Nitta, Ts., 2001. Diurnal variations of tropical convection observed during the TOGA-COARE. J. Meteorol. Soc. Jpn. 79, 815–830.
Kubota, H., Chan, J.C.L., Matsumoto, J., Ginn, E.W.L., 2012. Shifts in typhoon tracks over the western North Pacific during the 20th century based on the recovery of historical data. 30th AMS Conference on Hurricanes and Tropical Meteorology. The American Meteorological Society 1B, p. 7.
Kubota, H., Shirooka, R., Hamada, J.-I., Syamsudin, F., 2011. Interannual rainfall variability over the eastern maritime continent. J. Meteorol. Soc. Jpn. 89A, 111–122.
Kurita, N., Ichiyanagi, K., Matsumoto, J., Yamanaka, M.D., Ohata, T., 2009. The relationship between the isotopic content of precipitation and the precipitation amount in tropical regions. J. Geochem. Explor. 102, 113–122.
Lau, K.M., Lim, H., 1982. Thermally induced motion in an equatorial β-plane; Hadley and Walker circulation in the winter monsoon. Mon. Weather Rev. 110, 336–353.
Lau, K.M., Ding, Y., Wang, J.-T., Johnson, R., Keenan, T., Cifelli, R., Gerlach, J., Thiele, O., Rickenbach, T., Tsay, S.-C., Lin, P.-H., 2000. A report of the field operations and early results of the South China Sea Monsoon Experiment (SCSMEX). Bull. Am. Meteorol. Soc. 81, 1261–1270.
Lestari, S., Hamada, J.-I., Syamsudin, F., Sunaryo, Matsumoto, J., Yamanaka, M.D., 2016. ENSO influences on rainfall extremes around Sulawesi and Maluku Islands in the eastern Indonesian maritime continent. SOLA 12, 37–41.
Lindzen, R.S., 1990. Dynamics in Atmospheric Physics. Cambridge University Press (310 pp).
LMG (Meteorological and Geophysical Institute), 1973a. Rainfall Atlas of Indonesia. Vol. I: Java and Madura (1931–1960)*Meteorological Note* **9**(1). Department of Communications, Republic of Indonesia (30 pp).
LMG (Meteorological and Geophysical Institute), 1973b. Rainfall Atlas of Indonesia. Vol. II: Sumatra, Kalimantan, Sulawesi, Nusatenggara, Maluku, Irian Jaya (1911–1940) *Meteorological Note* **9**(2). Department of Communications, Republic of Indonesia (47 pp).
Love, B.S., Matthews, A.J., Lister, G.M.S., 2011. The diurnal cycle of precipitation over the Maritime Continent in a high-resolution atmospheric model. Q. J. R. Meteorol. Soc. 137, 934–947.
Lukas, R., Yamagata, T., McCreary, J.P., 1996. Pacific low-latitude western boundary currents and the Indonesian throughflow. J. Geophys. Res. 101, 12209–12216.
Madden, R.A., Julian, P.R., 1971. Detection of a 40–50 day oscillation in the zonal wind in the tropical Pacific. J. Atmos. Sci. 28, 702–708.
Manton, M.J., Della-Marta, P.M., Haylock, M.R., Hennessy, K.J., Nicholls, N., Chambers, L.E., Collins, D.A., Daw, G., Finet, A., Gunawan, D., Inape, K., Isobe, H., Kestin, T.S., Lefale, P., Leyu, C.H., Lwin, T., Maitrepierre, L., Ouprasitwong, N., Page, C.M., Pahalad, J., Plummer, N., Salinger, M.J., Suppiah, R., Tran, V.L., Trewin, B., Tibig, I., Yee, D., 2001. Trends in extreme daily rainfall and temperature in Southeast Asia and the South Pacific: 1961–1998. Int. J. Climatol. 21, 269–284.
Marzuki, M., Kozu, T., Shimomai, T., Randeu, W.L., Hashiguchi, H., Shibagaki, Y., 2009. Diurnal variation of rain attenuation obtained from measurement of raindrop size distribution in equatorial Indonesia. IEEE Trans. Antennas Propag. 57, 1191–1196.
Marzuki, M., Kozu, T., Shimomai, T., Hashiguchi, H., Randeu, W.L., Vonnisa, M., 2010. Raindrop size distributions of convective rain over equatorial Indonesia during the first CPEA campaign. Atmos. Res. 96, 645–655.
Marzuki, M., Randeu, W.L., Kozu, T., Shimomai, T., Schonhuber, M., Hashiguchi, H., 2012. Estimation of raindrop size distribution parameters by maximum likelihood and L-moment methods: effect of discretization. Atmos. Res. 112, 1–11.
Marzuki, M., Randeu, W.L., Kozu, T., Shimomai, T., Hashiguchi, H., 2013a. Raindrop axis ratios, fall velocities and size distribution over Sumatra from 2D-video disdrometer measurement. Atmos. Res. 119, 27–37.
Marzuki, M., Hashiguchi, H., Yamamoto, M.K., Yamamoto, M., Mori, S., Yamanaka, M.D., Carbone, R.E., Tuttle, J.D., 2013b. Cloud episode propagation over the Indonesian maritime continent from 10 Years of infrared brightness temperature observations. Atmos. Res. 120-121, 268–286.
Marzuki, M., Hashiguchi, H., Yamamoto, M.K., Mori, S., Yamanaka, M.D., 2013c. Regional variability of raindrop size distribution over Indonesia. Ann. Geophys. 31, 1941–1948.
Matsuda, Y., 1980. Dynamics of the four-day circulation in the Venus atmosphere. J. Meteorol. Soc. Jpn. 58, 443–470.
Matsuda, Y., Kato, T., 1987. The linear response of a global atmosphere to tropical heating: effect of planetary rotation. J. Meteorol. Soc. Jpn. 65, 819–842.
Matsumoto, J., 1992. The seasonal changes in Asian and Australian monsoon regions. J. Meteorol. Soc. Jpn. 70, 257–273.
Matsumoto, J., Murakami, T., 2000. Annual changes of tropical convective activities as revealed from equatorial symmetric OLR data. J. Meteorol. Soc. Jpn 78, 543–561.
Matsumoto, J., Wang, B., Wu, G.-X., Li, J.-P., Wu, P.-M., Hattori, M., Mori, S., Yamanaka, M.D., Hamada, J.-I., Syamsudin, F., Koike, T., Tamagawa, K., Ikoma, E., Kinutani, H., Kamahori, H., Kamiguchi, K., Harada, Y., 2016. An overview of the Asian Monsoon Years 2007–2012 (AMY) and multi-scale interactions in the extreme rainfall events over the Indonesian maritime continent. In: Chang, C.-P. (Ed.), The Global Monsoon System Research and Forecast III. World Scientific Publication Company (in press).
Matsuno, T., 1966. Quasi-geostrophic motions in the equatorial area. J. Meteorol. Soc. Jpn. 44, 25–43.
McBride, J.L., 1992. The meteorology of Indonesia and the maritime continent. *Extended Abstract, Fourth Int. Symp.Equatorial Atmos. Obs. over Indonesia*. I-1 (7 pp).
McBride, J., 1998. Indonesia, Papua New Guinea, and tropical Australia: the southern hemisphere monsoon. Meteorol. Monogr. 27, 89–100.
McBride, J.L., Haylock, M.R., Nicholls, N., 2003. Relationships between the Maritime Continent heat source and the El Niño-Southern Oscillation phenomenon. J. Clim. 16, 2905–2914.
McPhaden, M., Meyers, G., Ando, K., Masumoto, Y., Murty, V.S.N., Ravichandran, M., Syamsudin, F., Vialard, J., Yu, L., Yu, W., 2009a. RAMA: the research moored array for African–Asian–Australian monsoon analysis and prediction. Bull. Am. Meteorol. Soc. 90, 459–480.
McPhaden, M., Meyers, G., Ando, K., Masumoto, Y., Murty, V.S.N., Ravichandran, M., Syamsudin, F., Vialard, J., Yu, L., Yu, W., 2009b. Supplement to RAMA: the research moored array for African–Asian–Australian monsoon analysis and prediction. Bull. Am. Meteorol. Soc. 90, ES5–ES8.
Mega, T., Yamamoto, M.K., Luce, H., Tabata, Y., Hashiguchi, H., Yamamoto, M., Yamanaka, M.D., Fukao, S., 2010. Turbulence generation by Kelvin–Helmholtz instability in the tropical tropopause layer observed with a 47-MHz range imaging radar. J. Geophys. Res. 115, D18115. http://dx.doi.org/10.1029/2010JD013864.

Mega, T., Yamamoto, M.K., Abo, M., Shibata, Y., Hashiguchi, H., Nishi, N., Shimomai, T., Shibagaki, Y., Yamamoto, M., Yamanaka, M.D., Fukao, S., Manik, T., 2012. First simultaneous measurement of vertical air velocity, particle fall velocity, and hydrometeor sphericity in stratiform precipitation: results from 47-MHz wind profiling radar and 532–nm polarization lidar observations. Radio Sci. 47, RS3002. http://dx.doi.org/10.1029/2011RS004823.

Mori, S., Hamada, J.-I., Tauhid, Y.I., Yamanaka, M.D., Okamoto, N., Murata, F., Sakurai, N., Sribimawati, T., 2004. Diurnal rainfall peak migrations around Sumatera Island, Indonesian maritime continent observed by TRMM satellite and intensive rawinsonde soundings. Mon. Weather Rev. 132, 2021–2039.

Mori, S., Hamada, J.-I., Yamanaka, M.D., Kodama, Y.-M., Kawashima, M., Shimomai, T., Shibagaki, Y., Hashiguchi, H., Sribimawati, T., 2006. Vertical wind characteristics in precipitating cloud systems over west Sumatera, Indonesia, observed with Equatorial Atmosphere Radar: case study of 23–24 April 2004 during the first CPEA campaign period. J. Meteorol. Soc. Jpn. 84A, 113–131.

Mori, S., Hamada, J.-I., Sakurai, N., Fudeyasu, H., Kawashima, M., Hashiguchi, H., Syamsudin, F., Arbain, A.A., Sulistyowati, R., Matsumoto, J., Yamanaka, M.D., 2011. Convective systems developed along the coastline of Sumatera Island, Indonesia observed with an X-band Doppler radar during the HARIMAU2006 campaign. J. Meteorol. Soc. Jpn. 89A, 61–81.

Murakami, T., Matsumoto, J., 1994. Summer monsoon over the Asian Continent and western North Pacific. J. Meteorol. Soc. Jpn. 72, 719–745.

Murata, F., Yamanaka, M.D., Fujiwara, M., Ogino, S.-Y., Hashiguchi, H., Fukao, S., Kudsy, M., Sribimawati, T., Harijono, S.W.B., Kelana, E., 2002. Relationship between wind and precipitation observed with a UHF radar, GPS rawinsonde and surface meteorological instruments at Kototabang, West Sumatera during September–October 1998. J. Meteorol. Soc. Jpn. 80, 347–360.

Murata, F., Yamanaka, M.D., Hashiguchi, H., Mori, S., Kudsy, M., Sribimawati, T., Suhardi, B., Emrizal, 2006. Dry intrusions following eastward-propagating synoptic-scale cloud systems over Sumatera Island. J. Meteorol. Soc. Jpn. 84, 277–294.

Nakamura, K., 1994. Regional difference and seasonality of rainfall in Java, with special reference to Bogor. Tropics 4, 93–103.

Nakazawa, T., 1988. Tropical super clusters within intraseasonal variations over the western Pacific. J. Meteorol. Soc. Jpn. 66, 823–839.

Nastrom, G.D., Gage, K.S., 1985. A climatology of atmospheric wavenumber spectra of wind and temperature observed by commercial aircraft. J. Atmos. Sci. 42, 950–960.

Neale, R., Slingo, J., 2003. The Maritime Continent and its role in the global climate: a GCM study. J. Clim. 16, 834–848.

Nguyen, H., Evans, A., Lucas, C., Smith, I., Timbal, B., 2013. The Hadley circulation in reanalyses: climatology, variability, and change. J. Clim. 26, 3357–3376.

Nieuwolt, S., 1968. Diurnal rainfall variation in Malaya. Ann. Assoc. Am. Geogr. 58 (2), 313–326.

Niino, H., 1987. The linear theory of sea–land breeze circulation. J. Meteorol. Soc. Jpn. 65, 901–921.

Nitta, Ts, 1987. Convective activities in the tropical western pacific and their impact on the northern hemisphere summer circulation. J. Meteorol. Soc. Jpn. 65, 373–390.

Nitta, Ts, Sekine, S., 1994. Diurnal variation of convective activity over the tropical western Pacific. J. Meteorol. Soc. Jpn. 72, 627–641.

Nitta, Ts, Mizuno, T., Takahashi, K., 1992. Multiscale convective systems during the initial phase of the 1986/87 El Niño. J. Meteorol. Soc. Jpn. 70, 447–466.

Nurhayati, Nakajima, T., 2012. A study of aerosol optical properties at the global GAW station Bukit Kototabang, Sumatra, Indonesia. Atmos. Environ. 46, 597–606.

Ogino, S.-Y., Yamanaka, M.D., Fukao, S., 1995. Meridional variation of lower stratospheric gravity wave activity: a quick look at Hakuho–Maru J-COARE cruise rawinsonde data. J. Meteorol. Soc. Jpn. 73, 407–413.

Ogino, S.-Y., Yamanaka, M.D., Mori, S., Matsumoto, J., 2016. How much is the precipitation amount over the tropical coastal region? J. Clim. 29, 1231–1236.

Ogura, Y., Yoshizaki, M., 1988. Numerical study of orographic-convective precipitation over the eastern Arabian Sea and the Ghat Mountains during the summer monsoon. J. Atmos. Sci. 45, 2097–2122.

Ohsawa, T., Ueda, H., Hayashi, T., Watanabe, A., Matsumoto, J., 2001. Diurnal variations of convective activity and rainfall in tropical Asia. J. Meteorol. Soc. Jpn. 79, 333–352.

Okamoto, N., Yamanaka, M.D., Ogino, S.-Y., Hashiguchi, H., Nishi, N., Sribimawati, T., Numaguti, A., 2003. Seasonal variation of tropospheric wind over Indonesia: comparison between collected operational rawinsonde data and NCEP reanalysis for 1992–99. J. Meteorol. Soc. Jpn. 81, 829–850.

Peatman, S.C., Matthews, A.J., Stevens, D.P., 2014. Propagation of the Madden–Julian oscillation through the Maritime Continent and scale interaction with the diurnal cycle of precipitation. Q. J. R. Meteorol. Soc. 140, 814–825.

Qian, J.-H., 2008. Why precipitation is mostly concentrated over islands in the Maritime Continent. J. Atmos. Sci. 65, 1428–1441.

Qian, J.-H., Robertson, A.W., Moron, V., 2013. Diurnal cycle in different weather regimes and rainfall variability over Borneo associated with ENSO. J. Clim. 26, 1772–1790.

Ramage, C.S., 1968. Role of a tropical "maritime continent" in the atmospheric circulation. Mon. Weather Rev. 96, 365–369.

Ramage, C.S., 1971. Monsoon Meteorology. Academic Press (296 pp).

Rauniyar, S.P., Walsh, K.J.E., 2011. Scale interaction of the diurnal cycle of rainfall over the Maritime Continent and Australia: influence of the MJO. J. Clim. 24, 325–348.

Rauniyar, S.P., Walsh, K.J.E., 2013. Influence of ENSO on the diurnal cycle of rainfall over the Maritime Continent and Australia. J. Clim. 26, 1304–1321.

Reid, J.S., Hyer, E.J., Johnson, R.S., Holben, B.N., Yokelson, R.J., Zhang, J., Campbell, J.R., Christopher, S.A., Girolamo, L.D., Giglio, L., Holz, R.E., Kearney, C., Miettinen, J., Reid, E.A., Turk, F.J., Wang, J., Xian, P., Zhao, G., Balasubramanian, R., Chew, B.N., Janjai, S., Lagrosas, N., Lestari, P., Lin, N.-H., Mahmud, M., Nguyen, A.X., Norris, B., Oanh, N.T.K., Oo, M., Salinas, Santo V., Welton, E.J., Liew, S.C., 2013. Observing and understanding the Southeast Asian aerosol system by remote sensing: an initial review and analysis for the Seven Southeast Asian Studies (7SEAS) program. Atmos. Res. 122, 403–468.

Renggono, F., Hashiguchi, H., Fukao, S., Yamanaka, M.D., Ogino, S.-Y., Okamoto, N., Murata, F., Harijono, S.W.B., Kudsy, M., Kartasasmita, M., Ibrahim, G., 2001. Precipitating clouds observed by 1.3-GHz L-band boundary layer radars in equatorial Indonesia. Ann. Geophys. 19, 889–897.

Renggono, F., Yamamoto, M.K., Hashiguchi, H., Fukao, S., Shimomai, T., Kawashima, M., Kudsy, M., 2006. Raindrop size distribution observed with the Equatorial Atmosphere Radar (EAR) during the Coupling Processes in the Equatorial Atmosphere (CPEA-I) observation campaign. Radio Sci. 41, RS5002. http://dx.doi.org/10.1029/2005RS003333.

Robock, A., Ammann, C.M., Oman, L., Shindell, D., Levis, S., Stenchikov, G., 2009. Did the Toba volcanic eruption of 74 ka B.P. produce widespread glaciation? J. Geophys. Res. 114, D10107. http://dx.doi.org/10.1029/2008JD011652.

Rotunno, R., 1983. On the linear theory of the land and sea breeze. J. Atmos. Sci. 40, 1999–2009.

Saito, K., Keenan, T., Holland, G., Puri, K., 2001. Numerical simulation of the diurnal evolution of tropical island convection over the maritime continent. Mon. Weather Rev. 129, 378–400.

Saji, N.H., Goswami, B.N., Vinayachandran, P.N., Yamagata, T., 1999. A dipole mode in the tropical Indian Ocean. Nature 401, 360–363.

Sakazaki, T., Fujiwara, M., Zhang, X., Hagan, M.E., Forbes, J.M., 2012. Diurnal tides from the troposphere to the lower mesosphere as deduced from TIMED/SABER satellite data and six global reanalysis data sets. J. Geophys. Res. 117, D13108. http://dx.doi.org/10.1029/2011JD017117.

Sakurai, N., Murata, F., Yamanaka, M.D., Hashiguchi, H., Mori, S., Hamada, J.-I., Tauhid, Y.-I., Sribimawati, T., Suhardi, B., 2005. Diurnal cycle of migration of convective cloud systems over Sumatera Island. J. Meteorol. Soc. Jpn. 83, 835–850.

Sakurai, N., Kawashima, M., Fujiyoshi, Y., Hashiguchi, H., Shimomai, T., Mori, S., Hamada, J.-I., Murata, F., Yamanaka, M.D., Tauhid, Y.I., Sribimawati, T., Suhardi, B., 2009. Internal structures of migratory cloud systems with diurnal cycle over Sumatera Island during CPEA-I campaign. J. Meteorol. Soc. Jpn. 87, 157–170.

Sakurai, N., Mori, S., Kawashima, M., Fujiyoshi, Y., Hamada, J.-I., Shimizu, S., Fudeyasu, H., Tabata, Y., Harjupa, W., Hashiguchi, H., Yamanaka, M.D., Matsumoto, J., Emrizal, Syamsudin, F., 2011. Migration process and 3D wind field of precipitation systems associated with a diurnal cycle in west Sumatera: dual Doppler radar analysis during the HARIMAU2006 campaign. J. Meteorol. Soc. Jpn. 89, 341–361.

Sasaki, T., Wu, P.-M., Mori, S., Hamada, J.-I., Tauhid, Y.I., Yamanaka, M.D., Yoshikane, T., Kimura, F., 2004. Vertical moisture transport above the mixed layer around mountains in western Sumatera. Geophys. Res. Lett. 31, L08106. http://dx.doi.org/10.1029/2004GL019730.

Sato, Kaori, Okamoto, H., Yamamoto, M.K., Fukao, S., Kumagai, H., Ohno, Y., Horie, H., Abo, M., 2009b. 95-GHz Doppler radar and lidar synergy for simultaneous ice microphysics and in-cloud vertical air motion retrieval. J. Geophys. Res. 114, D03203. http://dx.doi.org/10.1029/2008JD010222.

Sato, Kaoru, Kumakura, T., Takahashi, M., 1999. Gravity waves appearing in a high-resolution GCM simulation. J. Atmos. Sci. 56, 1005–1018.

Sato, T., Miura, H., Satoh, M., Takayabu, Y.N., Wang, Y., 2009a. Diurnal cycle of precipitation in the tropics simulated in a global cloud-resolving model. J. Clim. 22, 4809–4826.

Satoh, M., Matsuno, T., Tomita, H., Miura, H., Nasuno, T., Iga, S., 2008. Nonhydrostatic icosahedral atmospheric model (NICAM) for global cloud resolving simulations. J. Comput. Phys. 227, 3486–3514.

Schmidt, F.H., Ferguson, J.H.A., 1951. Rainfall types based on wet and dry period ratios for Indonesia with western New Guinee. Verhandelingen Djawatan Meteorologi dan Geofisik 42 (77 pp).

Scott, J.R., 1956. The zonal wind in the upper troposphere and weather at Singapore. Q. J. R. Meteorol. Soc. 82, 340–341.

Seto, T.H., Yamamoto, M.K., Hashiguchi, H., Fukao, S., Abo, M., Kozu, T., Kudsy, M., 2006. Observational study on westerly wind burst over Sumatera, Indonesia by the Equatorial Atmosphere Radar: a case study during the first CPEA observation campaign. J. Meteorol. Soc. Jpn. 84A, 95–112.

Seto, T.H., Tabata, Y., Yamamoto, M.K., Hashiguchi, H., Mega, T., Kudsy, M., Yamanaka, M.D., Fukao, S., 2009. Comparison study of lower-tropospheric horizontal wind over Sumatera, Indonesia using NCEP/NCAR reanalysis, operational radiosonde, and the Equatorial Atmosphere Radar. SOLA 5, 21–24.

Shibagaki, Y., Kozu, T., Shimomai, T., Mori, S., Murata, F., Fujiyoshi, Y., Hashiguchi, H., Fukao, S., 2006a. Evolution of a super cloud cluster and the associated wind fields observed over the Indonesian maritime continent during the first CPEA Campaign. J. Meteorol. Soc. Jpn. 84A, 19–31.

Shibagaki, Y., Shimomai, T., Kozu, T., Mori, S., Fujiyoshi, Y., Hashiguchi, H., Yamamoto, M.K., Fukao, S., Yamanaka, M.D., 2006b. Multi-scale convective systems associated with an intraseasonal oscillation over the Indonesian maritime continent. Mon. Weather Rev. 134, 1682–1696.

Shimizu, A., Tsuda, T., 1997. Radiosonde observations of equatorial atmosphere dynamics over Indonesia. J. Geophys. Res. 102, 26159–26172.

Shimizu, A., Tsuda, T., 2001. Seasonal and QBO-related variations in gravity wave activities observed with radiosondes at Bandung, Indonesia. J. Meteorol. Soc. Jpn. 79, 185–200.

Siswanto, S., van Oldenborgh, G.J., van der Schrier, G., Jilderda, R., van den Hurk, B., 2015. Temperature, extreme precipitation, and diurnal rainfall changes in the urbanized Jakarta city during the past 130 years. Int. J. Climatol. http://dx.doi.org/10.1002/joc.4548.

Sprintall, J., Gordon, A.L., Koch-Larrouy, A., Lee, T., Potemra, J.T., Pujiana, K., Wijffels, S.E., 2014. The Indonesian seas and their role in the coupled ocean-climate system. Nat. Geosci. 7, 487–492.

Sugimoto, N., Matsui, I., Shimizu, A., Pinandio, M., Sugondo, S., 2000. Climatological characteristics of cloud distribution and planetary boundary layer structure in Jakarta, Indonesia reveald by lidar observation. Geophys. Res. Lett. 27, 2909–2912.

Sulistyowati, R., Hapsari, R.I., Syamsudin, F., Mori, S., Oishi, S.T., Yamanaka, M.D., 2014. Rainfall-driven diurnal variations in the Ciliwung River, West Jawa, Indonesia. SOLA 10, 141–144.

Suwarman, R., Ichiyanagi, K., Tanoue, M., Yoshimura, K., Mori, S., Yamanaka, M.D., Kurita, N., Syamsudin, F., 2013. The variability of stable isotopes and water origin of precipitation over the maritime continent. SOLA 9, 74–78.

Syamsudin, F., van Aken, H.M., Kaneko, A., 2010. Annual variation of the southern boundary current in the Banda Sea. Dyn. Atmos. Oceans 50, 129–139.

Syamsudin, F., Kaneko, A., 2013. Ocean variability along the southern coast of Java and Lesser Sunda Islands. J. Oceanogr. 69, 557–570.

Tabata, Y., Hashiguchi, H., Yamamoto, M.K., Yamamoto, M., Yamanaka, M.D., Mori, S., Syamsudin, F., Manik, T., 2011a. Lower tropospheric horizontal wind over Indonesia: a comparison of wind-profiler network observations with global reanalyses. J. Atmos. Sol. Terr. Phys. 73, 986–995.

Tabata, Y., Hashiguchi, H., Yamamoto, M.K., Yamamoto, M., Yamanaka, M.D., Mori, S., Syamsudin, F., Manik, T., 2011b. Observational study on diurnal precipitation cycle in equatorial Indonesia using 1.3-GHz wind profiling radar network and TRMM precipitation radar. J. Atmos. Sol. Terr. Phys. 73, 1031–1042.

Takasuka, D., Miyakawa, T., Satoh, M., Miura, H., 2015. Topographical effects on internally produced MJO-like disturbances in an aqua-planet version of NICAM. SOLA 11, 170–176.

Takayabu, Y.N., Nitta, Ts., 1993. 3 — 5 day-period disturbances coupled with convection over the tropical Pacific Ocean. J. Meteorol. Soc. Jpn. 71, 221–246.

Takayabu, Y.N., Lau, K.-M., Sui, C.-H., 1996. Observation of a quasi-2-day wave during TOGA COARE. Mon. Weather Rev. 124, 1892–1913.

Takayabu, Y.N., Iguchi, T., Kachi, M., Shibata, A., Kanzawa, H., 1999. Abrupt termination of the 1997–98 El Niño in response to a Madden- Julian oscillation. Nature 402, 279–282.

Tangang, F.T., Juneng, L., 2004. Mechanisms of Malaysian rainfall anomalies. J. Clim. 17, 3616–3622.

Tangang, F.T., Juneng, L., Salimun, E., Vinayachandran, P.N., Seng, Y.K., Reason, C.J.C., Behera, S.K., Yasunari, T., 2008. On the roles of the northeast cold surge, the Borneo vortex, the Madden–Julian oscillation, and the Indian Ocean dipole during the extreme 2006/2007 flood in southern Peninsular Malaysia. Geophys. Res. Lett. 35, L14S07. http://dx.doi.org/10.1029/2008GL033429.

Trilaksono, N.J., Otsuka, S., Yoden, S., Saito, K., Hayashi, S., 2011. Dependence of model-simulated heavy rainfall on the horizontal resolution during the Jakarta flood event in January — February 2007. SOLA 7, 193–196.

Trilaksono, N.J., Otsuka, S., Yoden, S., 2012. A time-lagged ensemble simulation on the modulation of precipitation over west Java in January–February 2007. Mon. Weather Rev. 140, 601–616.

Tsuda, T., Murayama, Y., Wiryosumarto, H., Harijono, S.W.B., Kato, S., 1994a. Radiosonde observations of equatorial atmosphere dynamics over Indonesia: 1. Equatorial waves and diurnal tides. J. Geophys. Res. 99, 10491–10505.

Tsuda, T., Murayama, Y., Wiryosumarto, H., Harijono, S.W.B., Kato, S., 1994b. Radiosonde observations of equatorial atmosphere dynamics over Indonesia: 2. Characteristics of gravity waves. J. Geophys. Res. 99, 10507–10516.

Tsuda, T., Fukao, S., Yamamoto, M., Nakamura, T., Yamanaka, M.D., Adachi, T., Hashiguchi, H., Fujioka, N., Tsutsumi, M., Kato, S., Harijono, S.W.B., Sribimawati, T., Sitorus, B.P., Yahya, R.B., Karmini, M., Renggono, F., Parapat, B.L., Djojonegoro, W., Mardio, P., Adikusumah, N., Endi, H.T., Wiryosumarto, H., 1995. A preliminary report on observations of equatorial atmosphere dynamics in Indonesia with radars and radiosondes. J. Meteorol. Soc. Jpn. 73, 393–406.

Tsuda, T., Nishida, M., Rocken, C., Ware, R.H., 2000. A global morphology of gravity wave activity in the stratosphere revealed by the GPS occultation data (GPS/MET). J. Geophys. Res. 105, 7257–7273.

Ueki, I., Fujii, N., Masumoto, Y., Mizuno, K., 2010. Data evaluation for new developed slack-line mooring buoy deployed in the eastern Indian Ocean. J. Atmos. Ocean. Technol. 27, 1195–1214.

Ueki, I., 2011. Evidence of wind–evaporation–sea surface temperature (WES) feedback in the western Pacific warm pool during the mature phase of the 1997–98 El Niño. Geophys. Res. Lett. 38. http://dx.doi.org/10.1029/2011GL047179.

Van Andel, T.H., 1994. *New Views on an Old Planet*: *A History of Global Change*. Cambridge University Press (458 pp).

van Bemmelen, W., 1913. Die Erforschungdes tropischen Luftoszeans in Niederländische-Ost-Indien. Luftfahrt und Wissenschaft 5, 1–50 (in German).

van Bemmelen, W., 1922a. Land- und Seebrise in Batavia. Beitr. Phys. Frei. Atmos. 10, 169–177 (in German).

van Bemmelen, W., 1922b. The antitrades. Nature 109, 172–173.

Villafuerte, M.Q., Matsumoto, J., 2015. Significant influences of global mean temperature and ENSO on extreme rainfall in Southeast Asia. J. Clim. 28, 1905–1919.

Virts, K.S., Wallace, J.M., Hutchins, M.L., Holzworth, R.H., 2013a. Highlights of a new ground-based, hourly global lightning climatology. Bull. Am. Meteorol. Soc. 94, 1381–1391.

Virts, K.S., Wallace, J.M., Hutchins, M.L., Holzworth, R.H., 2013b. Diurnal lightning variability over the Maritime Continent: impact of low-level winds, cloudiness, and the MJO. J. Atmos. Sci. 70, 3128–3146.

Wallace, J.M., 2002. General circulation: overview. Encyclopedia of Atmospheric Sciences. Academic Press, pp. 821–829.

Wallace, J.M., Hobbs, P.V., 2006. *Atmospheric Science*: *An Introductory Survey*. second ed. Academic Press (483 pp).

Webster, P.J., 1994. The role of hydrographic processes in ocean-atmosphere interactions. Rev. Geophys. 32, 427–476.

Webster, P.J., Clark, C., Cherikova, G., Fasullo, J., Han, W., Loschnigg, J., Sahami, K., 2002. The monsoon as a self-regulating coupled ocean-atmosphere system. Int. Geophys. 83, 198–219.

Widiyatmi, I., Yamanaka, M.D., Hashiguchi, H., Fukao, S., Tsuda, T., Ogino, S.-Y., Harijono, S.W.B., Wiryosumarto, H., 1999. Quasi-four-day mode observed by the boundary layer radar at Serpong (6S, 107E), Indonesia. J. Meteorol. Soc. Jpn. 77, 1177–1184.

Widiyatmi, I., Hashiguchi, H., Fukao, S., Yamanaka, M.D., Ogino, S.-Y., Gage, K.S., Harijono, S.W.B., Diharto, S., Djojodihardjo, H., 2001. Examination of 3-6 day disturbances over equatorial Indonesia based on boundary layer radar observations during 1996-1999 at Serpong, Biak and Bukittinggi. J. Meteorol. Soc. Jpn. 79, 317–331.

Winchester, S., 2003. *Krakatoa*: *The Day the World Exploded*: *August 27*, *1883*. Harper Collins Publishers, New York (416 pp).

Wu, P.-M., Hamada, J.-I., Mori, S., Tauhid, Y.I., Yamanaka, M.D., Kimura, F., 2003. Diurnal variation of precipitable water over a mountaneous area in Sumatera Island. J. Appl. Meteorol. 42, 1107–1115.

Wu, P.-M., Hara, M., Fudeyasu, H., Yamanaka, M.D., Matsumoto, J., Syamsudin, F., Sulistyowati, R., Djajadihardja, Y.S., 2007. The impact of trans-equatorial monsoon flow on the formation of repeated torrential rains over Java Island. SOLA 3, 93–96.

Wu, P.-M., Yamanaka, M.D., Matsumoto, J., 2008a. The formation of nocturnal rainfall offshore from convection over western Kalimantan (Borneo) Island. J. Meteorol. Soc. Jpn. 86A, 187–203.

Wu, P.-M., Mori, S., Hamada, J.-I., Yamanaka, M.D., Matsumoto, J., Kimura, F., 2008b. Diurnal variation of rainfall and precipitable water over Siberut Island off the western coast of Sumatera Island. SOLA 4, 125–128.

Wu, P.-M., Hamada, J.-I., Yamanaka, M.D., Matsumoto, J., 2009a. The impact of orographically-induced gravity wave on the diurnal cycle of rainfall over southeast Kalimantan Island. Atmos. Ocean. Sci. Lett. 2, 35–39.

Wu, P.-M., Hara, M., Hamada, J.-I., Yamanaka, M.D., Kimura, F., 2009b. Why heavy rainfall occurs frequently over the sea in the vicinity of western Sumatera Island during nighttime. J. Appl. Meteorol. Climatol. 48, 1345–1361.

Wu, P.-M., Fukutomi, Y., Matsumoto, J., 2011. An observational study of the extremely heavy rain event in northern Vietnam during 30 October–1 November 2008. J. Meteorol. Soc. Jpn. 89A, 331–344.

Wu, P.-M., Arbain, A.A., Mori, S., Hamada, J.-I., Hattori, M., Syamsudin, F., Yamanaka, M.D., 2013. The effects of an active phase of the Madden–Julian oscillation on the extreme precipitation event over western Java Island in January 2013. SOLA 9, 79–83.

Wyrtki, K., 1987. Indonesian through flow and the associated pressure gradient. J. Geophys. Res. 92, 12941–12946.

Xie, P., Arkin, P.A., 1997. Global precipitation: A 17-year monthly analysis based on gauge observations, satellite estimates, and numerical model outputs. Bull. Am. Meteorol. Soc. 78, 2539–2558.

Xie, S.-P., Xu, H., Saji, N.H., Wang, Y., Liu, W.T., 2006. Role of narrow mountains in large-scale organization of Asian monsoon convection. J. Clim. 19, 3420–3429.

Yamamoto, M.K., Ohno, Y., Horie, H., Nishi, N., Okamoto, H., Sato, K., Kumagai, H., Yamamoto, M., Hashiguchi, H., Mori, S., Hashiguchi, N.O., Nagata, H., Fukao, S., 2008. Observation of particle fall velocity in cirriform cloud by VHF and millimeter-wave Doppler radars. J. Geophys. Res. 113, D12210. http://dx.doi.org/10.1029/2007JD009125.

Yamamoto, M.K., Abo, M., Kishi, T., Nishi, N., Seto, T.H., Hashiguchi, H., Yamamoto, M., Fukao, S., 2009. Vertical air motion in midlevel shallow-layer clouds observed by 47-MHz wind profiler and 532-nm Mie lidar: Initial results. Radio Sci. 44, RS4014. http://dx.doi.org/10.1029/2008RS004017.

Yamanaka, M.D., Mori, S., Wu, P.-M., Hamada, J.-I., Sakurai, N., Hashiguchi, H., Yamamoto, M.K., Shibagaki, Y., Kawashima, M., Fujiyoshi, Y., Shimomai, T., Manik, T., Erlansyah, W., Setiawan, B., Tejasukmana, F., Syamsudin, Y., Djajadihardia, S., Anggadiredja, J.T., 2008. HARIMAU radar-profiler network over Indonesian maritime continent: A GEOSS early achievement for hydrological cycle and disaster prevention. J. Disaster Res. 3, 78–88.

Yamashita, A., 2011. Comparative analysis on land use distributions and their changes in Asian mega cities. In: Taniguchi, M. (Ed.), Groundwater and Subsurface Environments: *Human Impacts in Asian Coastal Cities*. Springer, pp. 61–81.

Yang, G.-Y., Slingo, J., 2001. The diurnal cycle in the tropics. Mon. Weather Rev. 129, 784–801.

Yasunari, T., 1981. Temporal and spatial variations of monthly rainfall in Java, Indonesia. Southeast Asian Stud. 19, 170–186.

Yasunari, T., Suppiah, R., 1988. Some problem on the interannual variability of Indonesian monsoon rainfall. *Toropical Rainfall Measurement*. DEEPAK Publ., pp. 113–121.

Yoden, S., Otsuka, S., Trilaksono, N.J., Hadi, T.W., 2016. Recent progress and achievements in research on the maritime continent monsoon. Global Monsoon System III (in press).

Yokoi, S., Matsumoto, J., 2008. Collaborative effects of cold surge and tropical depression–type disturbance on heavy rainfall in central Vietnam. Mon. Weather Rev. 136, 3275–3287.

Yoneyama, K., Masumoto, Y., Kuroda, Y., Katsumata, M., Mizuno, K., Takayabu, Y.N., Yoshizaki, M., Shareef, A., Fujiyoshi, Y., McPhaden, M.J., Murty, V.S.N., Shirooka, R., Yasunaga, K., Yamada, H., Sato, N., Ushiyama, T., Moteki, Q., Seiki, A., Fujita, M., Ando, K., Hase, H., Ueki, I., Horii, T., Yokoyama, C., Miyakawa, T., 2008. MISMO field experiment in the equatorial Indian Ocean. Bull. Am. Meteorol. Soc. 89, 1889–1903.

Yoneyama, K., Zhang, C., Long, C.N., 2013. Tracking pulses of the Madden–Julian oscillation. Bull. Am. Meteorol. Soc. 94, 1871–1891.

Zhang, C., 2005. Madden–Julian oscillation. Rev. Geophys. 43, RG2003. http://dx.doi.org/10.1029/2004RG000158.

Zhang, C., 2013. Madden–Julian oscillation bridging weather and climate. Bull. Am. Meteorol. Soc. 43, 1849–1870.